# Environmental Effects on Recycled Plastics

**By**

**Kan Li**

**School of Chemical Engineering**

**Faculty of Engineering, Computer and Mathematical Sciences**

**The University of Adelaide**


**A thesis submitted for the degree of**

**Master of Engineering Science**

# CHAPTER 1 INTRODUCTION

## 1.1 BACKGROUND

The ever increasing tonnage of plastic waste has driven the need for sustainability of renewable resources through plastic recycling. Nowadays, many products are manufactured using recycled plastic, including vineyard posts, garden sleepers, and decking boards for children's playgrounds [1]. However, there exist disadvantages in the use of recycled plastic when compared to virgin polymer or timber as raw materials: they generally exhibit lower stiffness and strength [2], which limits their use in high load-bearing applications. To improve the mechanical properties of these products, manufacturers normally add fillers, which affects the morphology and structure of the polymer [3], to reinforce the polymer matrix [2]. Another complication limiting the utility of these products in outdoor applications is their deterioration on exposure to adverse weathering conditions, which eventually leads to shorter life spans [4]. Previous work has demonstrated that certain fillers (such as calcium carbonate, talc and fibre glass) can be added to recycled low/high density polyethylene (LDPE/HDPE) to improve their mechanical properties [5]. However, it is still unclear if environmental factors, such as temperature, sunlight, oxidation and moisture may cause any loss of lifetime or compromise the durability and mechanical integrity of the composites. Further research is required to improve knowledge in this area.

This work investigated weathering effects on the mechanical properties of recycled LDPE composites and the potential of two types of fillers, talc and glass fibre, to act as reinforcing agents. Tested specimens were produced by injection moulding after the constituents were mixed in a twin screw extruder and then granulated using a pelletiser. The samples were then subjected to accelerated weathering conditions in a QUV/SE weathering chamber (Q-Panel Co.), after which a series of physical and chemical tests were undertaken. These results provide information in regards to the influence of the fillers on the degradation mechanism of recycled plastic matrix, as well as the anticipated rate of deterioration in their performance. This project

will contribute enormously to the usage of recycled plastic and mitigate current environmental issues.

## 1.2 SCOPE AND OBJECTIVE

The primary aim of this project has been to investigate environmental effects on recycled plastic composites. In order to accomplish this goal, the achievement of several milestones was necessary:

1) As the addition of fillers is an effective method to improve the mechanical properties of plastic materials, it was necessary to investigate the type of filler that is capable of reinforcing recycled LDPE more effectively. Furthermore, the effects of varying the content of fillers were examined.

2) The damaging effect of irradiating recycled plastics was explored. UV radiation is an important contributing factor in plastic ageing and degradation, and sustained exposure will reduce key mechanical properties of plastic products. Its effect on recycled plastics, however, has not been extensively studied. Therefore, the second aim of this work was to determine the life span of recycled plastics under UV irradiation, taking into consideration the change of internal structure caused by adding fillers to the polymer matrix.

3) The third and final goal of this work was to study the effect of temperature on recycled plastic products. It is well established that changes in the temperature can alter a plastic's physical characteristics. However, temperature does not have the same influence on the mechanical properties of virgin materials as recycled ones, due to the impurities in the latter. Experiments were therefore undertaken to determine the ability of the fillers to resist the effects of temperature change on the matrix.

## 1.3 THESIS OUTLINE

Chapter One of this work presents the background, scope and objectives of this project, as well as a brief summary of this thesis.

Chapter Two focuses on the literatures devoted to describing the effects of fillers on plastic, and the ageing of plastics in the environment. Additionally, the methods traditionally used to evaluate the degradation of plastic are discussed. Overall, this chapter is dedicated to highlighting previous research and providing the theoretical framework for this project.

Chapter Three highlights the methodologies and materials used in this project, including descriptions of the physical properties of each material. Based on previous research and test standards, the experiments within this project were designed specifically for recycled LDPE composites. Details of each experiment, including samples preparation, mechanical testing, DSC testing, FTIR spectroscopy analysis and SEM observation are also introduced

Chapter Four focuses on the experimental results, and is divided into three main parts. The first details the composition of recycled LDPE pellets, while the reinforcement effects provided by the fillers are discussed in the second part. Part three discusses investigations into environmental effects on recycled LDPE composites, specifically those resulting from UV irradiation and temperature.

Chapters Five and Six provide the conclusions and recommendations of this project. Furthermore, the outcomes from this investigation are summarized.

# CHAPTER 2 LITERATURE REVIEW

## 2.1 INTRODUCTION

Plastic recycling is more important than ever as a consequence of the ever-expanding rates of plastic consumption. However, the low stiffness and strength commonly associated with recycled plastics limits their use in high load-bearing applications [6]. Commonly, fillers have been used to improve the mechanical properties of polymer products, increasing their utility. However, strength reinforcements may not be sufficient, as plastic degradation upon exposure to weathering effects such as temperature and sunlight may restrict their life span [7]. Though there have been a few investigations into the effects of weathering on the properties of virgin plastics, environmental effects on recycled plastic composites have been poorly investigated.

This chapter summarizes the current state of plastic recycling, while also describing the effects of fillers on the mechanical properties of recycled plastic. Furthermore, this review describes the degradation of polymer under different weathering conditions and various experimental methods to measure this.

## 2.2 BACKGROUND

Plastic consumption is steadily increasing worldwide. In Australia, the total consumption increased from 1,553,475 tonnes to 1,710,085 tonnes in one year (2006 to 2007) [1]. In order to reduce the pollution levels associated with such high usage, plastic recycling is essential. According to PACIA (2008), the total amount of plastic recycled in Australia in 2007 were merely 261,109 tonnes [1], this value has not significantly increased despite the increases in consumption because poor mechanical properties and short life span limit the usage of products made from recycled plastic [8]. However, materials can be incorporated into the polymer matrix of recycled plastics to restore their mechanical properties and extend the life spans of the composites; these materials are often called fillers. For this research, talc and glass fibre were chosen as fillers in the reinforcement of recycled LDPE.

## 2.3 FILLERS

Fillers can be defined as the solid additives that are incorporated into the polymer matrix in order to improve its mechanical properties. The two most widely used types of fillers in these applications are extender and reinforcing fillers. The former are generally used to increase polymer bulk and reduce the cost of final products; reinforcing fillers, on the other hand, have the ability to improve the mechanical and physical properties of polymer. Further, anti-ageing agent also can be used as filler in polymer product and slow down the degradation during use [9].

The ability of reinforcing fillers to strengthen polymer can be attributed to three main mechanisms of action. The first is the ability of certain kinds of reinforcing fillers to create new chemical backbone in the polymer structure (i.e. by crosslinking). The connection of molecular chains to form a crosslinked structure provides significant improvements in the hardness and tensile strength of the material. The second possible action of reinforcing fillers is to change the morphological characteristics of polymer; fine talc act as crystal nuclei which, upon mixing with a semi-crystalline polymer, improves the latter's degree of crystallinity. Finally, certain reinforcing fillers, particular fibre fillers, are able to share stress loads with other matrix materials along the surface by sliding [10].

A filler's characteristics, such as particle shape, particle size, and, for fibre fillers, length have impact on their reinforcement capacities [11]. Generally, fillers have five major shapes: fibrous, spherical, cubical, block and flake. Fibrous filler can improve tensile strength, whereas sheet-like and plate-like are more sensitive to rigidity [12]. By contrast, round filler can produce lower tensile strength and higher ductility than irregularly shaped particles [13]. In terms of size, smaller fillers can provide higher tensile and flexural strength; due to the increased contact surface area provided by the fine particles, increased stress is transferred to the filler [14]. In contrast, larger particles contribute to larger cavities, which eventually decrease the tensile strength of specimens [15].

Fibrous filler can improve the tensile strength of a recycled polymer and this ability is dependent upon its length. This parameter is compared with the critical fibre length to evaluate its ability to act as a reinforcing agent. Critical fibre length, $L_c$, is defined as the minimum fibre length for a given diameter which will allow tensile failure of the fibre rather than shear failure of the interface. There exist three possibilities for fibre length: (a) $L<L_c$, (b) $L=L_c$, (c) $L>L_c$. In situation (a), applied stresses are insufficient to cause fibre breakage; instead fracture occurs on the polymer matrix. When the fibre length is equal to critical length, the fibre fillers are loaded to the peak stress only at their centers and the average stress across the entire fibre is only half that of peak stress. Finally, in situation (c), fibre fillers break under stress, rather than pulling out at the matrix fracture. Increasing fibre length from $L_c$ to five times that amount of effectively improves a composite's strength, but further increases in length above this value are of relatively little value [16-19].

### 2.3.1 Talc

Talc is commonly used as reinforcing filler for thermoplastics. It is a finely ground platy material composed of: $SiO_2$(40-62%), MgO(30-33%), $H_2O$(16-17%), $Al_2O_3$(0.2-11%), and $Fe_2O_3$(0.1-1.5%) [20]. Due to its shape and size, fine talc can provide significant reinforcements for polymer matrices [5] and because it is an inert substance, it will not react with matrix material. Talc can cause heterogeneous crystallization in a semicrystalline polymer, acting as the nuclei of crystal units [20], such improvements in crystallinity reinforce the mechanical properties of the composite polymer. Literature review on different sizes of calcium carbonate particles has demonstrated that the properties of the composites changes dramatically when particulate inorganic filler sizes reaches nano-level [11]. However, when using talc as filler, it is important to control particle dispersion, so as to maximize the reinforcement effect.

### 2.3.2 Glass fibre

Glass fibres comprise mainly of silica ($SiO_2$), display very stable physical and chemical

properties in all kinds of weathering conditions [21]. Thus, glass fibre is a very popular reinforcing agent for many polymer products and carries with it two distinct advantages. Firstly, glass fibres are able to strengthen plastic matrices. Whereas the tensile strength of most polymers is no more than 100 MPa, that of glass fibre is 3.45 GPa [22], because of this disparity, glass fibres are able to share tensile stress with a polymer's matrix upon mixing, resulting in a plastic with increased tensile strength. Another advantage of glass fibre is its chemical inertness that renders the composite useful in a variety of corrosive environments. The vitreous and crystalline states of silica provide glass fibres with extremely stable chemical properties [23]. This ensures the absence of a chemical reaction between the polymer matrix and reinforcing glass fibres. Furthermore, the chemical inertness of the latter is also able to slow down the degradation of a composite polymer in corrosive environments [23]. However, the surface characteristics of specimens reinforced by glass fibre are extremely important, because surface flaws can deleteriously lead to losses in tensile properties. Thus, the most effective method to improve the mechanical properties of polymer specimens reinforced by glass fibre is to ensure the avoidance of flaws on the surface between the fillers and matrix [24].

## 2.4 ENVIRONMENTAL FACTORS

The degradation of polymer products can be caused by environmental effects, such as temperature, sunlight, oxidation, moisture and microbiological attack [25]. Among these factors, temperature and sunlight are normally cited as the main environmental concerns leading to the loss of mechanical properties of plastic products and these effects will be subsequently discussed.

### 2.4.1 Temperature

Polymer materials are sensitive to temperature and their mechanical properties change as a function of this parameter [16]. The effect of temperature can be divided into two groups: those associated with low temperatures and those observed at high temperatures.

Molecular chains within polymer materials are bonded via Van der Waals forces. At lower

temperatures, there is insufficient energy to weaken these bonds, leading to decreases in molecular activity [26]. In this situation, the polymer structure is much harder and more brittle than those at room temperature (20$^{o}$C). However, if the environmental temperature is close to a plastic's glass transition temperature (which, for LDPE is approximately -78$^{o}$C), a shift to the glass phase is initiated, leading to increases in tensile strength and tensile modules and a decrease in tensile strain [27].

High temperatures, on the other hand, can lead to two distinct changes in the mechanical properties of polymer. The first involves bonding among molecular chains, increased temperatures provide sufficient energy to weaken the attractive forces among molecular chains [28]. This results a significant elongation of materials; whilst, at the same time, tensile strength decreases slightly. The second noticeable effect of high temperatures is the acceleration of photo-degradation, a process that occurs upon a plastic product's exposure to sunlight. Described mathematically, by using the reaction rate constant K as function of temperature T, is in the following manner: $K=Ae^{-Eq/RT}$, where $K$: Reaction rate constant; $A$: Pre-exponential factor; $E_q$: Activation energy; $R$: Gas constant; $T$: Absolute temperature

Since the values for $A$ and $E_q$ are dependent on the reaction, it is clear that K is dependent on temperature, and increases exponentially with increasing temperature, a relationship which is reflected by faster photo-degradation reactions at high temperatures. Thus, high temperatures accelerate losses in the mechanical properties of plastic products.

### 2.4.2 UV Radiation

Many polymeric materials are sensitive to the effects of the UV fraction of solar radiation [29], despite the fact that pure polyolefins cannot absorb it. Polymer sensitivity to sunlight can be attributed to the fact that polyolefin products generally contain some form of impurity or chromophores. These impurities can absorb the UV radiation, subsequently driving the photo-oxidation of commercial polylolefins [30]. It is therefore clear that photo-degradation causes the physical and chemical changes of polymers associated with exposure to UV

radiation or visible light. However, various binding energies lead to different spectral sensitivities of various polymers, some of which are highlighted in Table 2.1 [29].

**Table 2.1 Spectral sensitivity of some polymers**

| Polymer | Wavelength(nm) |
|---|---|
| Polyester | <315 |
| Polystyrene | <340 |
| Polyethylene | <300 |
| Polybutadiene | <380 |
| Polyvinyl chloride | 310 and 370 |
| Polyvinyl alcohol | <280 |

It is clear from Table 2.1 that visible light between 400 and 800 nanometres cannot have direct effect to the polymer. Photo-degradation caused by UV radiation results from the latter's delivery of additional energy to the electrons in the polymer. This results in the formation of free radicals which subsequently react with oxygen and water. The process of photo-degradation can be described in four stages: initiation, propagation, branching and termination [29], which are represented in the following chemical reactions.

(P: Alkyl, *: free Radical, O: Oxygen, H: Hydrogen POO: Peroxy, POOH: Hydroperoxide, OH: Hydroxy, PO: Alkoxy) [31]:

a. Initiation

b. Propagation

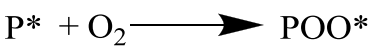

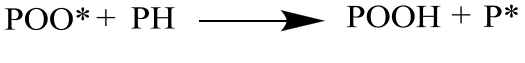

c. Branching

$$POOH \longrightarrow PO^* + OH^*$$

d. Termination

$$POO^* + POO^* \longrightarrow POOP + O_2$$

$$P^* + P^* \longrightarrow P\text{-}P\,(\text{cross linked})$$

$$PO^* + H^* \longrightarrow POH$$

$$P^* + H^* \longrightarrow PH$$

At the beginning of photo-oxidative degradation, the free hydrogen radical and free alkyl radical are dissociated from the polymer by photons from UV irradiation. Next, the process can be propogated by the conversion of the free alkyl radicals to free hydroperoxides radicals, which, in turn, can react with free hydrogen radicals to create hydroperoxide. Alternatively, the peroxy radicals can react with another alkyl to form hydroperoxide and a free alkyl radical. In the branching process, hydroperoxide may decompose into yield alkoxy and hydroy radicals. Finally, there are four possible chemical reactions involved in the termination of photo-oxidative degradation, resulting in one of the following products: hydroperoxide, cross-linking polymer, hydoxyl and short chain alkyl polymer. Depending on which final products result, photo-oxidative degradation could lead to one of two structural changes in a polymer: chain scission or crosslinking [31].

If, during the degradation reactions, free alkyl radicals in different molecular chains react with each other, adjacent linear chains will covalently link to another at various positions by covalent bonds [32]. Once this crosslinking occurs, the mechanical properties of the polymer may be improved significantly. On the other hand, the termination of the photo-oxidative degradation process could result in the breakage of molecular chains into shorter pieces via a phenomenon known as chain scission [29]. In direct contrast to crosslinking, a polymer's mechanical properties are significantly degraded by chain scission. The result of the degradation reactions is crosslinking or chain scission depends on the relative amount of alkyl radicals and absorbed oxygen within the polymer matrix. After long periods of UV irradiation,

chain scission dominates crosslinking. Curiously, it has been demonstrated that crosslinking occurs at the beginning of degradation and it is a precursor to the chain scission [29].

The ageing of plastic products not only depends on the exposure time under UV radiation but also the varying thickness of specimen can have substantial effects on the degradation. Thus it is difficult to just only refer to the standard.

According to previous research, it is believed that in the accelerated weathering system, UVB-313nm lamps produce more damaged specimens and are more effective than UVA-340nm lamps [25, 26, 33, 34]. The reason is shorter wavelength radiation provides higher energy and causes more free radicals to form.

### 2.4.3 The photo-oxidative degradation of polyethylene

Because this work utilized, polyethylene, it is essential to clarify the specifics of this material's photo-oxidative degradation process. Again, the process is divided into four steps [33]:

a. Initiation

(1)

b. Propagation

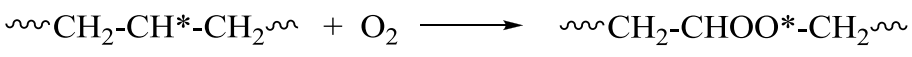

(2)

I 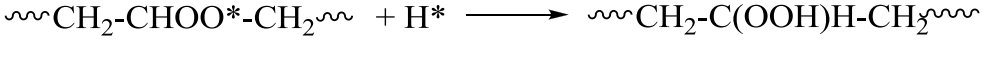

(3)

II 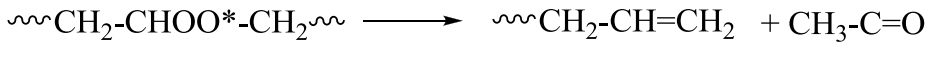

(4)

c. Branch

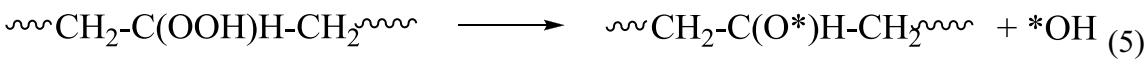

(5)

d. Termination

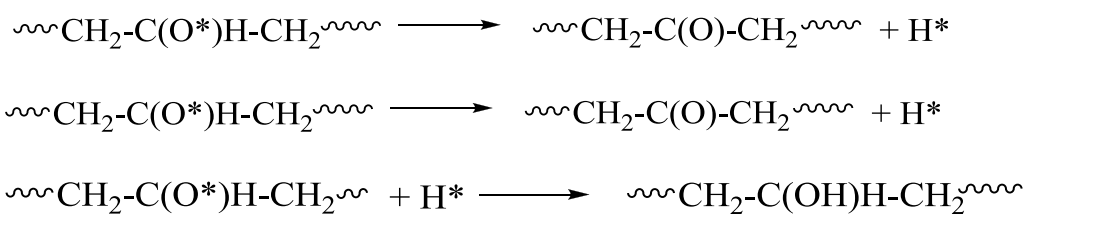

(6)

(7)

(8)

As discussed above, the photo-oxidative reactions are initiated by UV radiation. In the first reaction, polyethylene loses one hydrogen atom and becomes active. The active polyethylene is oxidized in the second reaction. After this, one of two degradation reactions follows: Norrish type I and type II, as described in the third and fourth reactions, respectively. With respect to Norrish type I regime, acyl radical is formed. This radical would further decompose with the loss of carbon monoxide. However, in the Norrish type II regime, the adjacent hydroxyl and vinyl are rearranged to form a ketone [33]. This ketone, which consists of carbonyl group, is consider as one of the groups that can be detected during the FTIR spectroscopy process to indicate the oxidation rate [35]. The final two steps of the photo-degradation of polyethylene are driven by UV radiation. The new free radicals initiate the new reactions cycle. After the termination process, the original molecules decompose into several shorter chain molecules.

In the process of photo-degradation, UV radiation is regarded as the catalytic agent, and radiation intensity limits the speed of reactions. Furthermore, the structural changes in the molecules may lead to different mechanical properties in materials [36].

## 2.5 MECHANICAL PROPERTIES

The mechanical properties of polymers can be determined by measuring various parameters such as the modulus of elasticity, yield strength, tensile strength and %elongation. For many polymer products, the simple stress-strain test is employed for the characterisation of these mechanical parameters [22].

### 2.5.1 Tensile properties

Polymer materials can display three different types of stress-strain behavior, as shown in Figure 2.1 [37]. Curve A illustrates the stress-strain behavior of a brittle polymer. These materials fracture while deforming elastically. The behavior of a plastic material, represented by curve B, is similar to ductile metallic materials. Elastic deformation occurs in the beginning of the tensile test, followed by yielding and a region of plastic deformation. In curve C, the deformation of elastic polymer displays similar characteristics to that of rubber [22].

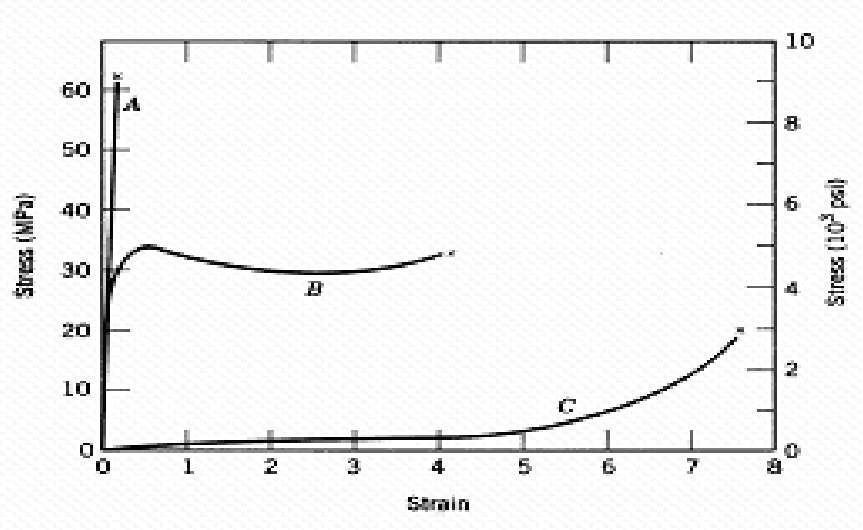


**Figure 2.1 The stress-strain behavior for brittle (curve A), plastic (curve B), and highly elastic (curve C) polymers (Reproduced from [22])**

From the stress-strain curve, there are a number of parameters that can be determined to evaluate material characteristics of a plastic, including modulus of elasticity, yield strength, tensile strength and % elongation. Modulus of elasticity is defined as the ratio of stress to strain when deformation is totally elastic and can be thought of as material's stiffness. The yield strength ($\sigma_y$) is defined as the maximum point just beyond the termination of the maximum elastic region for the plastic polymer (curve B, Figure 2.1). Tensile strength is the maximum stress load experienced in the tensile test, and may be greater or less than the yield strength. Tensile strain is used to describe the change in a sample's length at fracture point. Each parameters may be used to evaluate different aspects of a polymer's mechanical properties [22].

Mechanical properties of polymers are very sensitive to temperature changes. For instance,

increasing the temperature from 40 to 60$^{o}$C may lead to a reduction in tensile strength and elastic modulus, and an enhancement of tensile strain. On the other hand, a decrease in temperature may result in the opposite behaviour, with tensile strain becoming lower than that at room temperature [37].

### 2.5.2 Factors that influence the mechanical properties

Molecular weight, degree of crystallinity, and crosslinking are some of the parameters that influence the mechanical properties of polymeric materials. A polymer's molecular weight depends on the number of repeat units in one molecular chain; more repeat units lead to high molecular weight and long molecular chains. Long molecular chains, in turn, can provide more chain entanglements. Thus, high molecular weight leads to increased tensile strain and tensile strength.

The degree of crystallinity has a significant effect on the mechanical properties as well, since it influences the intermolecular secondary bonding. Most polymers are of a semi-crystalline structure; in the crystalline region, the molecular chains are closely packed in an ordered parallel arrangement, which causes high secondary bonding. Therefore, polymers with a high degree of crystallinity may have a high tensile strength and elastic modulus. However, these materials tend to be more brittle with the increasing of degree of crystallinity, which leads to the decreasing of tensile strain.

Crosslinking is another parameter that influences the mechanical properties of polymers. In crosslinked samples, linear chains are joined by covalent bonds, as represented in Figure 2.2. Similar to the properties conferred by a high molecular weight, crosslinking can reinforce the tensile strength and the tensile strain of a polymer, due to restricting relative chain mobility. Thus many rubbers are crosslinked elastic materials.

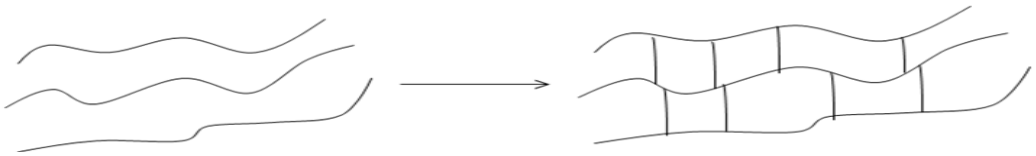

**Figure 2.2 The crosslinking of linear chains**

## 2.6 DETECTION OF PHOTO-OXIDATION DEGRADATION

Photo-oxidative degradation can only be identified using chemical detection methods. There are two obvious features which results from photo-oxidation degradation: the formation of new functional groups, as previously described, and a change in the molecular weight of the polymer, due to crosslinking or chain scission. The former can be detected using Fourier transform infrared (FTIR) spectroscopy which is an effective method to identify the functional groups present in materials and to determine the degree of degradation by quantifying the amount of newly formed functional groups [38]. To determine the change in molecular weight of a polymer, as occurs during crosslinking or chain scission, gel permeation chromatography (GPC) is commonly used [39]. Unfortunately, the results from GPC are not always reliable, particularly when impurities are present. Since this project involved investigating recycled plastics by the addition of fillers, the presence of impurities was impossible to avoid. Therefore, FTIR spectroscopy was used to evaluate the photo-oxidation degradation in this work.

FTIR is used commonly to identify an unknown material, to determine the quality of a sample and the relative amounts components in a mixture by the process illustrated in Figure 2.3. Different functional groups in a materials can be detected by the absorption of IR at a particular wavelength [40].

NOTE:
This figure is included on page 16 of the print copy of the thesis held in the University of Adelaide Library.

**Figure 2.3 Principle of FTIR (Reproduced from [40])**

Carbonyl groups (C=O) are a product of chain scission and oxidation. The ketone groups of LDPE, and can be detected by FTIR after thermal degradation [35]. The presence of carbonyl groups, as determined by FTIR analysis, is therefore often used to verify the occurrence of photo-degradation in polymer samples.

Based on the research from Gulmine (2000), the new functional groups can be seen in Figure 2.4 after UV accelerated weathering testing. It is clear that the presence of carbonyl group can be observed from the absorption of IR at 1714 $cm^{-1}$ (ketone group) [35].

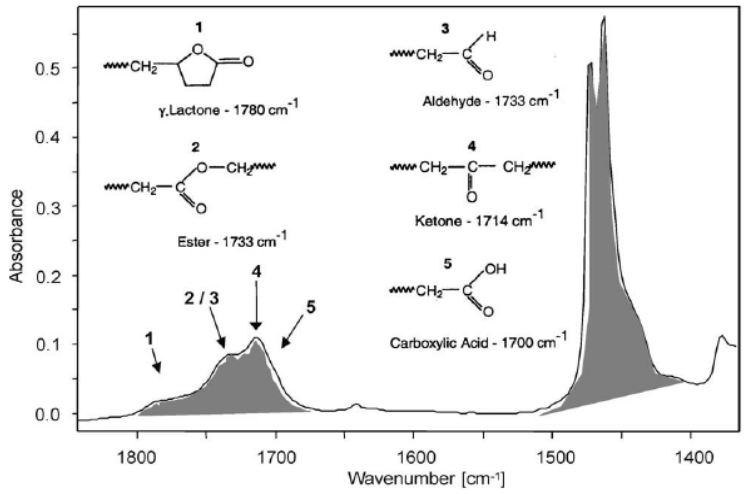


**Figure 2.4 The spectrum of LDPE after accelerated weathering test (Reproduced from [41])**

However, due to instrumental errors in FTIR testing, it is impossible to evaluate the process of photo-oxidation degradation by comparing the absorbance of carbonyl group (ketone group). The absorbance polyethylene polymer band (in the range of 1470 $cm^{-1}$) is set as the reference, and another modulus has been introduced namely carbonyl index [33, 41]. The carbonyl index is defined as the ratio of the integrated band absorbance of the carbonyl in the ketone group to the absorbance of the polyethylene polymer band, which exhibits the degree of photo-oxidation in each LDPE samples. Figure 2.5 shows the method of calculated the carbonyl index.

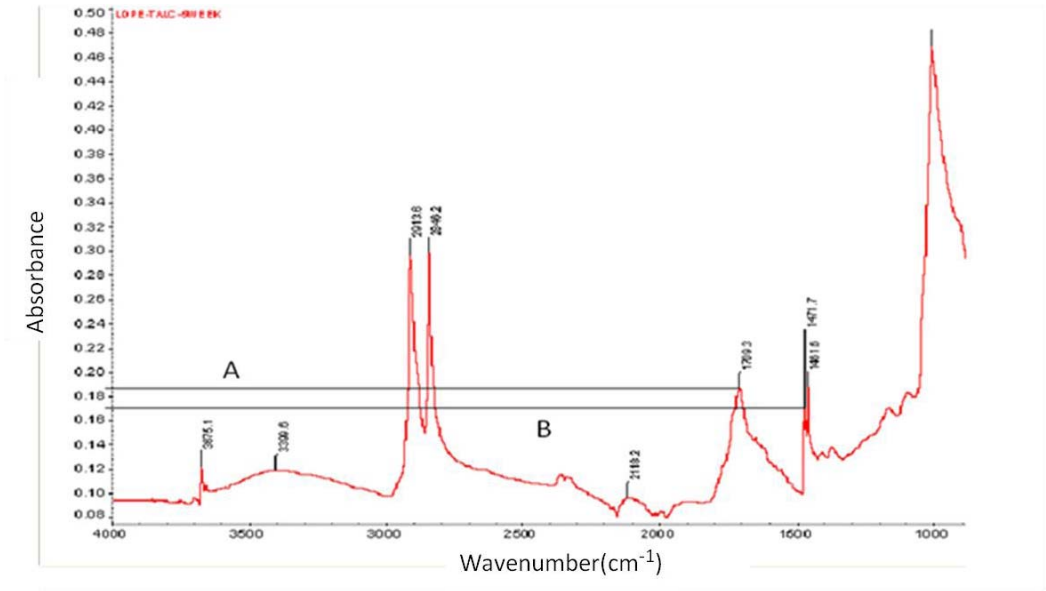


**Figure 2.5 Definition of carbonyl index**

Peak A represents the carbonyl group, while peak B represents the polyethylene polymer band. The carbonyl index equals to A/B, which can be calculated from the new spectrum after an FTIR test [38, 39].

## 2.7 CRYSTALLIZATION PROPERTIES

The crystallization properties of a polymer can be elucidated using differential scanning calorimetry (DSC). In this technique, the heat flow in the sample is measured as a function of time or temperature by scanning its temperature in a controlled atmosphere [42]. The main application of DSC is for determining the phase transitions of materials, such as the glass transition and the crystallization temperature, because the energy and heat capacity changes associated with these transitions can be measured by DSC [43].

In this work, DSC was used to detect the degree of crystallinity in LDPE composites. As a sample's temperature increases, the bonding energy among its molecular chains is weakened. Eventually, these molecular chains may obtain enough freedom to form a new crystalline structure and the energy lost in this process can be determined by DSC. A peak in the DSC signal represents the transition from amorphous solid to crystalline solid and the area of that peak is used to calculate the energy lost [44].

The polymer molecules in most plastic materials are only partially crystalline, or "semi-crystalline". In such a structure, crystalline regions appear within the amorphous materials. Because a polymer's internal structure has a great effect on its mechanical properties [22], the degree of crystallinity is an important factor to evaluate in defining its mechanical properties. Figure 2.6 shows a typical DSC thermogram of pure HDPE. The temperature corresponding to the inverse peak is the melting point ($T_m$). The area above this on a DSC thermogram can be translated to the degree of crystallinity. Furthermore, it can be used to determine the melting enthalpies ($\Delta H_m$) of a polymer. A larger area indicates a higher degree of crystallinity of the test material [45]. To determine the precise peak area for different types of polyethylene, different temperature ranges are utilised. For instance, those for HDPE, LDPE, and LLDPE are 70-160$^oC$, 65-140$^oC$, 75-155$^oC$, respectively. Because the heat of fusion ($\Delta H_0$) of the polyethylene crystal phase is known to be 292.5 kJ/kg, the degree of crystallinity ($\chi$) of any polyethylene sample can be estimated by the following equation: $\Delta \chi = \Delta H_m/\Delta H_0$ [46].

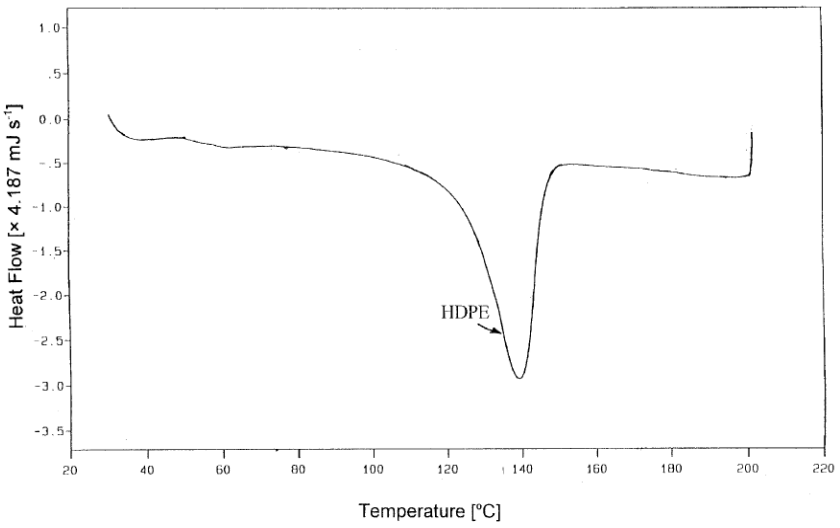


**Figure 2.6 Typical DSC themogram of pure HDPE (Reproduced from [46])**

## 2.8 MORPHOLOGICAL OBSERVATION

The morphology of a polymer sample is influenced by the shape, size and distribution of the particles on its surface, and it generally detected by Scanning Electron Microscopy (SEM) (Figure 2.7).

In this process a small area of the specimen is bombarded with electrons, which can lead to several effects: 1) the electrons may be elastically reflected from the specimen without any loss of energy; 2) the specimen could absorb the electrons and generates secondary electrons with lower energy; or 3) a visible light could be emitted when the electrons are absorbed by the specimen. The SEM image is generated in accordance with these different reflected effects, though the secondary electrons are usually the main contributor to the resulting image. It is important, when using SEM, that the sample is coated with an electric conductor such as carbon in order to generate a clear image on the screen [47].

**Figure 2.7 The structure of Scanned Electron Microscopy (Reproduced from [47])**

In the research on polymer composites, SEM can be employed to provide information on the morphology of fillers on the surface. As the molecular weight of the polymer generally decreases during photo-degradation, this process will result in some cracks on the specimen's surfaces and such flaws can be detected by SEM. Therefore, analysing the surface images can provide an understanding of the mechanical properties of a polymer as well as its degree of photo-oxidation.

# CHAPTER 3 MATERIALS AND EXPERIMENTS

## 3.1 MATERIALS

This work focuses on the use of recycled low density polyethylene when fine talc and glass fibre were employed as reinforcing fillers.

### 3.1.1 Recycled Low Density Polyethylene

Polyethylene ($-CH_2-CH_2-$), the simplest of all polymers and a common thermoplastic, can be subdivided into low density polyethylene (LDPE) and high density polyethylene (HDPE). LDPE is a commercially popular material, due to its dielectric properties combined with its durability, low-cost and easy manufacturability.

The recycled LDPE used in this study was supplied by Plastic Granulating Service (PGS), South Australia, in the form of pellets. In order to extend recycled LDPE's life span, PGS mixed them with carbon black. Thus, a sample control test was necessary for each batch of pellets.

### 3.1.2 Talc

Talc ($3MgO \cdot 4SiO_2 \cdot H_2O$) is a naturally occurring hydrated magnesium silicate. The talc used in this work is a yellow powder with an average particle size of roughly 106 μm, a sample of which is shown in Figure 3.1.

**Figure 3.1 Fine Talc**

### 3.1.3 Glass Fibre

Glass fibre is the most widely used reinforcing fibre in the plastic recycling industry and can be modified to promote adhesion to the polymer matrix. The effect of reinforcement depends on the length of fibre, a length of 6 mm was chosen for this research, a sample of which is shown in Figure 3.2. This filler was supplied by George Fethers & Co.

**Figure 3.2 Glass Fibre**

## 3.2 EXPERIMENTS

### 3.2.1 Sample Preparation

*3.2.1.1 Blending of LDPE pellets and fillers*

The blending of LDPE and filler (either talc or glass fibre), was performed by using a Brabendar 32-mm co-rotating intermeshing twin screw extruder (RMIT University, Victoria, Australia) as shown in Figure 3.3. The extruder was preheated to three different zone temperatures at 150$^{o}$C, 170$^{o}$C and 200$^{o}$C, respectively. The extruded plastic strands were granulated into 2-3 mm pellets in a Berlyn pellister (RMIT University, Victoria, Australia), shown in Figure 3.4. The content of the recycled LDPE composites made in this manner is shown in Table 3.1.


**Figure 3.3 Brabender twin screw**

**Figure 3.4 Berlyn pellister**

**Table 3.1 The content of recycled LDPE composites**

| No. | Matrix (wt%) | Filler (wt%) |
|---|---|---|
| 1 | 70% R-LDPE(1) | 30% Talc |
| 2 | 65% R-LDPE(1) | 35% Talc |
| 3 | 60% R-LDPE(2) | 40% Talc |
| 4 | 55% R-LDPE(2) | 45% Talc |
| 5 | 50% R-LDPE(2) | 50% Talc |
| 6 | 70% R-LDPE(1) | 30% Glass Fibre |
| 7 | 65% R-LDPE(2) | 35% Glass Fibre |
| 8 | 60% R-LDPE(2) | 40% Glass Fibre |
| 9 | 55% R-LDPE(2) | 45% Glass Fibre |
| 10 | 50% R-LDPE(2) | 50% Glass Fibre |

* (1) denotes the first batch of recycled LDPE received from PGS, whereas (2) indicates samples from the second batch

*3.2.1.2 Injection Moulding*

After granulation, the composite pellets were injection moulded into specimens for tensile testing by a Battenfeld injection moulder (PGS, South Australia, Australia), shown in the Figure 3.5, based upon ASTM D256 and D790. The pressure of injection was set at 137 bars for all specimens, and the front, mixing and feeding temperatures across the barrel were set at 245$^{o}$C, 235$^{o}$C and 200$^{o}$C, respectively.

**Figure 3.5 Battenfeld Injection Moulder**

The pellets of recycled LDPE composites were moulded into specimens based on the standard ASTM D638 procedure [48]. The type II standard specimen for tensile testing was applied in our testing. The configuration and size of specimen are shown in Figure 3.6.



**Figure 3.6 Dimension of tensile test specimen (Reproduced from[49])**

### 3.2.2 Weathering accelerating process

The QUV Accelerated Weathering Tester (Q-Lab Corporation, USA) is widely used in the research on plastic degradation. The type of weathering damage that might be caused by a specimen over months or years of outdoor exposure can be reproduced by the QUV in just a few days or weeks. The damaging effects of natural weathering due to factors such as sunlight, dew and rain can be realistically simulated by the QUV short wavelength UV-light and moisture cycles. Given this, weathering accelerating process, undertaken in this research was accomplished using a QUV Accelerated Weathering Tester. The chamber was equipped with UVB-313 fluorescent lamps which reached maximum peak at 313 nm. ASTM (G5396)

procedure specifies UV irradiation for 8 hours at radiation level of 0.6 W/m$^2$ at 60$^o$C followed by condensation for 4 hours at 50$^o$C [50]. The ageing process employed in this work ranged from one to eight weeks for eight sets of specimens and six repeated specimens were used for each set. During the process of accelerated weathering, UV sensors were calibrated for every 500 hours.


**Figure 3.7 QUV Accelerated Weathering Tester**

The specimens for accelerated weathering test are listed below in Table 3.2.

**Table 3.2 The specimens for accelerated weathering test**

| Quantity | Specimens |
|---|---|
| 48 | R-LDPE |
| 48 | 70% R-LDPE -30% Talc |
| 48 | 65% R-LDPE –35% Talc |
| 48 | 70% R-LDPE –30% Glass Fibre |

### 3.2.3 Mechanical Testing

Mechanical tests were conducted both at room temperature and in an environmental chamber using an Instron 5543 mechanical tester (Figure 3.8).This is a single column system for tests requiring less than 1 kN, whose design provides a small footprint and accessibility to the test area from three sides. The system can be installed with a diverse selection of grips and fixtures

for tensile, compression, bending and component testing. Additional accessories, which include extensometer for strain measurement and environmental chambers for high or low temperature tests, can be installed onto the system as well.

The environmental chamber (Figure 3.9) is designed for use at temperature up to +250$^{o}$C and down to -70$^{o}$C; the latter being accomplished with an optional cooling package which utilizes liquid nitrogen to reach subzero temperatures. All internal surfaces are stainless steel and are insulated by glass fibre and Microtherm insulation.

As noted, testing under both conditions was carried out by the INSTRON 5543 with a maximum load capacity of 1 kN at a speed of 50 ± 10% mm/min with every set of tests repeated at least five times. Repetitive testing is required when stand deviation value is more than 0.5 with five or more samples. Room temperature studies were carried out at 23±2$^{o}$C in order to match the condition utilized in the accelerated weathering tests previously conducted on the specimens as it is useful to determine the UV effects on the mechanical properties under the same environmental conditions.

**Figure 3.8 INSTRON 5543**

**Figure 3.9 Environmental Chamber**

The second test condition employed the environmental chamber, in order to investigate the effects of temperature on the mechanical properties of the specimens. The environmental chamber has a temperature range from -70$^{o}$C to 250$^{o}$C, and the temperature selected for this study range from -20$^{o}$C to 80$^{o}$C, in 20$^{o}$C increments.

### 3.2.4 FTIR spectroscopy analysis

The components of the polymers and their photo-degradation rate were characterized using a FTIR spectrometer (Nicolet 6700, Thermo Scientific) with wavelength numbers ranging from 500 to 4000 cm$^{-1}$. A Smart Orbit ATR fitted with a diamond crystal functioned as the detector, and is capable of analyzing solids, thin and thick films, powders, pastes and liquids, thus allowing our specimens to be tested directly. Results from FTIR analysis determine the carbonyl index which, in turn, represents the amount of carbonyl compounds produced in the photo-oxidation process.


**Figure 3.10 FTIR Nicolet 6700**

### 3.2.5 DSC analysis

The DSC equipment from Setaram Instrumentation, model S60/52920, was applied to test the degree of crystallinity of the recycled LDPE composites reinforced with talc. Heating and cooling rates of 13$^{o}$C/min and -13$^{o}$C/min were used, respectively, in the range from 40$^{o}$C to 210$^{o}$C. The heating and cooling steps were repeated twice for every test. During the second cooling down cycle, the values of the temperature and crystallization enthalpy were recorded. Small-sized samples within the mass range of 5-20 mg were required for DSC analysis.

NOTE:
This figure is included on page 28 of the print copy of the thesis held in the University of Adelaide Library.

**Figure 3.11 Differential scanning calorimetry (DSC)**

### 3.2.6 SEM observation

The Philips XL-20 Scanning Electron Microscope (SEM) produces various images by focusing a high energy beam of electrons onto surface of a sample and detecting signals from the interaction of the incident electrons with the sample's surface. The types of signals gathered in an SEM vary and can include secondary electrons, characteristic x-rays, and back-scatter electrons. Three-dimensional SEM images can be obtained by the scanning of secondary electrons.

Prior to SEM observation, small portions adjacent to the fracture area of the tensile-tested specimens were cut and sputter coated with carbon by Adelaide Microscopy staff using the Cressington sputter coater. Sputter coating is a process of coating a specimen with an ultra fine layer of electrically-conducting material, generally gold or a gold/palladium mixture. This coating acts as a "stain" and increases the ability of a specimen to conduct electricity and emit secondary electrons when placed in a scanning electron microscope.

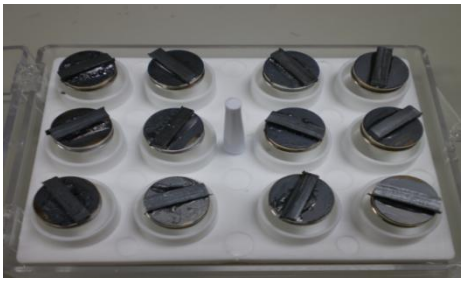

**Figure 3.12 Philips XL-20 and Specimens**

Morphology studies were carried out using the Philips XL-20 scanning electron microscope (Adelaide Microscopy, South Australia), with 10 kV acceleration. Observations were made using magnifications of 35X, 200X, 500X and 800X.

# CHAPTER 4 RESULTS AND DISCUSSION

## 4.1 INTRODUCTION

This section highlights the results obtained from a series of experiments and determines the characteristics of each recycled low density polyethylene composite. This section is divided into three parts according to the steps of experiments. The first part investigates the composition of recycled LDPE pellets owing to the difficulties in obtaining consistency in the content of recycled LDPE from batch to batch. The reinforcing effects of fillers are discussed in the second part, which also examines the function of filler in recycled LDPE composites. Finally, the environmental effects, such as UV irradiation and temperature, on the recycled LDPE composites are actively looked at. By comparing the characteristics among the recycled LDPE composites in weathering conditions, the resistance to ageing among different kinds of material is obtained.

## 4.2 SAMPLE CONTROL

During recycling, the purity of materials was often unpredictable, leading to variations in properties. The matrix material used in this work, recycled LDPE, was obtained from the supplier in two separate batches, necessitating a sample control before any study was undertaken. Tensile test curves of these two batches of recycled LDPE samples are shown in Figure 4.1.

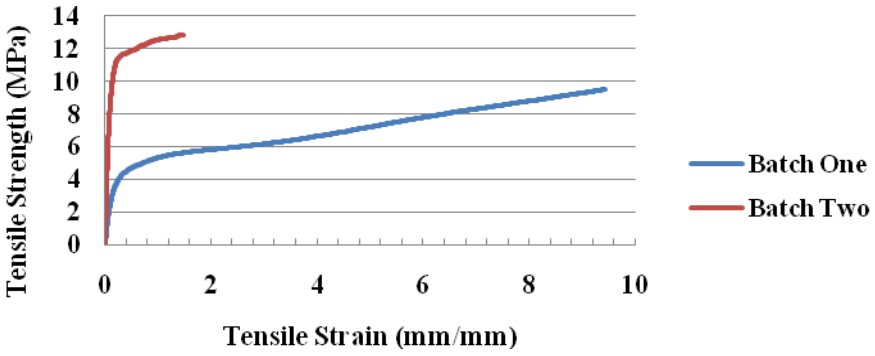


**Figure 4.1 Tensile strength-strain curves of two recycled LDPE batch**

It is obvious that there is a significant difference between these two batches of recycled LDPE. Batch two has much lower tensile strain than that of batch one, which reaches to 1.42 mm/mm. However, since the elongation of batch one at fracture point is longer than the stretch range of the INSTRON 5543 testing machine, the actual tensile strain and tensile strength might be higher than those at the maximum point on the strength-strain curve. Thus, the tensile strength of these samples is not comparable. Also clear from Figure 4.1 is the fact that the specimens made from batch two are much more brittle than those made from batch one.

The difference in mechanical properties between two samples of the same materials is attributable to the existence of impurities. In the plastic recycling process, packaging material is one of the most common contaminants. It is difficult to avoid mixing other plastics with LDPE during the recycling process. The contents of both batches of recycled LDPE were determined via FTIR testing. The spectra of which are shown in Figure 4.2.

It is clear from this figure that polyethylene is the main content of these two materials from the peaks at 2913 $cm^{-1}$ and 2847 $cm^{-1}$. Furthermore, there is no obvious change in the other peaks between the two batches, except at the peak around 1000 $cm^{-1}$, which has a much higher absorbance in batch two than in batch one. Thus, it can be concluded that the existing functional group at 1000 $cm^{-1}$ is the main cause for any difference observed in the mechanical properties of these two batches of recycled LDPE. According to Table B-5 in Appendix B , which lists the characteristic IR absorption frequencies of organic functional groups, there are three possible functional that groups absorbing IR around at 1000 $cm^{-1}$, the “C-F” group in the alky halide polymer, the “C-N” group in the amine polymer, and “C-O” group in the ether polymer. Since most recycled plastics come from packaging materials, the “C-F” group in the alkyl halide polymer is the most likely of the three to present in recycled LDPE pellets. Halogenated polyethylene is widely used in packaging materials such as polyvinyl chloride (PVC) and polytetrafluoroethylene (PTFE), because of its remarkable mechanical properties. Hence, it may be concluded that “C-F” the functional group is present in the second batch of recycled LDPE. Thus, the explanation for sample #2 being much harder and more brittle than sample #1 is reasonable. It should be noted that, due to the number of unknown impurities

existing in both materials, the quantitative analysis for the content of each impurity is not practical.

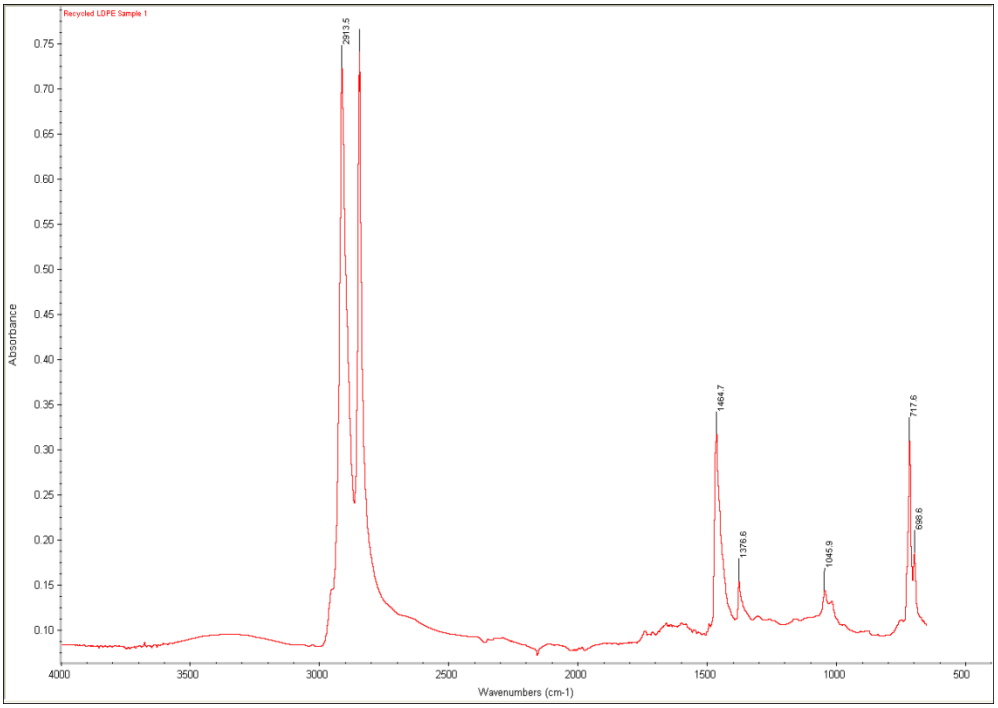


(a) Batch One

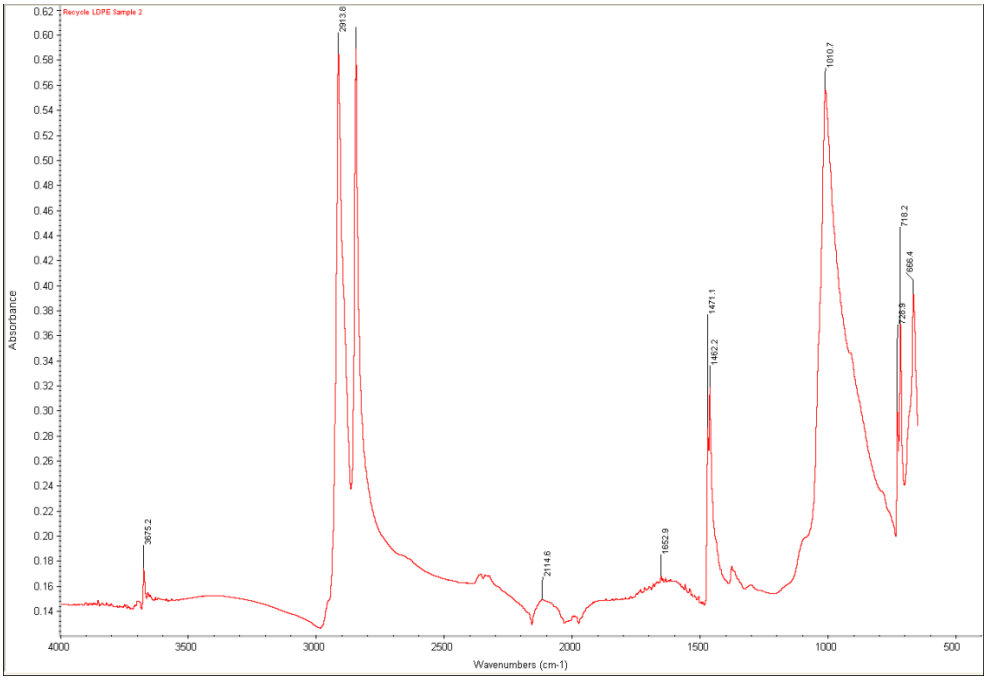


(b) Batch Two

**Figure 4.2 FTIR spectra for two batches of recycle LDPE sample**

Since the two batches of matrix show great differences in mechanical properties and content, only specimens from the same batch are compared in any individual test in this work. The details of each specimen's content have been previously described and are listed in Table 3.1. In order to accurately compare the effects of fillers on recycled LDPE, the specimens were divided into two groups according to the matrix and tested in the different experimental conditions, as listed in Table 4.1

**Table 4.1 Specimens for different tests**

| Test | | Specimen |
|---|---|---|
| **Filler Effect** | | R-LDPE (Batch 2), R-LDPE-Talc (40, 45, 50 wt%)<br>R-LDPE-Glass fibre (40, 45, 50 wt%) |
| **Environmental Effecct** | **UV** | R-LDPE (Batch 1), R-LDPE-Talc (30, 35 wt%)<br>R-LDPE-Glass fibre (30 wt%) |
| | **Temperature** | R-LDPE (Batch 2), R-LDPE-Talc (40, 45, 50 wt%)<br>R-LDPE-Glass fibre (40, 45, 50 wt%) |

As noted, it has been assumed that the reduction of impurities in the recycled LDPE samples could be the most practical method to keep the mechanical properties of recycled material stable consistent between batches. Moreover, the sample control test functions as a calibration and is essential before doing any further research on the recycled plastics.

## 4.3 REINFORCEMENT EFFECTS OF FILLERS ON MECHANICAL PROPERTIES

Fine talc and glass fibres were used as reinforcing fillers for the recycled LDPE matrix in this study. The reinforcement effect not only depends on the types of filler, but also related to the filler's content in the material. This research focused on these two aspects, filler type and concentration, to determine their reinforcement effects and to obtain the optimal concentration of filler by comparing the specimens' mechanical properties.

### 4.3.1 Reinforcement by fine talc

Fine talc was blended with recycled LDPE to achieve concentration of 40, 45, and 50 weight percent (wt%) of the total composite weight. The reinforcement effects of fine talc were determined by investigation into the mechanical properties, internal structure and morphology of each sample.

#### *4.3.1.1 Mechanical Properties*

Figures 4.3 and 4.4 show the changes in tensile properties with increasing content of fine talc. It is observed that as fine talc content increases, (%) elongation with respected to tensile strength drops significantly whereas tensile strength rises by the same magnitude. Figure 4.3 shows that a decrease of 65% in elongation of the unfilled sample is achieved at 50 wt% fine talc, but there is a slight change between 45 wt% and 50 wt%, whose changing rate just results 1%. In other words, (%) elongation almost reaches the minimum value of recycled LDPE with fine talc composites.

From the curve displaying tensile strength versus fine talc content (Figure 4.4), it is clear that tensile strength increase significantly from 13.28 MPa to 16.62 MPa with an increase in fine talc content. At 50 wt% talc addition, tensile strength increases by 15% compared with that of samples without filler, and there is only 9% increase for 45 wt% fine talc. Thus, it is clear that the increasing ratio in tensile strength is much higher when the content of fine talc is in the range from 40 wt% to 50 wt%. Furthermore, it is postulated that increases in tensile strength would continue beyond 50 wt% fine talc loading, though there is insufficient evidence to definitively state this. Thus, the optimal concentration of fine talc is not detectable from the data presented herein.

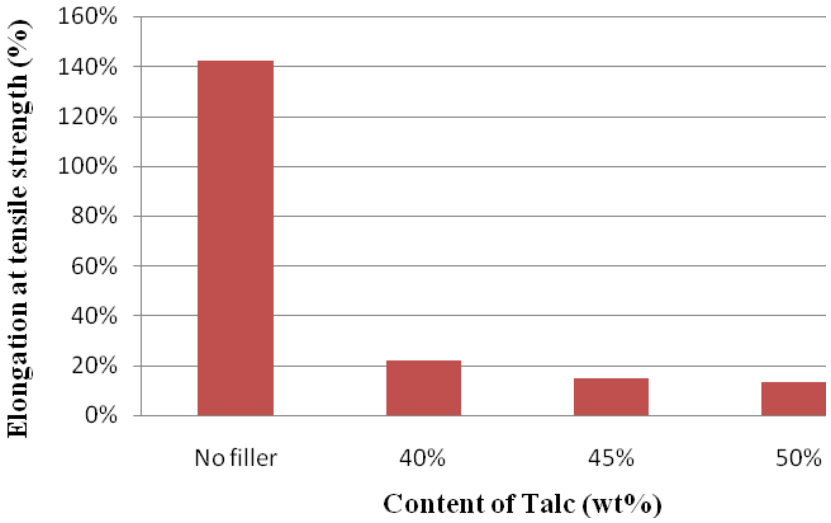


**Figure 4.3 Elongation at tensile strength (%) of recycled LDPE composites with the content of talc**

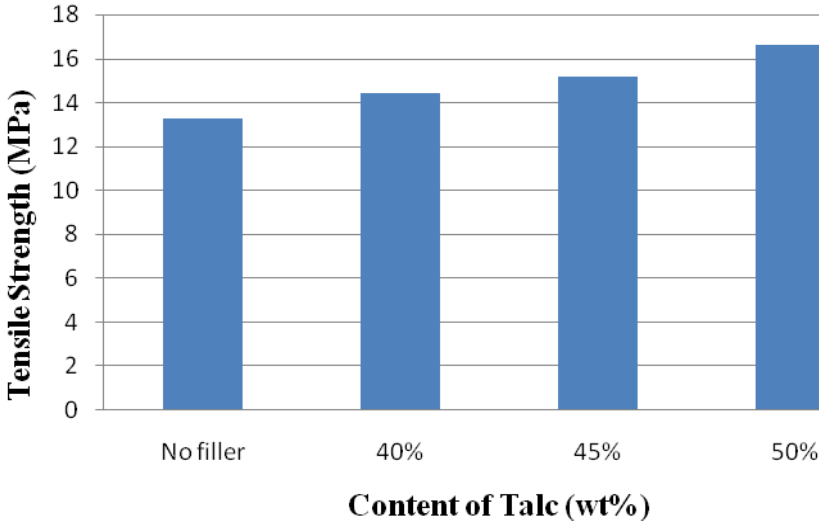


**Figure 4.4 Tensile-strength of recycled LDPE composites with the content of talc**

Overall, with the increase of fine talc content from 0 to 50 wt%, recycled LDPE composites are able to bear more tensile load. Meanwhile, filled specimens exhibit a higher level of brittleness than unfilled samples.

*4.3.1.2 Degree of crystallinity*

As mentioned in Chapter Two, fine talc is a strong nucleating agent for polymer materials. The improvement on the degree of crystallinity is an effective method to increase the tensile strength of specimens. The degree of crystallinity is measured by detection of the crystallization temperature peak and the heat of crystallization. Materials with a higher degree of crystallinity are capable of absorbing more energy during the crystallization process. Therefore enthalpy is an important factor in determining the crystallization characteristics of each specimen. Table 4.2 shows the crystallization properties of recycled LDPE with various talc weight percentages of talc.

**Table 4.2 Crystallization properties of recycled LDPE filled by talc**

| | Unfilled | 40 wt% | 45 wt% | 50 wt% |
|---|---|---|---|---|
| Crystallization Temperature Peak ($^{o}$C) | 133.9 | 134.1 | 135.4 | 136.1 |
| Heat of Crystallization (J/g of LDPE) | 69.01 | 78.28 | 81.36 | 95.3 |
| Degree of Crystallinity | 24% | 27% | 28% | 33% |

It is obvious that the heat of crystallization increases proportionally to the talc concentration, which may also be related to the degree of crystallinity. Moreover, it has been observed that the temperature of crystallization peak increase slightly when specimens include more fine talc filler. Similar phenomena were also reported in the work by Karrad [34], who claimed that it may be ascribed to different heterogeneous nucleation mechanisms. Thus, the crystallization temperature peak provides the evidence to support the theory that the increase of degree of crystallinity is caused by fine talc. Since the change in the degree of crystallinity is in accordance with varying tensile strength, it can be deduced that crystallization properties play an important role in the mechanical properties of recycled LDPE. In addition, fine talc increases the degree of crystallinity of recycled LDPE regardless of concentration, and significantly reinforce s the mechanical properties.

*4.3.1.3 Morphology*

Micrographs of the recycled LDPE/fine talc composites at different talc contents and after tensile testing by SEM are shown in Figure 4.6.

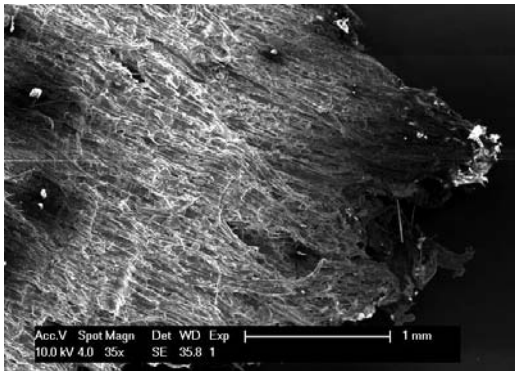


(a) Recycled LDPE-Talc (40wt%) 35X

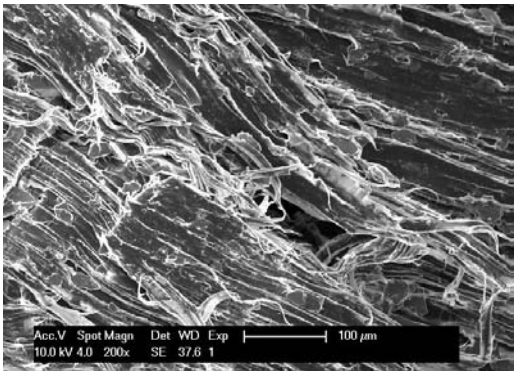


(b) Recycled LDPE-Talc (40wt%) 200X

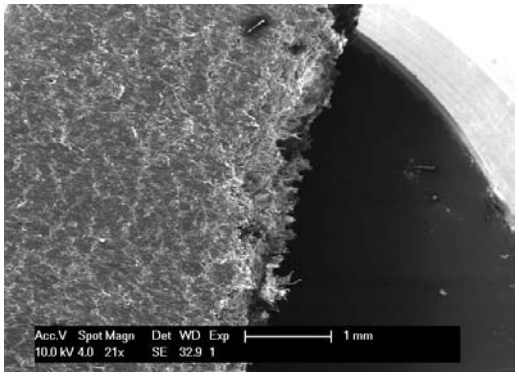


(c) Recycled LDPE-Talc (45wt%) 35X

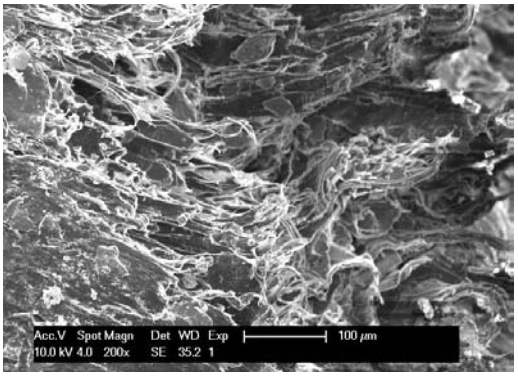


(d) Recycled LDPE-Talc (45wt%) 200X

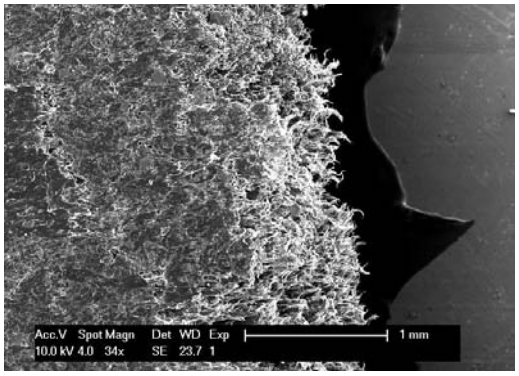


(e) Recycled LDPE-Talc (50wt%) 35X

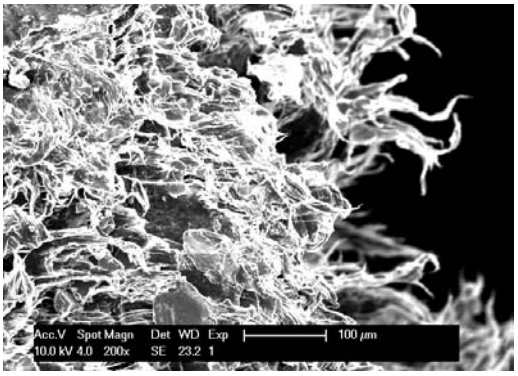


(f) Recycled LDPE-Talc (50wt%) 200X

**Figure 4.6 SEM photographs of recycled LDPE filled by talc (40, 45, 50 wt%)**

These micrographs, obtained by SEM, show the cross-sectional areas of filled recycled LDPE at both high and low magnifications. It is clear from these images that a layered structure appears at cross-section of recycled LDPE filled by 40 wt% fine talc, which suggests that tensile stress should lead to the deformation of matrix. However, this phenomenon is not

observed in images (c) and (e), which shows the cross-section morphologies of specimens filled by 45 wt% and 50 wt% fine talc, respectively, both of which lack any obvious deformation. It is deduced that the molecular chains in these samples are fractured at the same plane. The high-profiled images, magnified by 200X times and shown in Figures 4.6 (d) and (f), offer more visible structure changes of materials.

Differences in the crystalline structure can also be determined from these images. Image (a) shows linear structure on the surface of specimens after tensile testing, but block structures are observed in images (c) and (d) under the same test condition. This phenomenon can be explained by differences in the degree of crystallinity between the samples.

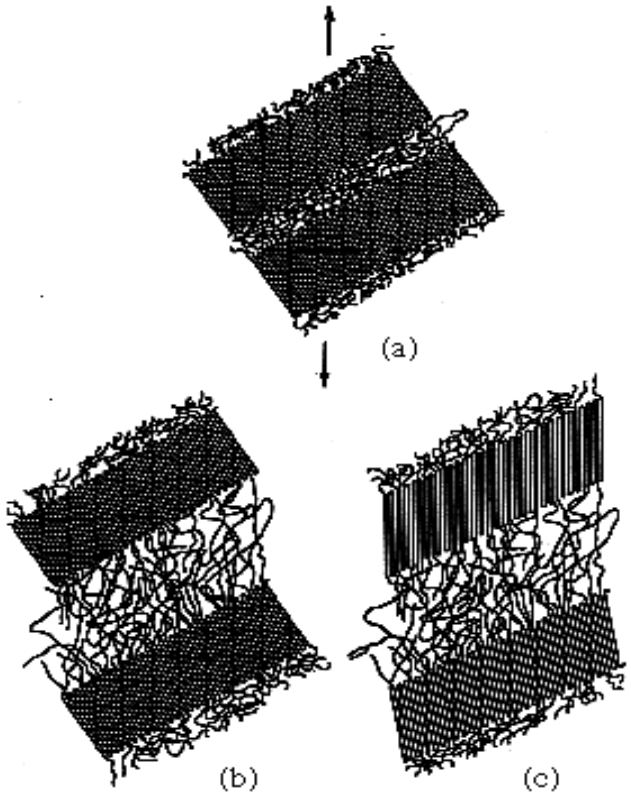


**Figure 4.7 Structure of a semicrystalline polymer (Reproduced from [31])**

LDPE, as mentioned in Chapter Two, is a semicrystalline polymer, an example of whose structure can be seen in Figure 4.7. This illustration shows the transformation of a semicrystalline polymer under tensile stress. In image (a), chain-folded lamellae parts are in crystalline structure whereas other parts are in amorphous structure. When the specimen

undergoes tensile stress, the molecular chains in the amorphous part tend to align along the stress direction, resulting in no obvious deformation in the crystalline part. Finally, the amorphous part breaks when sufficient tensile stress is applied, which can be explained for the break in linear structure found in Figure 4.6 (a). However, with increasing crystallinity, the crystalline structure becomes dominant. The block structures in Figure 4.6 (c) and (e) are assumed to be small LDPE crystal with fine talc nucleus. In the specimens containing 45 wt% and 50 wt% fine talc, the amorphous linear molecular chains still exist, which can be seen in Figure 4.6 (d) and (f). Those linear structures also indicate that fracture of specimens under tensile stress concentrates on the amorphous parts. Moreover, amorphous linear molecular chains with short length lead to the drop in tensile strain and the increase of tensile strength. The analysis of SEM images in another aspect supports the change of mechanical properties with the content of fine talc.

### 4.3.2 Reinforcement by glass fibre

Glass fibre was blended with recycled LDPE in the same weight percentages as fine talc (40, 45 and 50 wt%). The analysis of the mechanical properties combined with morphology images subsequently allowed the determination of the reinforcement effects of glass fibre.

#### *4.3.2.1 Mechanical properties*

Figures 4.8 and 4.9 show the effects of increasing glass fibre content on the tensile strain and tensile strength of recycled LDPE composites. It can be seen from Figure 4.8 that the value of (%) elongation drops rapidly until the content of glass fibre reaches 40 wt%. Decreases in (%) elongation up to 85% are observed between unfilled specimens and filled specimens. The elongation tends to be stable from 40 to 45 wt% with a further decrease observed when the glass fibre content is increased to 50 wt%. Since the recycled LDPE with 50 wt% glass fibre reflects the elongation of 0.05 mm/mm, the toughness of these specimens is close to that of ceramics materials.

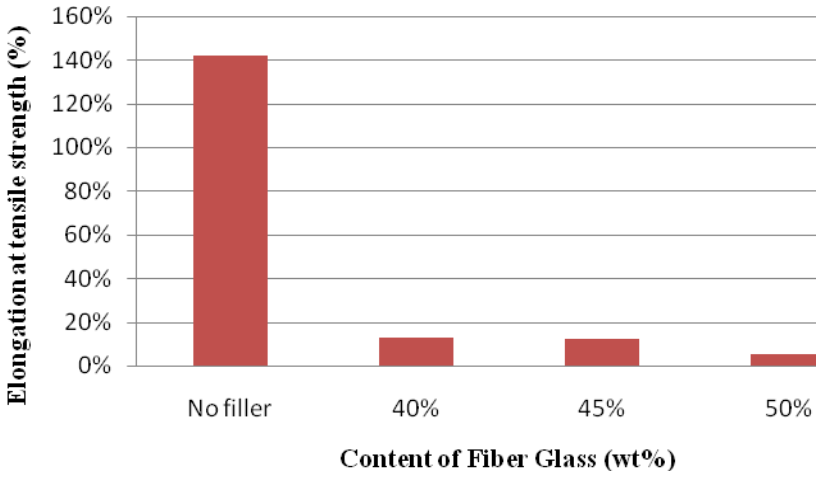


**Figure 4.8 Elongation at tensile strength (%) of recycled LDPE composites with the content of glass fibre**

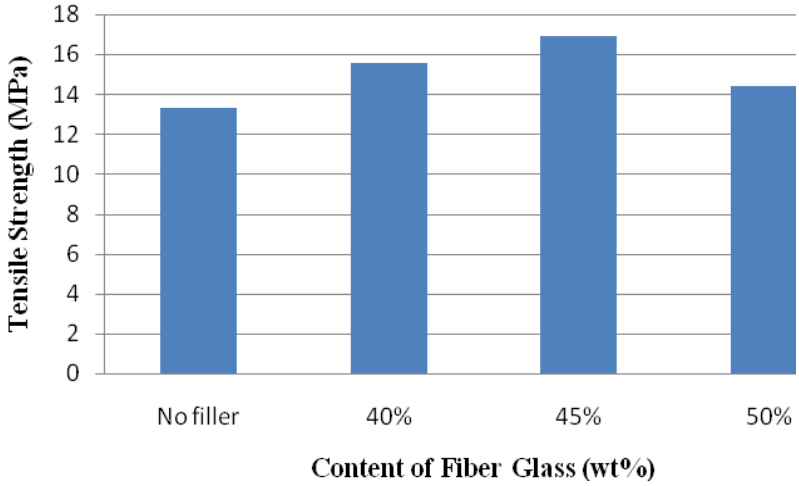


**Figure 4.9 Tensile-strength of recycled LDPE composites with the content of glass fibre**

The change in tensile strength of recycled LDPE composites with increasing glass fibre content is shown in Figure 4.9. Tensile strength gradually rises until the content of filler reaches 45 wt%, followed by a sudden drop between 45 and 50 wt%. Similar to the reinforcement effect of fine talc, growth rate is much higher between 40 and 45 wt% than between 0 and 40 wt%, as indicated by comparing the slope of the lines connecting these points. Although the specimens filled by 50 wt% glass fibres still have a higher tensile strength than unfilled samples, there will be a continued decline in tensile strength if addition of glass fibre exceeds 50 wt%.

Figure 4.9 demonstrates that the addition of glass fibre, up to concentrations of 45 wt%, helps matrix materials undertake more applied stress, while still retaining the same toughness. However, the mechanical properties start dropping after the glass fibre content exceeds 45 wt%. Thus it can be deduced that the optimum concentration of glass fibre for recycled LDPE in mechanical properties resides between 45 to 50 wt%.

*4.3.2.2 Morphology*

Images in Figure 4.10 illustrate the cross sections of each category of specimen after tensile testing. The magnification of images (a), (c) and (e) is 35X, whereas the others are magnified to 500X. Comparing the lower magnification images, more layer structures are observed in images (a) and (c), but the cross section of specimens filled by 50 wt% glass fibre in image (e) is in better order. This difference is due to the change in tensile strain among these three recycled LDPE composites. Images (b), (d) and (f) have clearer morphologies of cross sections. It is observed that fractured plastic fragments gather at the cross section in images (b) and (f), but in image (f) more glass fibres are localized in the same location. These observations indicate that plastic deformation occurs in specimens of recycled LDPE with 40 wt% and 45 wt% glass fibre prior to fracture. However specimens filled by 50 wt% glass fibre break at the joint between glass fibre and matrix without much plastic deformation while under tensile stress. This explains to the sudden drop in tensile strain when the content of filler changes from 45 wt% to 50 wt%.

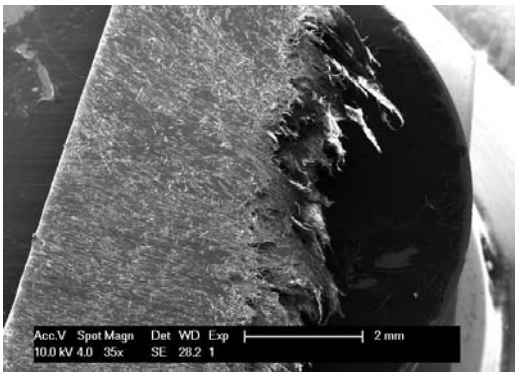


(a)Recycled LDPE-FG (40wt%) 35X

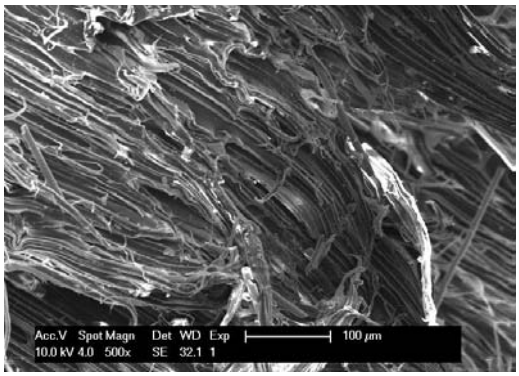


(b) Recycled LDPE-FG (40wt%) 500X

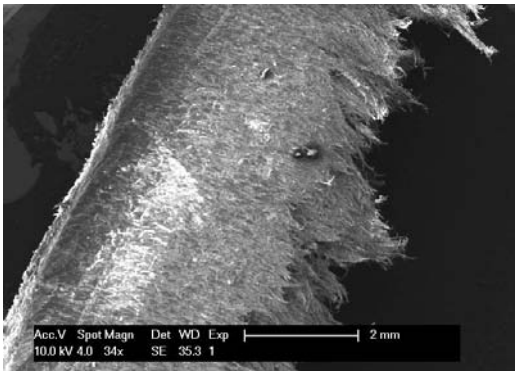


(c) Recycled LDPE-FG (45wt%) 35X

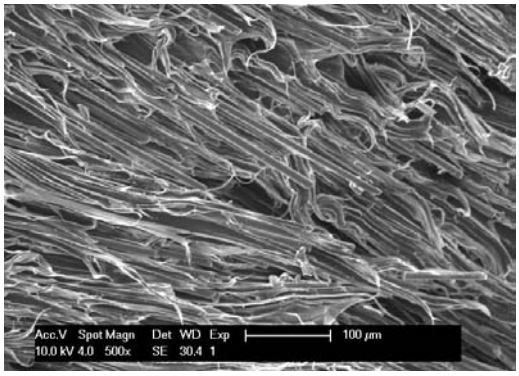


(d) Recycled LDPE-FG (45wt%) 500X

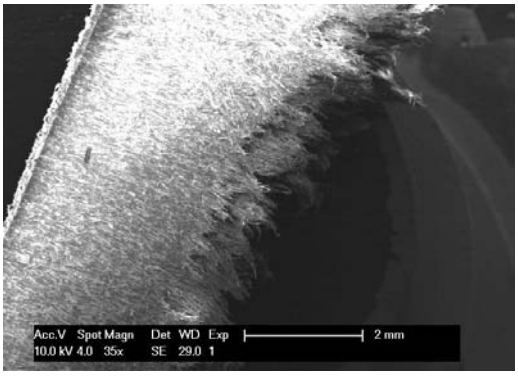


(e) Recycled LDPE-FG (50wt%) 35X

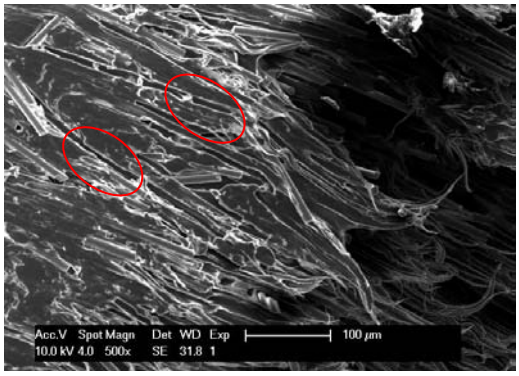


(f) Recycled LDPE-FG (50wt%) 500X

**Figure 4.10 SEM photographs of recycled LDPE filled by fibre glass (40, 45, 50 wt%)**

Images (b), (d) and (f) show that glass fibres are aligned, which allows them to share the tensile stress with the matrix material and improve the tensile strength of specimen. However, some flaws appear in the surface of sample with 50 wt% glass fibre, which have been annotated as circles in image (f). When the concentration of glass fibre reaches to 50 wt%, there would be not LDPE molecular chains to wrap each glass fibre. Thus, glass fibres are easy to slide past one another under the applied tensile stress, and some flaws come out in this situation. Since any minute surface flaws might deter the tensile properties, the tensile strength and (%) elongation of samples decrease significantly as the concentrate of glass fibre increases from 45 wt% to 50 wt%.

### 4.3.3 Comparison on the reinforcement effect between fine talc and glass fibre

A comparison between the reinforcement effect of glass fibre and fine talc is shown in Figure 4.11. It is clear that the use of glass fibre reinforces recycled LDPE more effectively than fine talc at the same filler concentration, when the content of filler is below 45 wt%. Although the tensile strength of specimens filled by 45 wt% glass fibre is still relatively higher than specimens reinforced by 50 wt% fine talc, it cannot be assumed that the maximum tensile strength is afforded by filling with glass fibre, because the optimal concentration of fine talc was not determined in these studies.

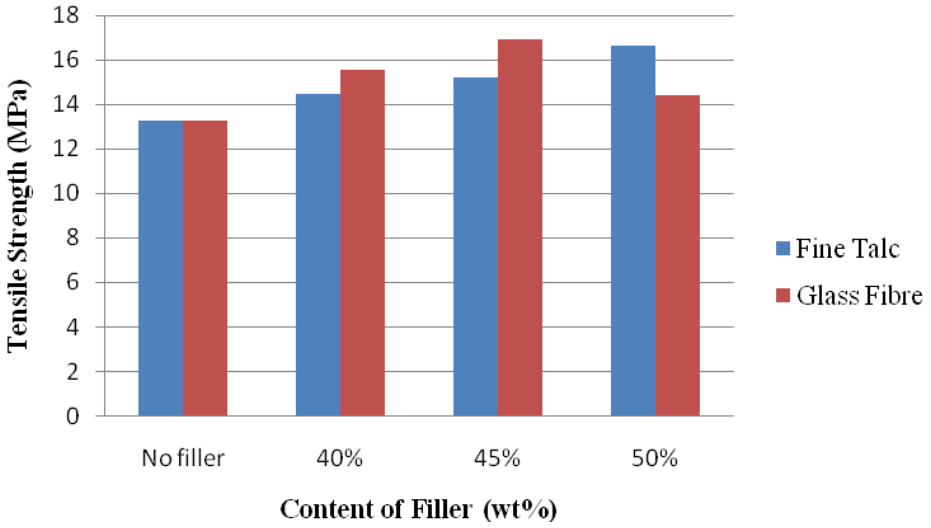


**Figure 4.11 Tensile-strength of recycled LDPE composites with the content of filler**

The growth rates of each reinforced specimen by filler are listed in Table 4.3 according to filler type. Particle filler can improve the degree of crystallinity of recycled LDPE, as well as its mechanical properties, by modifying its internal structure. However, fine talc cannot transform recycled LDPE into a crystalline material and the existence of amorphous molecular chains prevents improvements in tensile strength.

**Table 4.3 Growth rate in tensile strength of each reinforced specimen**

| **Content of Filler** | Fine Talc | Glass Fibre |
|---|---|---|
| 40 wt% | 8.8% | 17% |
| 45 wt% | 14.3% | 27.3% |
| 50 wt% | 25.2% | 8.2% |

As the fibre reinforcement agent, fibre filler can share stress from the matrix phase, which is effective on reducing the actual stress on recycled LDPE matrix. However, there is not enough matrix material in the specimens with too high concentration of glass fibres (more than 50 wt%); glass fibres would slip on the surface of samples under the applied tensile stress. Thus, it is important to keep the compact structure for recycled LDPE with glass fibres to obtain better mechanical properties.

## 4.4 WEATHERING EFFECTS ON THE COMPOSITES

Weathering factors include sunlight, temperature, moisture and microbiologic attack. Among these, sunlight is the most critical variable for plastic ageing, inducing photo-degradation and leading to a loss in mechanical properties. Additionally, temperature is important factor contributing to change in a plastic's properties. This section therefore focuses on these two parameters in analysing weathering effects on recycled LDPE composites.

### 4.4.1 UV radiation effects

Based on results from the sample control test, four kinds of specimens were selected for this aspect of this work: recycled LDPE (batch one) with no filler, with 30 and 35 wt% fine talc, and with 30 wt% glass fibre. The purpose of this test was to determine the effects of filler type and concentration on UV ageing by comparing mechanical properties of each kind sample after exposure under accelerated weathering condition. FTIR spectroscopy and SEM images were used to determine the degree of photo-degradation of specimens caused by UV irradiation.

#### *4.4.1.1 Mechanical Properties*

Tensile strength and (%) elongation bar charts of these four materials maintained at room temperature (23 $\pm$ 2 $^{o}$C) after exposure in the QUV chamber are shown in Figures 4.12 and 4.13.

A decrease in tensile strength with increasing exposure time was obtained for all samples.

However, the unfilled samples exhibit damage in response to UV at an earlier stage than other specimens. While the weathering process had little effect on their mechanical properties of the unfilled recycled LDPE initially, its tensile strength and (%) elongation dropped rapidly between weeks three and five. The tensile strength and (%) elongation of the third week samples had decreased by 47% and 39% respectively, as compared to initial samples. After five or six weeks of weathering, the mechanical properties of each sample tend to reach plateau point, resulting in increased brittleness (elongation is very low around 26%) and failure at lower loads (tensile strengths are around 2.5 MPa). From these data, it can be seen that the mechanical properties are in transition during weeks three and four, and are deteriorated from week five onwards.

For the LDPE composites reinforced by talc, the transition phase occurs later. LDPE samples with 30% talc begin to compromise their mechanical properties in the fifth week after weathering and plateau in the sixth week. On the other hand, the mechanical properties of the LDPE with 35% talc remained unchanged until the sixth week at which point, they exhibited a significant decrease followed by a plateau in week seven and eight. Thus, the properties' transition phase of the 35% talc-LDPE can be captured between the sixth and seventh week.

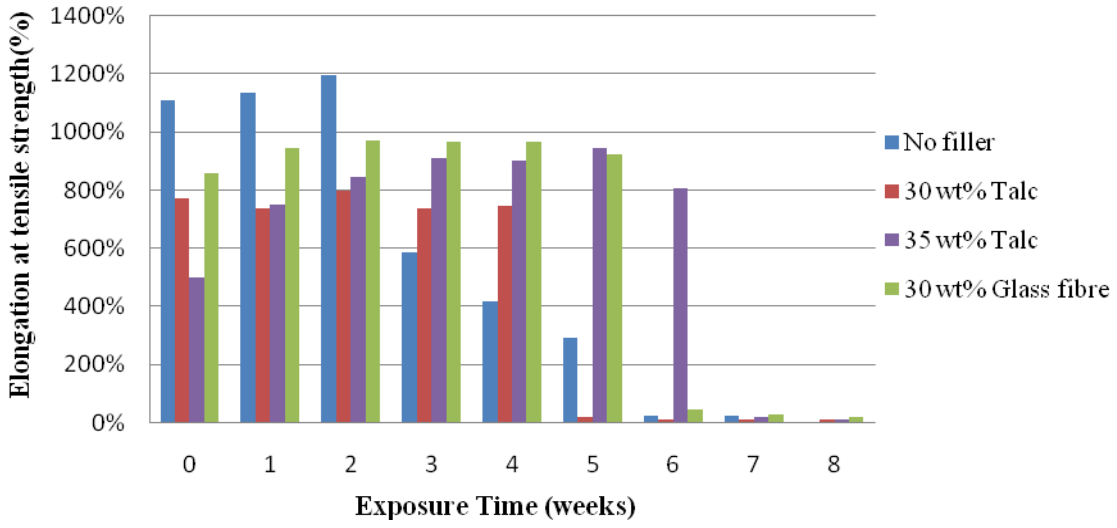


**Figure 4.12 Elongation at tensile strength (%) of recycled LDPE composites with various weathering exposure time**

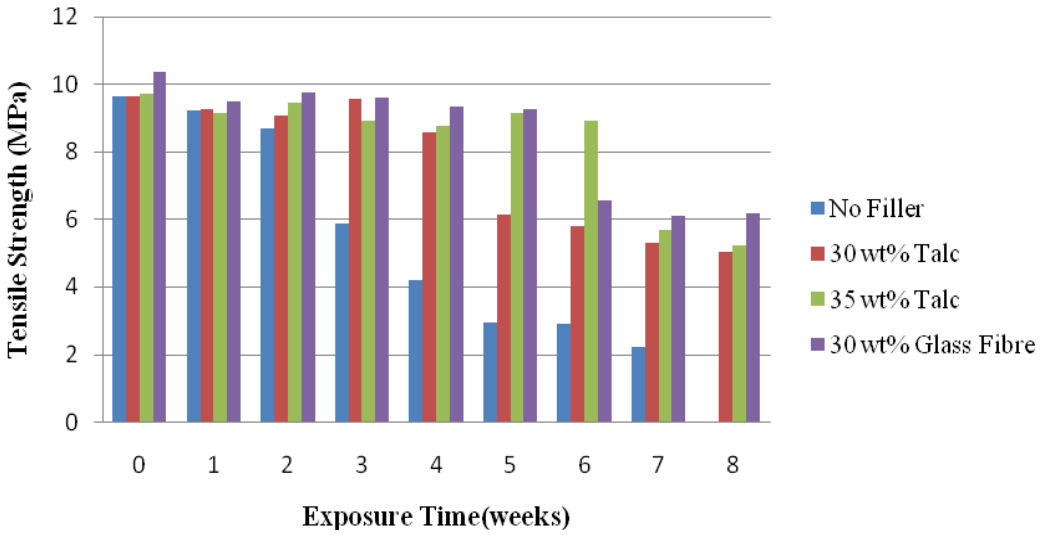


**Figure 4.13 Tensile strength of recycled LDPE composites with various weathering exposure time**

The difference between unfilled LDPE and LDPE with talc is noted not only at the onset of the transition phase, but also in the magnitude of tensile strength reduction. The tensile strength of recycled LDPE samples in the final stable stage decreased by 77% compared to the original. For the 30% talc-LDPE and 35% talc-LDPE there was a decline of 48% and 46%, respectively. The result indicates that the LDPE composites are more resistant to the effects of UV irradiation with the addition of fine talc.

Similar to other three materials, specimens reinforced by 30 wt% glass fibre also lost their mechanical properties after UV exposure. However, the presence of glass fibre was able to help the polymer matrix resist UV irradiation more effectively than the same concentration of talc, as shown in figure 4.12 and 4.13. In the first five weeks of the accelerated weathering test, no significant changes in (%) elongation and tensile strength were observed; however both of these values dropped suddenly when UV exposure was extended to six weeks. Sample stability reappeared again during the seventh and eighth weeks; however, demonstrating that the transition phase occurred during the sixth week, a slight delay as compared to that observed with the unfilled and talc-filled samples. Furthermore, the decrease rate in tensile strength of specimens reinforced by 30 wt% glass fibre is the lowest of these four samples, dropping merely 40% between the original stage and the final stable stage. It can therefore be stated that

glass fibre provides recycled LDPE with an increased capacity to resist UV ageing than does fine talc.

According to theoretical framework as presented in Chapter Two, chain scission is cited as the main reason for the loss of mechanical properties during the degradation process. However, the existence of fillers modifies the internal structure of matrix, which causes each specimen has their own characteristic in resisting photo-degradation ageing. The photo-oxidation reaction of these four types material can be investigated by analysing the results from FTIR spectra.

It should be mentioned that for all four kinds of recycled LDPE composites, (%) elongation slightly increases during the early stages of weathering. The increasing trend of unfilled specimens lasts for three weeks, which is slightly longer than others. These phenomena might be explained by crosslinking, which normally happens at the beginning of degradation process. This hypothesis also needs to be further proved by FTIR testing.

*4.4.1.2 FTIR spectroscopy analysis*

After specimens were exposed in the QUV chamber, FTIR spectrometry was used to characterize and quantify the oxidation products present within in the specimens. As mentioned in Chapter Two, the carbonyl index is an important parameter when evaluating the process of photo-oxidation in recycled LDPE composites.

Figure 4.14 shows the carbonyl index curves of the four samples following weathering. These data were processed from FTIR-ATR spectra. For unfilled recycled LDPE specimens, the carbonyl index increases with exposure time indicating that the oxidation reaction continuously occurs during the ageing process.

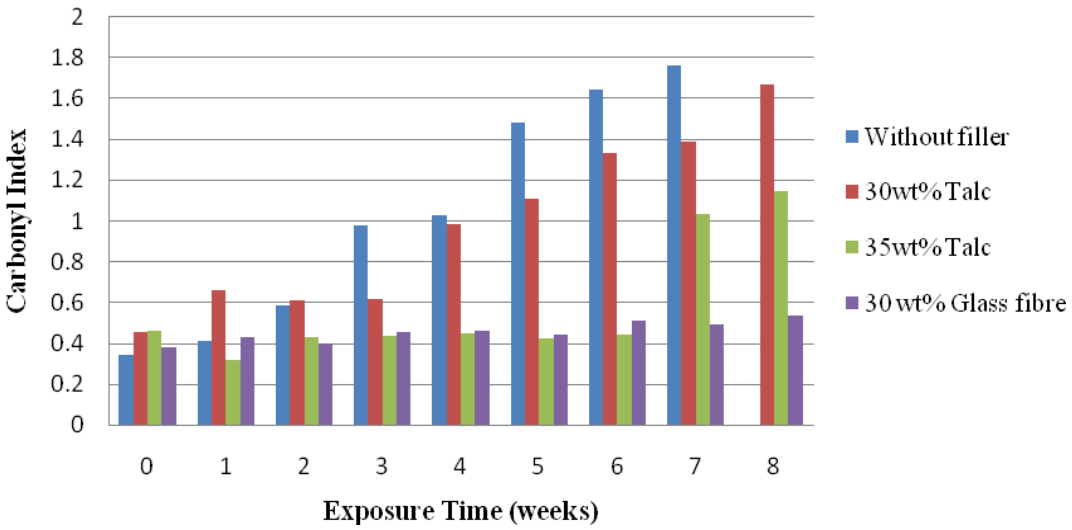


**Figure 4.14 Carbonyl indexes of recycled LDPE composites with different weathering exposure time**

Specimens reinforced by fine talc seem to be more stable than unfilled samples under the same weathering conditions. Almost no oxidation is detected for the 30 wt% talc-LDPE samples in the first three weeks of exposure, noted by the stability of the carbonyl index during the period. For 35 wt% talc-LDPE the carbonyl index remained unchanged until the seventh week. However, after the stable period, the photo-oxidation reaction takes place vigorously in both kinds of material. Since chain scission is the main cause for the increase in the carbonyl index, an increase in the carbonyl index theoretically leads to a reduction in mechanical properties during the ageing process. Figures 4.15- 4.17 show the relationship between the carbonyl index and tensile strength of the unfilled sample as well as those reinforced with talc, a relationship in which an increase in the former leads to a decrease in the latter in each case.

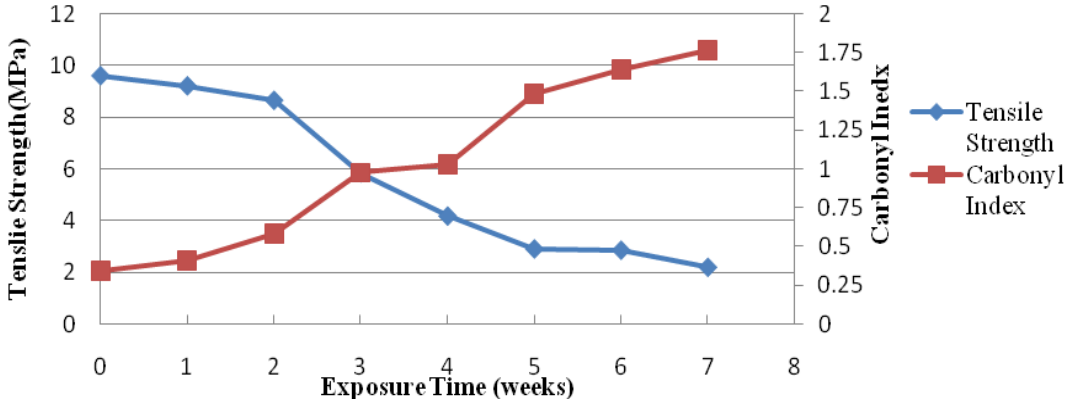


**Figure 4.15 Tensile strength and carbonyl index with exposure time for unfilled recycled LDPE**

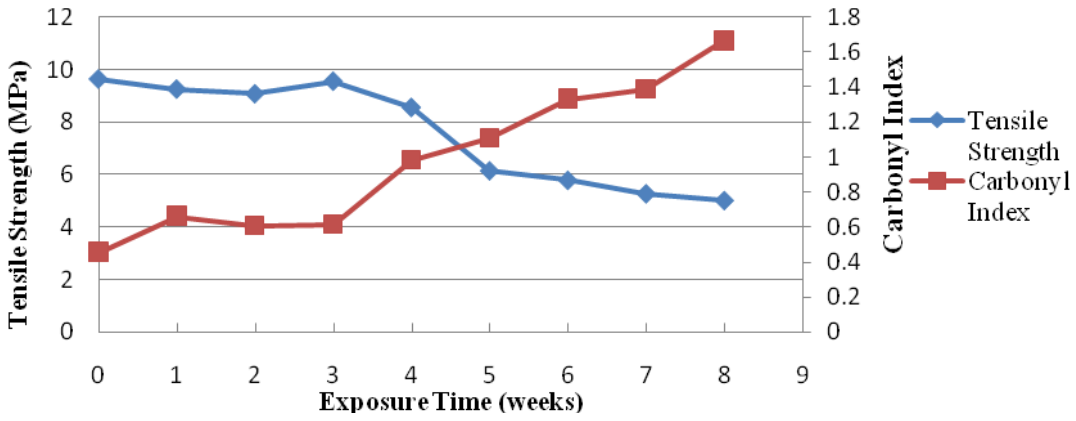


**Figure 4.16 Tensile strength and carbonyl index with exposure time for recycled LDPE with 30 wt% fine talc**

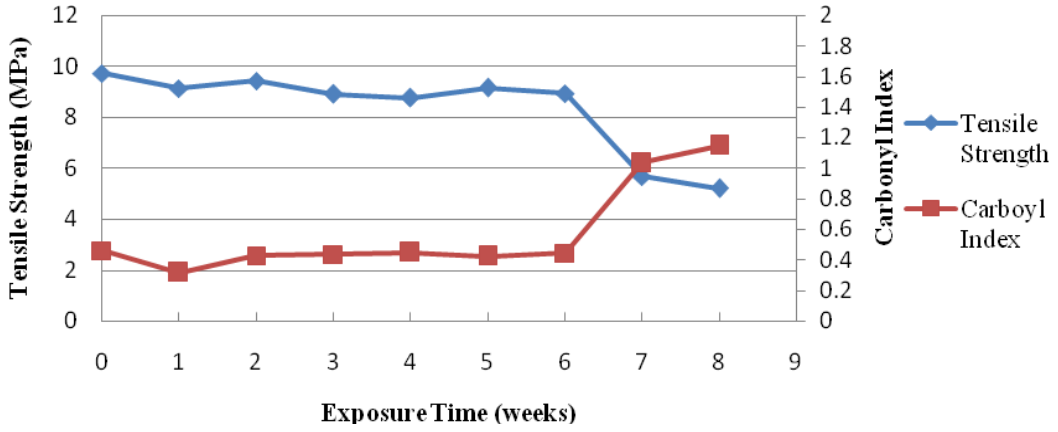


**Figure 4.17 Tensile strength and carbonyl index with exposure time for recycled LDPE with 35 wt% fine talc**

Conversely, when tensile strength increases slightly, the carbonyl index remains almost constant. These results suggest that crosslinking occurs at the beginning, preventing the formation of carbonyl in the ketone group. A number of researchers have demonstrated that photo-oxidation is the main cause of the loss in mechanical properties for unfilled and fine talc-reinforced specimens [16, 30, 33]. Moreover, fine talc has played a role in delaying chain scission, and increasing the concentration of fine talc provides a longer stable phase before mechanical property loss.

The discussion above does not necessarily apply to other specimens such as those filled by 30 wt% glass fibre, because the change in carbonyl index for these specimens is obviously different than to the other three materials. With increased exposure time, the carbonyl index of recycled LDPE reinforced with 30 wt% glass fibre increased only slightly, indicating that less photo-degradation occurred in the sample. However, the change of carbonyl index is still in accordance with the alteration of mechanical properties. Figure 4.18 shows the change of tensile strength and carbonyl index with increasing time in the QUV weathering machine. Both parameters remained stable for the first five weeks of exposure, but a slight increase in carbonyl index at the sixth week led to a sudden decrease in tensile strength.

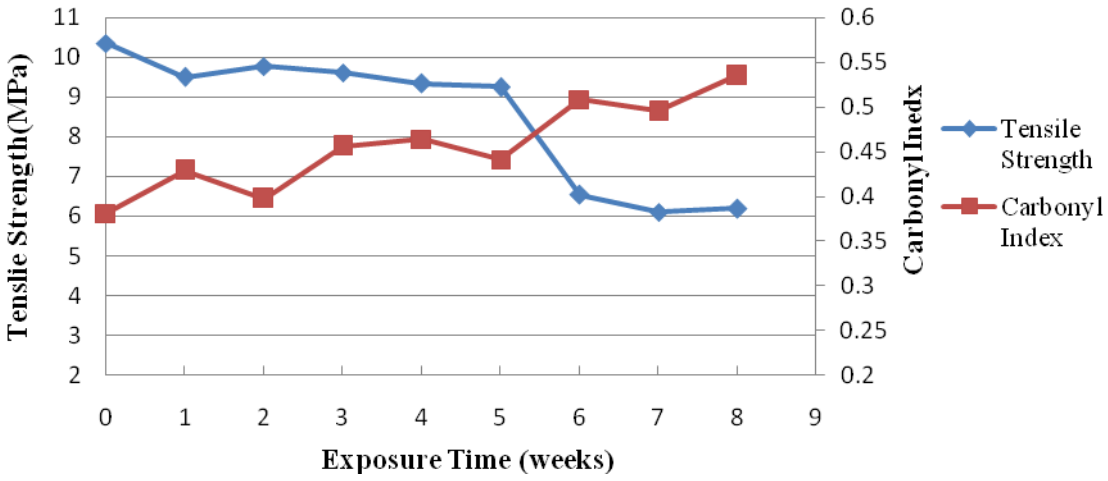


**Figure 4.18 Tensile strength and carbonyl index with exposure time for recycled LDPE with 30 wt% glass fibre**

For the other three specimens, the distinct growth of the carbonyl index over time may explain the decrease observed in tensile strain and strength. Although it is noted that glass fibre can prevent the damage from UV irradiation effectively, a significant decrease in the mechanical properties was detected at weeks seven and eight of the weathering test, indicating that the mechanical properties of specimens filled by glass fibre are very sensitive to photo-degradation. This hypothesis was verified by morphological analysis, as described in the following section.

*4.4.1.3 Morphology*

Figure 4.19 shows the changes in surface morphology of the unfilled LDPE specimen upon exposure to accelerated weathering conditions. Prior to the weathering test, the surface of the recycled LDPE samples looks almost smooth, as shown in image (a). However, with continued weathering, more and more cracks appear on the surface, a phenomenon which can be seen in images (b) and (c). In image (b), it is obvious that a large number of cracks are arranged randomly on the surface, dividing the specimen into small segments. However, when the accelerated weathering test reaches the seventh week, the surface cracks seem to be more aligned, as shown in image (c) which displays some deep lineal cracks along with numerous shallow gaps among the cracks. These two kinds of morphology can be regarded as being caused by photo-degradation.

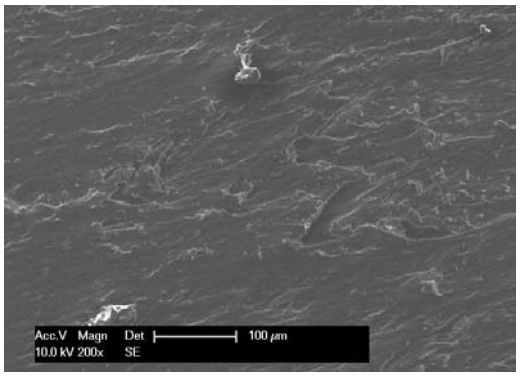


a. Without UV

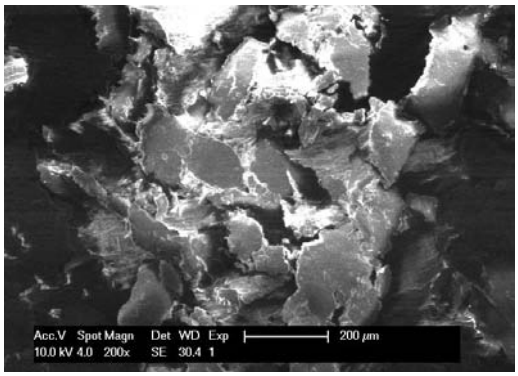


b. 4 weeks' weathering

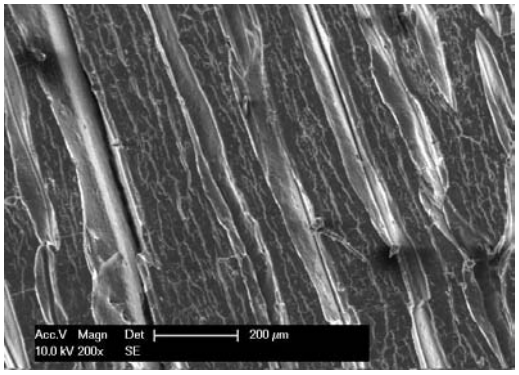


c. 7 weeks' weathering

**Figure 4.19 SEM surface photographs of specimen without filler after weathering**

Photo-degradation reactions can alter a material's structure in two ways: (i) crosslinking or (ii) chain scission. In the accelerated weathering test, a sample's molecular weight decreases constantly with the continuing of chain scission, and the polymer chains break into smaller molecular units. Thus some block structures appear in the fourth week. Since the polymer chains with the lower molecular weight do not easily entangle with other chains, the cracks on the surface would appear ordered, as in Figure 4.19 image(c). These images prove the decrease of molecular weight during the photo-degradation process. The loss of mechanical properties might be caused by the cracks on the sample surface as well.

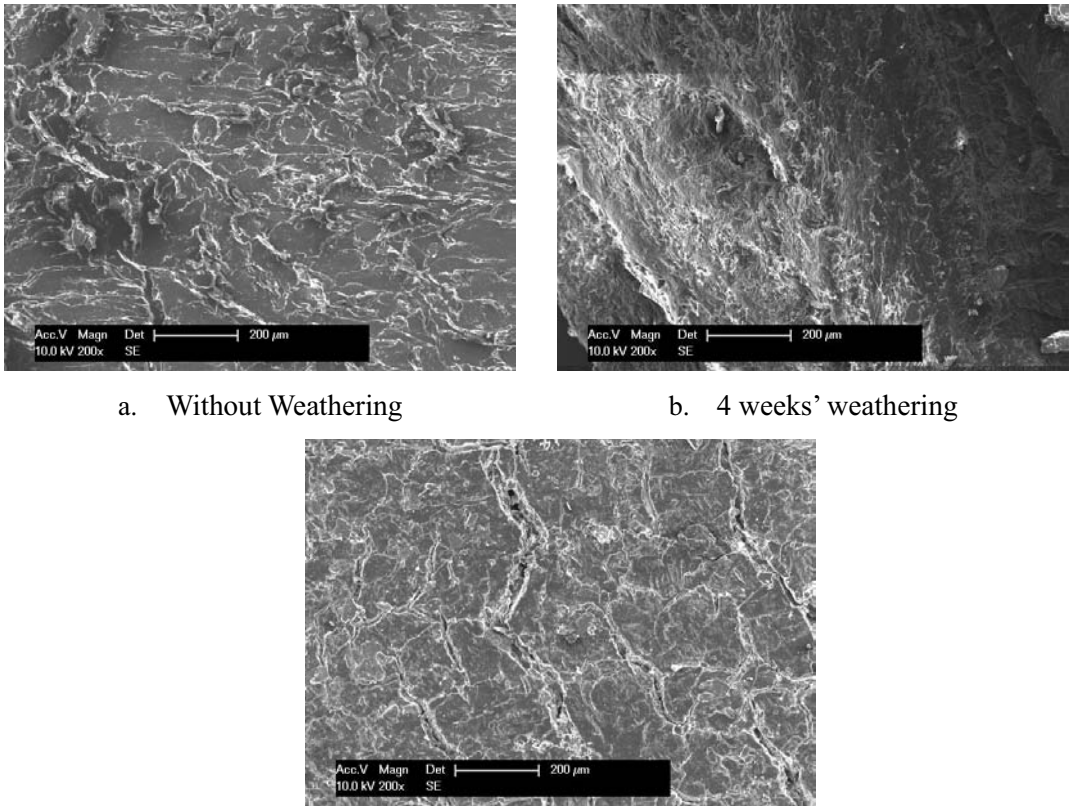


a. Without Weathering

b. 4 weeks' weathering

c. 7 weeks' weathering

**Figure 4.20 SEM surface photographs of specimen with 30 wt% fine talc after weathering**

Surface images of specimens reinforced by fine talc after weathering test are shown in Figure 4.20. Since fine talc effectively improves the degree of crystallinity, the surface of the specimen before the accelerated weathering test has a blocky structure instead of a linear one (Figure 4.20 (a)). For the first several weeks, there is no discernible change in the surface morphology, but by the seventh week of exposure in the QUV machine, some cracks appear on

the sample surface. It is clear in Figure 4.20 image(c) that the cracks are propagating along the bonding lines of each blocky structure. Since oxygen is difficult to enter into the compact crystalline structure, the photo-degradation takes place easily in amorphous structure. This theory can be used to explain why photo-degradation happens in gaps among crystalline units in advanced; and there is no significant damage on the crystalline structure. Considering less photo-degradation occurs in specimens reinforced by fine talc, these specimens still maintain a high tensile strength than unfilled samples.

The following SEM images (Figure 4.21) present the surface morphologies of recycled LDPE reinforced by 30 wt% glass fibre undertaken at different periods of the weathering test, from time zero (a) to eight weeks of exposure (d).

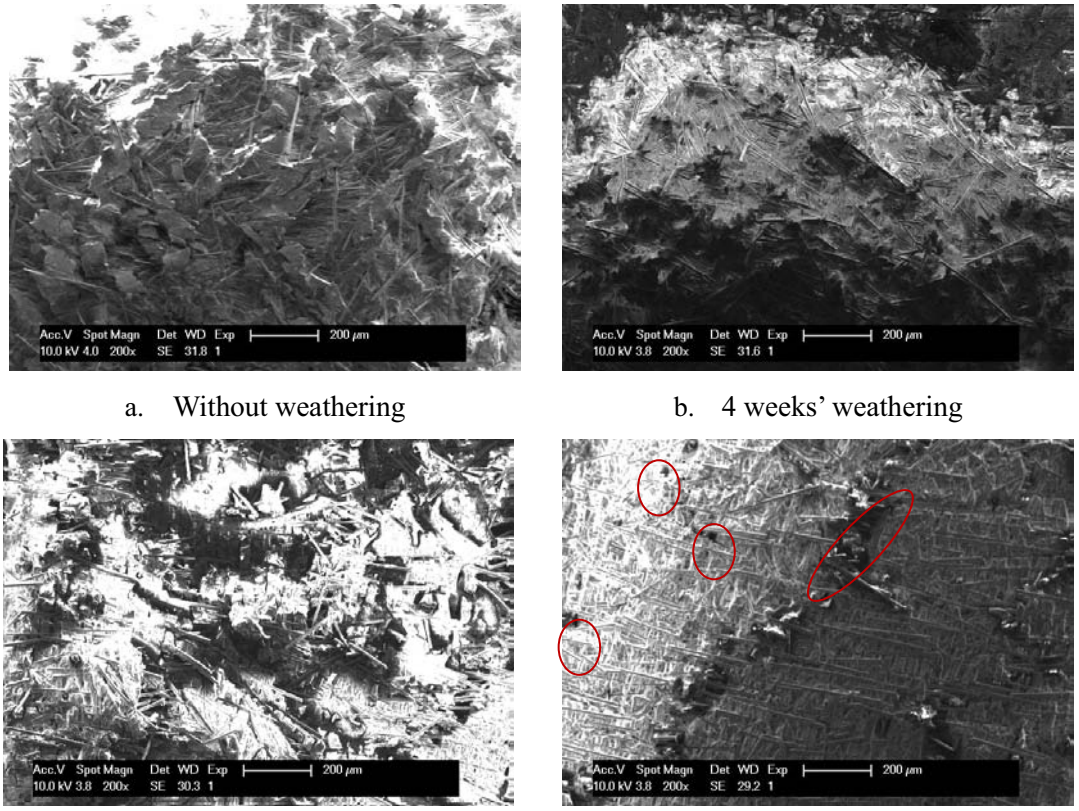


a. Without weathering

b. 4 weeks' weathering

c. 7 weeks' weathering

d. 8 weeks' weathering

**Figure 4.21 SEM surface photographs of specimen with 30 wt% glass fibre after weathering**

Before the weathering test, the glass fibres are randomly oriented on the surface. Considering the length of the glass fibres, the matrix is unable to connect with them properly, resulting in some gaps on the surface among fibres and matrix. Furthermore, it is observed that glass fibres almost cover the whole surface of specimens, acting as a protective layer. It can thus prevent exposure of the polymer surface to direct UV irradiation, slowing down the photo-degradation reaction. This phenomenon explains the reduction in the carbonyl index in specimens filled by glass fibre upon weathering.

In the first several weeks of weathering, given that there is no significant photo-degradation, very little difference can be seen between images (a) and (b). However, by the seventh or eighth week, the alignment of the glass fibres on the surface has changed. In image (c), although the matrix surface still appears rough, most of the glass fibres seem aligned. This situation is similar to that observed with unfilled samples, where it was caused by a reduction in the species' molecular weight. Since LDPE molecules with lower molecular weight cannot easily entangle the glass fibres, the glass fibres would all move in the same direction under the applied tensile stress. However, a distinct change can be seen in image (d), taken after the specimens had been in the QUV machine for eight weeks. The specimen's surface in this instance was much smoother than the other samples', and the glass fibres are all oriented in a single direction. While glass fibres cover most of the specimen surface, uncovered parts, particularly those in the cross sections between the glass fibres and the matrix, would undertake serious damage by UV irradiation. It is obvious that some cavities and cracks appear on the surface after eight weeks of weathering, as highlighted by red circle in image (d). Such cracks and cavities would reduce tensile strength and strain rapidly, attributing to a quick loss in mechanical properties under low photo-degradation.

Figure 4.21 demonstrates the change in glass fibre alignment during the accelerated weathering test. However, tensile strength of specimens filled by glass fibre is still higher than other composites, because UV irradiation cannot weaken the ability of glass fibres in sharing tensile stress for matrix.

*4.4.1.4 Reinforcement effect of recycled LDPE composites on resisting the accelerated weathering*

A series of experimental results obtained via different analysing techniques indicate that the internal structure of specimens, which can be altered by the use of different reinforcing fillers, directly influence the ability of recycled LDPE composites to resist accelerated weathering.

The following table, Table 4.4, shows the crystallization properties of recycled LDPE (batch one) with no filler and filled with talc. Since recycled LDPE mainly comes from packaging materials, it is difficult to control the molecular weight and structure of each molecular chain. Thus recycled LDPE has the lowest crystallization temperature and degree of crystallization. Crystallization properties of the matrix also suggest that amorphous molecular chains comprise the main structure of unfilled specimen, thus allowing oxygen easy access into the polymer structure and accelerating the rate of photo-degradation. The unfilled recycled LDPE is susceptible to photo-degradation in the accelerated weathering test, while the other three samples tested, the filled composites, are photo-degradation resistive.

**Table 4.4 Crystallization properties of recycled LDPE filled by talc**

| | Unfilled | 30 wt% | 35 wt% |
|---|---|---|---|
| Crystallization Temperature Peak ($^{o}$C) | 128.0 | 128.9 | 129.0 |
| Heat of Crystallization (J/g of LDPE) | 24.9 | 35.6 | 41.04 |
| Degree of Crystallinity | 9% | 12% | 14% |

It has been shown that fine talc is a strong nucleating agent for polymer materials, a characteristic that was demonstrated during its use as a reinforcement agent for recycled LDPE. The crystallization properties' improvement due to the presence of talc is evident in Table 4.4. Due to the higher degree of crystallinity, molecular chains are packed together tightly, preventing oxygen from entering into the internal structure of the specimens. This greatly reduces photo-degradation upon UV irradiation. Therefore, fine talc is able to extend the

lifespan of recycled LDPE under conditions of accelerated weathering. Furthermore, increases in fine talc concentration yield a higher degree of crystallinity, thus decreasing the photo-degradation reaction more effectively, and helping maintain a longer life span.

Although glass fibres seem to have no influence on the specimens' internal structure, they provide a protective film which helps the matrix maintain its mechanical properties better than other three composites. Table 4.5 shows the change rate of each specimen in tensile strength and carbonyl index after seven weeks' accelerated weathering test. In these four materials, specimens reinforced by 30 wt% glass fibre present the minimum change in both tensile strength and carbonyl index. In other words, the surface protection lowers the damage of photo-degradation to a larger extent, and also keeps the mechanical properties more stable than does altering the internal structure.

**Table 4.5 The change rate in tensile strength and carbonyl index at seven weeks' accelerated weathering test**

| | No filled | 30 wt% Talc | 35 wt% Talc | 30 wt% Glass fibre |
|---|---|---|---|---|
| Tensile strength | 77% | 45% | 42% | 41% |
| Carbonyl index | 413% | 206% | 125% | 40% |

Several conclusions can be drawn from these results and comparisons. Firstly, the decrease in molecular weight caused by the photo-degradation process leads to a loss in the mechanical properties of the plastic composites. Secondly, fine talc slows down the process of photo-degradation by improving the degree of crystallinity of recycled LDPE. In addition, high concentration of fine talc provides higher resistance against weathering. Finally, specimens reinforced by glass fibre are suitable for resisting accelerated weathering, due to the unique protection layer afforded by this reinforcing agent.

### 4.4.2 Temperature effects

Polymeric materials are well known in term of its sensitivity to temperature and display varying mechanical properties with change in temperature. In order to study the effects of temperature on the recycled LDPE composites, samples were first heated in the environmental chamber at various temperature conditions (i.e., -20$^{o}$C, 0$^{o}$C, 20$^{o}$C, 40$^{o}$C, 60$^{o}$C and 80$^{o}$C) and then subjected to tensile testing.at those temperatures. The specimens that were selected for testing are: recycled LDPE, recycled LDPE with fine talc (40, 45 and 50 wt%) and recycled LDPE with glass fibre (40, 45 and 50 wt%).

*4.4.2.1 Temperature effects on recycled LDPE reinforced by fine talc*

Figure 4.22 illustrates the changes in tensile strain for each specimen with increasing temperature. Recycled LDPE seemed to be more sensitive to temperature than other composites when environmental temperature is lower than room temperature (20$^{o}$C). At higher temperature, the elongation of recycled LDPE specimens deformed samples which reached the maximum allowable length within the environmental chamber before they fractured. Because of this equipment constraint, the actual (%) elongation at tensile strength of the samples at 40, 60 and 80$^{o}$C are likely higher than that shown in Figure 4.21. Thus it can be assumed that the curve representing specimens without filler would continue to increase rather than reaching a plateau.

For specimens reinforced by fine talc, temperature below 40$^{o}$C had no significant influence on (%) elongation. However, when the testing temperature was higher than this, the elongation of specimens increased slightly. Additionally, higher concentrations of fine talc were useful in assisting to maintain a stable (%) elongation with increasing temperature.

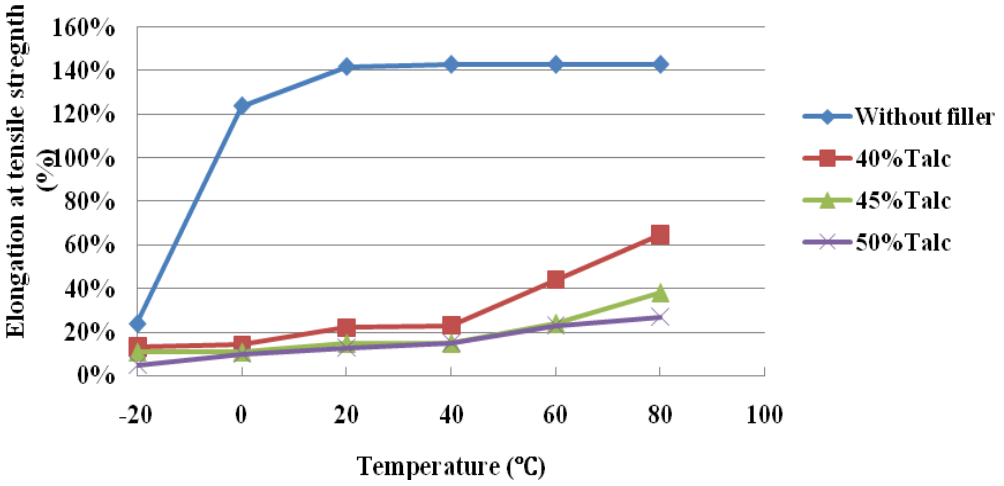


**Figure 4.22 Elongation at tensile strength (%) of recycled LDPE reinforced by fine talc with the increase of temperature**

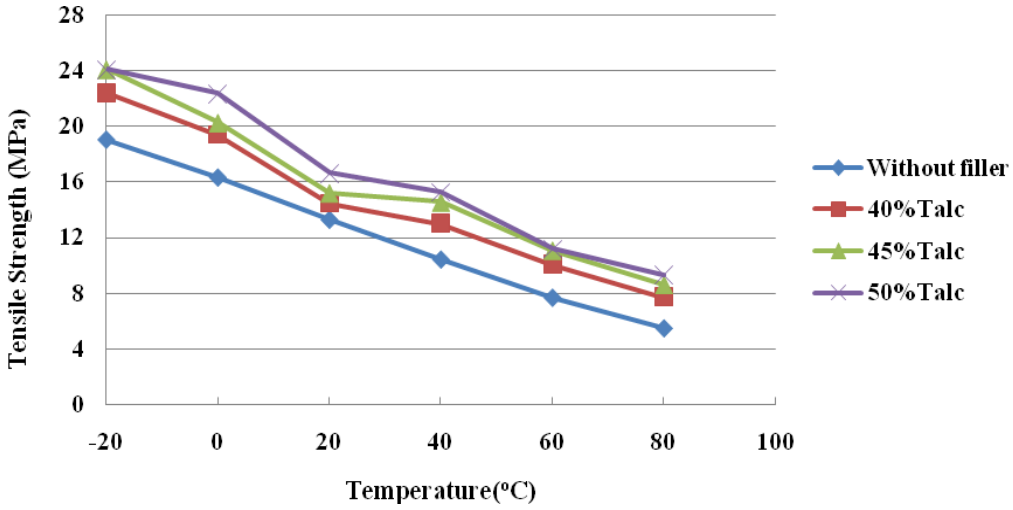


**Figure 4.23 Tensile strength of recycled LDPE reinforced by fine talc with the increase of temperature**

Figure 4.23 shows how the tensile strength of each specimen changes with temperature. All of tensile strength curves indicate a linear decrease with increasing temperature; given this result, it is difficult to determine which sample can maintain tensile strength stability most effectively under various temperatures. Table 4.6 illustrates the rate of change of tensile strength as a function of temperature for each sample, as compared to the value obtained at room temperature. Positive values indicate an increasing rate, while negative values represent decreases. When the temperature is below 20°C, the rate of increase in specimens reinforced with fine talc is higher than that of unfilled samples. This is highlighted by the matrix sample

supplemented with 45 wt% talc, where the change rate was 59% at -20°C. However, this increase rate did not continue with increasing talc concentration. Tensile strength of specimens with 50 wt% talc were equivalent to that of 45% sample, and was very similar to the result obtained with the unfilled samples.

When the testing temperature is higher than 20°C, the unfilled samples had greater losses in tensile strength than did the other specimens. When compared to (%) elongation achieved at 20°C, the rate of unfilled samples at 80°C was 59%, while that for the talc-reinforced samples was around 45%. Furthermore, among the reinforced samples, 45 wt% seemed to be the optimum concentration in resisting the effect of high temperature, as this sample's tensile strength was much more stable than the others' at 40, 60 and 80°C.

**Table 4.6 The changing rate of tensile strength in the different temperature compared with room temperature (20 °C )**

| | Without Filler | 40 wt% Talc | 45 wt% Talc | 50 wt% Talc |
|---|---|---|---|---|
| -20 °C | 43% | 55% | 59% | 45% |
| 0 °C | 23% | 34% | 33% | 34% |
| 20 °C | 0 | 0 | 0 | 0 |
| 40 °C | -22% | -10% | -4% | -8% |
| 60 °C | -42% | -30% | -27% | -33% |
| 80 °C | -59% | -47% | -43% | -44% |

These tensile strength and (%) elongation indicate that fine talc can reinforce the polymer matrix most effectively at lower temperatures, but can also reduce the influence of high temperatures on the samples' mechanical properties. The differences in the ability of these samples to resist temperature effects can be attributed to changes in internal structure.

Unfilled recycled LDPE is predominantly amorphous in structure with molecular chains occupying the greatest part of these specimens. Molecular chains are held together by van der Waals forces, but these bonds are sensitive to temperature. At higher temperatures, the activities of molecular chains increase significantly, possibly weakening van der Waals bonding. With these intermolecular forces decreasing, specimens cannot undertake the higher tensile stress than room temperature, which leads to the reduction of tensile strength. On the contrary, amorphous structure can obtain more elastic deformation at higher temperatures, potentially leading to increases in tensile strain. However, at temperature below $0^{o}C$, the environmental does not provide enough energy for the material, causing a reduction in the activities of the molecular chains. Thus, a slight increase in the tensile strength of recycled LDPE could cause a significant decrease in tensile strain.

As highlighted in section 4.3.1, the degree of crystallinity of a recycled LDPE sample can be improved by increasing the content of fine talc. Based on that hypothesis, more crystalline structures are assumed to appear in specimens instead of amorphous molecular chains in the semicrystalline polymer. Although crystalline units and amorphous molecular chains are both held together by van der Waals bonds, a more compact structure reduces the activity of each molecular chain at high temperatures. Since the crystallization temperature of recycled LDPE is higher than $100^{o}C$, the crystalline structure within the polymer composites were not damaged by these tests, which were conducted at temperatures lower than $100^{o}C$. Thus, van der Waals forces among the crystalline units were unchanged; the high temperature, however, did have an adverse effect on the amorphous molecular chains. This was noted when comparing the unfilled samples with those filled with talc; a latter would have fewer amorphous molecular chains leading to less movement in molecular chains, therefore reducing the influence from higher temperature. Thus, a compact structure will lead to higher tensile strength and lower tensile strain.

These experimental results and their analyses suggest that fine talc can improve the ability of recycled LDPE to maintain stable mechanical properties at different temperatures by increasing the degree of crystallinity of the matrix.

*4.4.2.2 Temperature effects on recycled LDPE reinforced by glass fibre*

Tensile tests of recycled LDPE samples reinforced with glass fibre were carried out using the sample temperature range as that employed for fine talc: namely -20°C to 80°C. The results of the tensile testing are shown in Figures 4.24 and 4.25.

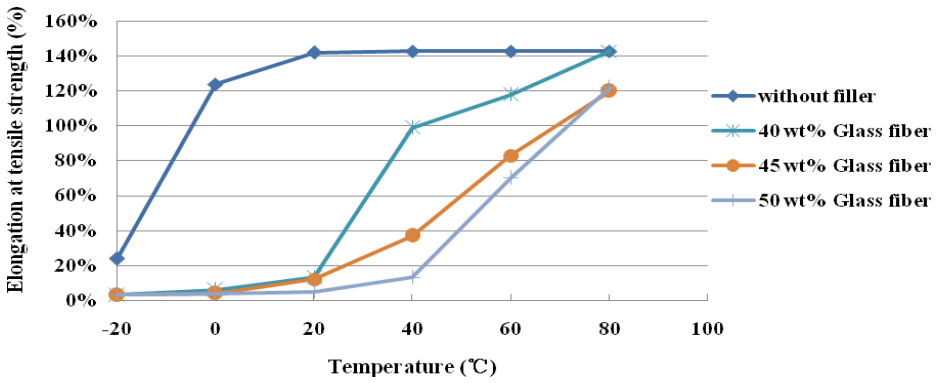


**Figure 4.24 Elongation at tensile strength of recycled LDPE reinforced by glass fibre with the increase of temperature**

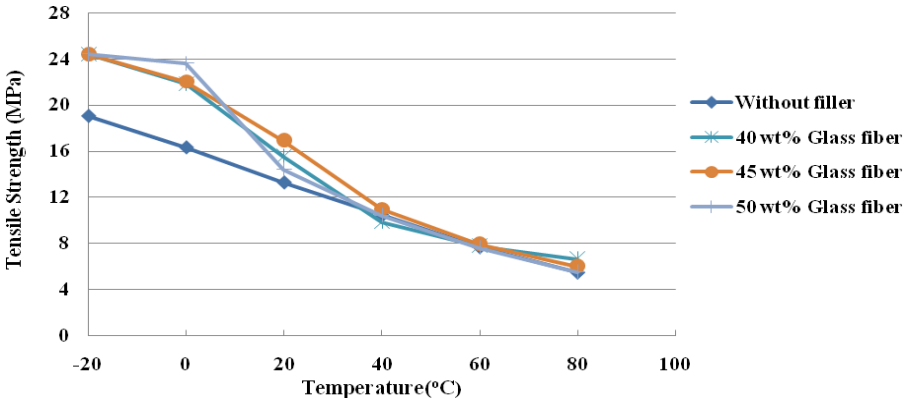


**Figure 4.25 Tensile strength of recycled LDPE reinforced by glass fibre with the increase of temperature**

At room temperature (20°C), the tensile strength of specimens filled by glass fibre is much higher than that of unfilled samples, as shown in Figure 4.25. However, filled samples present various characteristic under a range of temperatures. When the environmental temperature is below 20°C, the stiffness of glass fibre filled specimen increases, a trend which was noted in unfilled and fine talc filled specimens. The maximum load of the INSTRON 5543 is 1 KN; however, the specimens filled by glass fibre can undertake tensile stress greater than this value at - 20°C. Thus, the tensile strength and (%) elongation at - 20°C that are shown in Figures 4.24

and 4.25 are values obtained at 1KN tensile stress, and may not reflect the true values at this temperature. Because of this equipment limitation, the tensile strength and (%) elongation at $0^oC$ were used to determine the materials' characteristics at low temperature. Compared with unfilled samples, the glass fibre filled samples displayed around 5% elongation before their fracture. However, the increases in tensile strength are obvious. The growth rate of the 40, 45 and 50 wt% samples reached 40%, 30% and 64% at $0^oC$, respectively, relative to the tensile strength at $20^oC$. As each of these values is much higher than that obtained using unfilled samples, it can be concluded that the reinforcing effects of glass fibre on tensile strength are more effective at lower temperature; it must be noted, however, that the specimens become much more brittle under such conditions.

On the contrary, specimens filled with glass fibre are not stable in the high temperature range. When temperature increased to above $40^oC$, the tensile strength of samples dropped rapidly. Figure 4.25 shows that each specimen tested displayed almost identical tensile strengths at $60^oC$ and $80^oC$. In other words, the glass fibres lost their ability to effectively reinforce the polymer samples at high temperatures. At the same time, the filled specimens tended to get softer with increasing temperature, leading to increasing in (%) elongation, behavior which is analogous to that of unfilled specimens. Thus it could be concluded that high temperatures adversely affect recycled LDPE reinforced with glass fibre.

The compactness between matrix and glass fibres plays an important role in the reinforcement effect of glass fibre. Since the activity of molecular chain changes with temperature, recycled LDPE composites display different compactness at various temperatures.

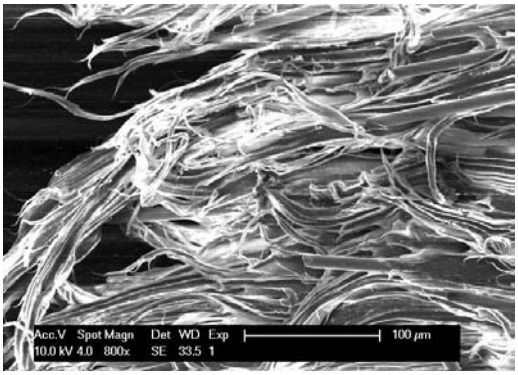


(a) 0°C

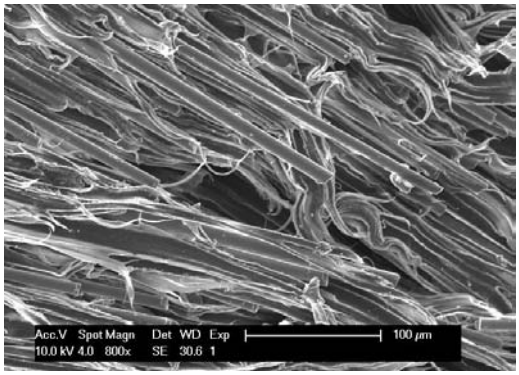


(b) 20°C

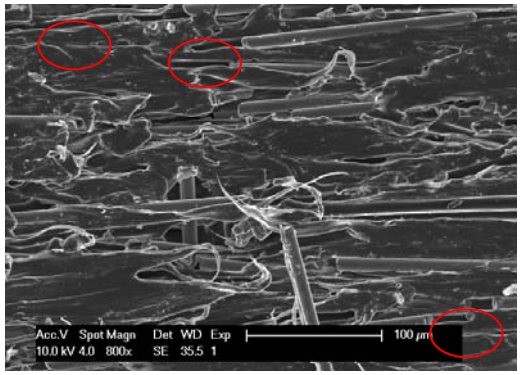


**(c) 80°C**

**Figure 4.26 SEM images of cross section at fracture point in the different temperature**

Specimens with 45 wt% glass fibre were selected to examine changes in structure compactness with temperature. Figure 4.26 shows the SEM images of the specimens' fracture surfaces at 0°C, 20°C and 80°C. Image (b) clearly shows that some glass fibres and fractured LDPE on the fracture surface, and demonstrates that these two materials pack tightly when the tensile test is operated at 20°C. The LDPE matrix is stable at room temperature, and wraps glass fibres at a suitable strength. The compactness at 20°C, therefore, can be a standard to which other specimens at different temperatures are compared.

Image (a) in Figure 4.26 shows the surface condition of specimens fractured at 0°C. Compared with image (b), almost no glass fibre is observed at the fracture point, and the recycled LDPE wraps the fibres more tightly than at 20°C, because the cooler test condition reduces the size of gaps between molecular chains and fillers. In this situation, glass fibres cannot slide in the matrix when undertaking tensile stress, which is useful in improving the tensile strength of

specimens. Furthermore, the small gaps improve the intensity of van der Waals bonding, allowing the matrix to undertake more tensile stress.

The surface condition of specimen at 80$^{o}$C is shown in image (c), and seems to be smooth as compared to the other two images. No obvious entanglement between the matrix and fibres is observed, which could be explained by the activity of molecular chains. High temperatures provide energy to molecular chains, increasing their activities as well as stretching the distance between molecules. Loose internal structure increases probability of fibres' movement in the matrix, which can be proved by image (c). The cavities highlighted within the red circles in image (c) are the vestiges after fibres' sliding. Since it is easy for glass fibres to slip into matrix under high temperature, they are not able to divert the tensile stress from matrix, thus losing their reinforcement ability. These factors explain the rapid loss in mechanical properties observed at high temperatures in glass fibre filled samples.

In conclusion, glass fibre can strengthen the mechanical properties of recycled LDPE at temperatures below 20$^{o}$C, but leads to significant weakening of specimens at high temperatures. So while fibre glass provides higher tensile strength for recycled LDPE at room temperature, fine talc can help matrix stability with changes in temperature.

# CHAPTER 5 CONCLUSION

The following conclusions can be drawn from this study:

- The mechanical properties of recycled LDPE are not consistent between batches because of the inevitable introduction of impurities during the recycling process. It is therefore necessary to analyze the content and characteristics of recycled materials before using them in practical applications.
- Fine talc is able to improve the mechanical properties of recycled LDPE. In addition, increase in concentration of fine talc provides the excellent reinforcement effect, when the content of filler ranged from 0 to 50 wt%.
- Glass fibre can effectively reinforce recycled LDPE and this reinforcement effect increases with the growth of the glass fibre's content up to concentration of 45 wt%.
- When used at the same concentration, glass fibre provides recycled LDPE with higher mechanical properties than fine talc.
- In accelerated weathering conditions, both fine talc and glass fibre can help recycled LDPE resist photo-degradation, and extend the life span of matrix, though the latter is able to prolong the original properties longer than the former. However, the life span can be extended with fine talc simply by increasing its concentration in the polymer composite.
- The addition of fine talc to recycled LDPE provides the polymer with the ability to resist influences of varying temperatures, though slight differences were noted in mechanical properties at the different testing temperature.
- Specimens with glass fibre show more sensitivity to temperature than other specimens. At lower temperature (< $20^{o}$C), the effectiveness of glass fibre for recycled LDPE is higher than that at room temperature ($20^{o}$C). However, specimens with glass fibre lose mechanical properties faster when testing temperature is higher than $20^{o}$C.

# CHAPTER 6 RECOMMENDATIONS

Based on the understanding gained from this study, some related aspects requiring further research have become apparent. There are summarized as follows:

- The existence of impurities limits the application of recycled plastic. Therefore, methods to identify recycling methods capable of improving the purity of recycled materials should be investigated.
- The optimum concentration of fine talc filler should be investigated, as it was not achieved from the conditions examined in this work. Doing so could lead to improvements in the maximum tensile strength that recycled LDPE composites can achieve.
- The addition of anti-aging agents to the recycled LDPE composites should be considered, thus investigating the span life of these new composites.
- It is recommended to find an additive for recycled plastics which would allow an improvement in the stability of specimens filled by glass fibres at higher temperature.

# REFERENCE


1. PACIA, *2008 National Plastics Recycling Survey (2007 Calendar Year) Main Survey Report.* 2008.

2. F. P. La Mantia, *Effect of fillers on the properties of recycled polymer.* Macromol. Symp, 2003(194): p. 101-110.

3. J. Stepek, H.Daoust, *Additives for plastic*. 1983, New York: Springer-Verlage.

4. W.Schnabel, *Polyemer degradation: principle and practical application* 1981: Munchen : Hanser.

5. H. D. Putra, Y. Ngothai, T. Ozbakkaloglu, R. Seracino, *Mineral filler reinforcemnet for commingled recycled plastic materials*. 2007.

6. M. Kostadinova Loultcheva, M.Proietto, N. Jilow, F. P. La Mantia, *Recycling of high density polylene containers.* Polymer degradation and stability, 1997. **57**: p. 77-81.

7. H. Hamid, M. B. Amin, A. G. Maadhah, *Handbook of polymer degradation*. Weathering degradation of polyethylene, ed. A.G.M. S.Halim Hamid, Mohamed B, Amin. 1992, New York: Marcel Dekker.

8. S. Bertin, J.J.Robin, *Study and chracterization of virgin and recycled LDPE/PP blends.* European polymer journal 2002. **38**: p. 2255-2264.

9. R. Gachter, H. Muller, *Plastic additives handbook*. 1993, Ohio: Hanger/Gardner Publications Inc. 525-531.

10. R. Gachter, H. Muller, *Plastic additives handbook*. 1993, Ohio: Hanger/Gardner Publiations Inc. 539-541.

11. K. Yang, Q. Yang, G. Li, Y. Sun, D. Feng, *Mechanical properties and morphologies of polypropylene with different sizes of calcium carbonate particles.* Polymer composites, 2006. **2006**: p. 443-450.

12. Y. W. Leong, M. B. Abu Bakar., Z. A. M. Ishak, A. Ariffin, B. Pukanszky, *Comparison of the mechanical properties and interfacial interactions between talc, kaolin, and calcium carbonate filled polypropylene composites.* Applied polymer science, 2003. **91**: p. 3315-3326.

13. C. Dearmitt, R. Rothen, *Filler and surface treatment.* Plastic additives & compounding,

2002.

14. T. Kauly, B. Keren, A. Siegmann, *Highly filled thermoplastic composites. II: Effects of particle size distribution on some properties.* Polymer composites, 1996. **17**: p. 806-815.

15. T. L. Wong, C. M. Barry, S. A. Orroth, *The effects of filler size on the properties of thermoplastic polyolefin blends.* Journal of vinyl & additive technology 1999. **5**: p. 235-240.

16. A. Davis, D. Sims, *Weathering of polymers*. Ultraviolet radiation. 1983, London: Applied science publishers. 21.

17. S. Y. Fu, B. Lauke, E. Mader, C. Y. Yue, X. Hu, *Tensile properties of short-glass-fibre and short-carbon-fibre-reinforced polypropylene composites.* Composites 2000. **Part A 31**: p. 1117-1125.

18. G. Ozkoc, G. Bayram, E. Bayramli, *Short glass fibre reinforced ABS and ABS/PA6 composites: Processing and characterization.* Polymer composites, 2005. **2005**: p. 745-755.

19. S. Shibata, I. Fukumoto, Y. Cao, *Effects of fibre compression and length ditribution on the flexural properties of short kenaf fibre-reinforced biodegradable composites.* Polymer composites, 2006. **27**: p. 170-176.

20. S.Karrad, J. M. Lopez Cuesta, A. Crespy, *Influence of a fine talc on the properties of composites with high density polyethylene and polyethylene polystyrene blends.* Materials science, 1998(33): p. 453-461.

21. D. W. Woodilliam, J. Callister, *The impact properties of hybrid composites reinforced with high-modulus polyethylene fibres and glass fibres.* Composites science and technology 1994. **52**: p. 397-405.

22. W. D. Callister, *Materials science and engineering: an introduction*. 2007: New York, NY: John Wiley & Sons, c2003.

23. Wikipedia, *Fibreglass*. 2010, Wikimedia Foundation, Inc.

24. J.L.Thomason, *Structure-property relationships in glass-reinforced polyamide, Part 1: the effect of fibre content.* Polymer composites, 2006. **DOI 10.1002**: p. 552-562.

25. H.Al-Madfa, Z. Mohamed, M. E. Kassem, *Weather ageing characterization of the mechanical properties of the low density polyethylene.* Polymer degradation and stability, 1997. **62**: p. 105-109.

26. K. Kadotani, *Mechanical properties of plastic composites under low temperature conditions.* Composites, 1980. **1980**: p. 87-93.

27. K. Ahlborn, *Mechanical relaxation of polymers at low temperature.* Cryogenics, 1988. **28**: p. 234-240.

28. M. R. Monaghan, P. J. Mallon, *High temperature mechancial characterisation of polyimide diaphragm forming films.* Applied science and manufacturing, 1998. **29**(3): p. 265-272.

29. A. Davis, D. Sims, *Weathering of polymers*. Ultraviolet radiation. 1983, London: Applied science publishers. 21.

30. J.Attwood, M. Philip, A. Hulme, G. Williams, P. Shipton, *The effects of ageing by ultraviolet degradation of recycled polyolefin blends.* Polymer degradation and stability, 2006. **91**: p. 3407-3415.

31. A. J. Peacock, *Hand book of polyethylene*. 2000, New York: Marcel Dekker Inc.

32. A. C.TAVARES, J. V. Gulmine, C. M. Lepienski, L. Akcelrud, *The effect of accelerated aging on the surface mechanical properties of polyethylene.* Polymer degradation and stability, 2002. **81**: p. 367-373.

33. R. Geetha, A. Torikai, S. Nagaya, K. Fueki, *Photo-oxidative degradation of polyethylene: effect of polymer characteristics on chemical changes and mechanical properties.* Polymer degradation and stability, 1987. **19**: p. 279-292.

34. S. El Raghi, R. R. Zahran, B. E. Gebril, *Effect of weathering on some properties of polyvinyl chloride/lignin blends.* Materials Letters, 1999. **46**: p. 332-342.

35. J. V. Gulmine, P. R. Janissek, H. M. Heise, L. Akcelrud, *Polyethylene characterization by FTIR.* Polymer testing, 2002(21 ): p. 557-563.

36. H. Hamid, M. B. Amin, A. G. Maadhah, *Handbook of polymer degradation*. Weathering degradation of polyethylene, 1992, New York: Marcel Dekker.

37. D. Kemiteknik, *Polymers in general* 2005.

38. J. V. Gulmine, L. Akcelrud, *FTIR characterization of aged XLPE.* Polymer testing, 2006. **25**: p. 932-942.

39. F. P. La Mantia, N. Tzankova Dintcheva, *Photooxidation and stabilization of photooxidized polyethylene and of its monopolymer blends.* Applied polymer science, 2003. **91**(2244-2255).

40. Shimadzu, *IRP restige-21 Fourier Transform Infrared Spectrophotometer*. 2000, Tokyo.

41. J. V. Gulmine, P. R. Janissek, H. M. Heise, L. Akcelrud, *Degradation profile of polyethylene after artifical accelerated weathering* Polymer degradation and stability 2003(79): p. 385-397.

42. Wikipedia, *Differential Scanning Calorimetry*. 2009, Wikimedia Foundation, Inc., a non-profit organization.

43. A. P. Gray, *Polymer crystallinity determination by DSC.* Thermochim Acta, 1970. **1**: p. 563-579.

44. A. C. Y. Wong, F. Lam, *Study of selected thermal characteristics of polypropylene/polyethylene binary blends using DSC and TGA.* Polymer testing, 2001. **21**: p. 691-696.

45. Y. Kong, J. N. Hay, *The measurement of the crystallinity of polymers by DSC.* Polymer, 2002. **43**: p. 3873-3878.

46. I. H. Craig, J. R. White, *Crystallization and chemi-crystallization of recycled photodegradation polyethylenes.* Polymer engineering and science, 2005: p. 588-595.

47. Arizona Collaborative for Excellene in Preparation Teachers, *Scanned electron microscopy*. 1999.

48. ASTM, *Standard test method for tensile properties of plastic.* 1999.

49. C. C. Wang, T. Lin, S. Hu, *Optimizing the rapid prototyping process by integrating the Taguchi method with the Gray relational analysis* Rapid prototyping journal 2007. **13**(5): p. 304-315.

50. ASTM, *Standard practice for fluorescent UV exposure of plastics.* 1999.

# APPENDIX A: TENSILE TEST RESULTS

**Table A-1 Tensile strain of recycled LDPE after UV exposing**

| Exposure Time(week) | 0 | 1 | 2 | 3 | 4 | 5 | 6 | 7 |
|---|---|---|---|---|---|---|---|---|
| 1 | 11.03 | 10.72 | 11.7 | 5.64 | 3.82 | 2.94 | 0.23 | 0.23 |
| 2 | 11.11 | 11.3 | 11.78 | 5.87 | 3.94 | 2.78 | 0.27 | 0.31 |
| 3 | 11.27 | 11.45 | 12.09 | 5.92 | 4.13 | 2.84 | 0.27 | 0.26 |
| 4 | 11.08 | 11.81 | 12.01 | 6.01 | 4.06 | 2.89 | 0.22 | 0.31 |
| 5 | 11.11 | 11.61 | 11.98 | 5.16 | 4.1 | 2.85 | 0.25 | 0.28 |
| Mean | 11.12 | 11.38 | 11.91 | 5.72 | 4.01 | 2.86 | 0.25 | 0.28 |
| Standard deviation | 0.09 | 0.41 | 0.16 | 0.34 | 0.13 | 0.06 | 0.02 | 0.03 |

**Table A-2 Tensile strength of recycled LDPE after UV exposing**

| Exposure Time(week) | 0 | 1 | 2 | 3 | 4 | 5 | 6 | 7 |
|---|---|---|---|---|---|---|---|---|
| 1 | 9.96 | 8.75 | 8.84 | 8.76 | 3.79 | 2.75 | 2.59 | 1.95 |
| 2 | 9.62 | 9.16 | 8.8 | 4.29 | 5.62 | 2.99 | 3.13 | 2.39 |
| 3 | 9.46 | 9.4 | 8.77 | 4.56 | 3.84 | 2.87 | 3.24 | 2.22 |
| 4 | 9.57 | 9.67 | 8.53 | 5.87 | 3.5 | 3.1 | 2.54 | 2.31 |
| 5 | 9.5 | 9.56 | 8.55 | 5.9 | 3.62 | 3.14 | 2.88 | 2.22 |
| Mean | 9.62 | 9.31 | 8.70 | 5.88 | 4.07 | 2.97 | 2.88 | 2.22 |
| Standard Deviation | 0.20 | 0.37 | 0.15 | 1.77 | 0.87 | 0.16 | 0.31 | 0.17 |

**Table A-3 Tensile strain of recycled LDPE with 30 wt% talc after UV exposing**

| Exposure Time(week) | 0 | 1 | 2 | 3 | 4 | 5 | 6 | 7 | 8 |
|---|---|---|---|---|---|---|---|---|---|
| 1 | 8.54 | 9.21 | 7.42 | 7.36 | 5.14 | 0.18 | 0.15 | 0.12 | 0.13 |
| 2 | 8.3 | 5.22 | 8.51 | 7.45 | 8.6 | 0.22 | 0.16 | 0.14 | 0.13 |
| 3 | 7.19 | 7.66 | 7.72 | 7.44 | 8.66 | 0.19 | 0.16 | 0.11 | 0.12 |
| 4 | 7.15 | 7.32 | 7.98 | 7.36 | 7.64 | 0.23 | 0.15 | 0.11 | 0.11 |
| 5 | 7.57 | 7.54 | 8.32 | 7.43 | 7.3 | 0.18 | 0.14 | 0.13 | 0.12 |
| Mean | 7.75 | 7.39 | 7.99 | 7.41 | 7.47 | 0.20 | 0.15 | 0.12 | 0.12 |
| Standard Deviation | 0.64 | 1.42 | 0.44 | 0.04 | 1.43 | 0.02 | 0.01 | 0.01 | 0.01 |

**Table A-4 Tensile strength of recycled LDPE with 30 wt% talc after UV exposing**

| Exposure Time(week) | 0 | 1 | 2 | 3 | 4 | 5 | 6 | 7 | 8 |
|---|---|---|---|---|---|---|---|---|---|
| 1 | 9.77 | 9.99 | 8.88 | 9.40 | 9.04 | 6.29 | 5.58 | 5.14 | 4.94 |
| 2 | 9.85 | 8.22 | 9.43 | 9.24 | 8.08 | 6.38 | 5.82 | 5.45 | 5.07 |
| 3 | 9.50 | 9.56 | 8.93 | 10.12 | 8.02 | 5.96 | 5.93 | 5.61 | 4.99 |
| 4 | 9.44 | 9.32 | 9.50 | 9.55 | 8.67 | 6.60 | 5.82 | 5.02 | 4.99 |
| 5 | 9.64 | 9.22 | 8.66 | 9.57 | 8.99 | 5.52 | 5.80 | 5.18 | 5.02 |
| Mean | 9.64 | 9.26 | 9.08 | 9.58 | 8.56 | 6.15 | 5.79 | 5.28 | 5.00 |
| Standard Deviation | 0.17 | 0.65 | 0.37 | 0.33 | 0.49 | 0.42 | 0.13 | 0.24 | 0.05 |

**Table A-5 Tensile strain of recycled LDPE with 35 wt% talc after UV exposing**

| Exposure Time(week) | 0 | 1 | 2 | 3 | 4 | 5 | 6 | 7 | 8 |
|---|---|---|---|---|---|---|---|---|---|
| 1 | 5.88 | 7.53 | 8.58 | 9.45 | 9.43 | 9.45 | 8.48 | 0.32 | 0.16 |
| 2 | 6.39 | 7.11 | 8.58 | 8.20 | 8.63 | 9.46 | 8.35 | 0.18 | 0.12 |
| 3 | 5.81 | 7.95 | 9.01 | 9.44 | 9.48 | 9.48 | 7.19 | 0.12 | 0.17 |
| 4 | 6.16 | 7.58 | 7.85 | 9.35 | 8.56 | 9.52 | 8.04 | 0.25 | 0.19 |
| 5 | 7.10 | 7.48 | 8.44 | 9.19 | 9.86 | 9.34 | 8.24 | 0.17 | 0.11 |
| Mean | 6.27 | 7.53 | 8.49 | 9.13 | 9.19 | 9.45 | 8.06 | 0.21 | 0.15 |
| Standard Deviation | 0.52 | 0.30 | 0.42 | 0.53 | 0.57 | 0.07 | 0.51 | 0.08 | 0.03 |

**Table A-6 Tensile strength of recycled LDPE with 35 wt% talc after UV exposing**

| Exposure Time(week) | 0 | 1 | 2 | 3 | 4 | 5 | 6 | 7 | 8 |
|---|---|---|---|---|---|---|---|---|---|
| 1 | 9.86 | 9.09 | 9.47 | 8.72 | 9.21 | 9.06 | 9.39 | 6.26 | 5.49 |
| 2 | 9.89 | 8.83 | 9.65 | 9.58 | 9.23 | 9.24 | 9.12 | 5.75 | 4.99 |
| 3 | 9.64 | 9.49 | 9.24 | 8.53 | 9.36 | 9.37 | 8.03 | 5.00 | 5.24 |
| 4 | 9.70 | 9.10 | 9.32 | 8.75 | 7.39 | 8.95 | 9.19 | 5.34 | 5.64 |
| 5 | 9.51 | 9.14 | 9.48 | 8.93 | 8.72 | 9.13 | 8.93 | 6.00 | 4.69 |
| Mean | 9.72 | 9.13 | 9.43 | 8.90 | 8.78 | 9.15 | 8.93 | 5.67 | 5.21 |
| Standard Deviation | 0.16 | 0.24 | 0.16 | 0.40 | 0.82 | 0.16 | 0.53 | 0.51 | 0.38 |

**Table A-7 Tensile strain of recycled LDPE with 30 wt% glass fibres after UV exposing**

| Exposure Time(week) | 0 | 1 | 2 | 3 | 4 | 5 | 6 | 7 | 8 |
|---|---|---|---|---|---|---|---|---|---|
| 1 | 8.96 | 9.01 | 9.70 | 9.66 | 9.69 | 9.71 | 0.50 | 0.41 | 0.29 |
| 2 | 9.14 | 9.72 | 9.73 | 9.66 | 9.69 | 9.64 | 0.34 | 0.40 | 0.18 |
| 3 | 8.09 | 9.73 | 9.72 | 9.65 | 9.72 | 9.67 | 0.31 | 0.26 | 0.27 |
| 4 | 8.10 | 9.55 | 9.75 | 9.78 | 9.71 | 8.51 | 0.79 | 0.27 | 0.19 |
| 5 | 8.61 | 9.41 | 9.78 | 9.67 | 9.54 | 8.72 | 0.47 | 0.22 | 0.27 |
| Mean | 8.58 | 9.48 | 9.74 | 9.68 | 9.67 | 9.25 | 0.48 | 0.31 | 0.24 |
| Standard Deviation | 0.48 | 0.30 | 0.03 | 0.05 | 0.07 | 0.58 | 0.19 | 0.09 | 0.05 |

**Table A-8 Tensile strength of recycled LDPE with 30 wt% glass fibres after UV exposing**

| Exposure Time(week) | 0 | 1 | 2 | 3 | 4 | 5 | 6 | 7 | 8 |
|---|---|---|---|---|---|---|---|---|---|
| 1 | 9.95 | 9.57 | 10.01 | 9.83 | 9.05 | 8.57 | 6.66 | 6.25 | 6.34 |
| 2 | 10.46 | 9.44 | 9.80 | 9.90 | 9.65 | 9.86 | 6.43 | 5.46 | 6.01 |
| 3 | 10.85 | 9.49 | 9.98 | 9.59 | 9.00 | 8.92 | 6.34 | 5.15 | 6.23 |
| 4 | 9.84 | 9.52 | 10.09 | 9.14 | 9.87 | 9.78 | 6.65 | 6.22 | 6.16 |
| 5 | 10.65 | 9.48 | 8.99 | 9.56 | 9.08 | 9.12 | 6.60 | 7.42 | 6.21 |
| Mean | 10.35 | 9.50 | 9.77 | 9.60 | 9.33 | 9.25 | 6.54 | 6.10 | 6.19 |
| Standard Deviation | 0.44 | 0.05 | 0.45 | 0.30 | 0.40 | 0.56 | 0.14 | 0.88 | 0.12 |

**Table A-9 Tensile strain (mm/mm) of recycled LDPE at different temperatures ($^{o}$C)**

| Temperature($^{o}$C) | -20 | 0 | 20 | 40 | 60 | 80 |
|---|---|---|---|---|---|---|
| 1 | 0.25 | 1.27 | 1.54 | 1.43 | 1.43 | 1.43 |
| 2 | 0.26 | 1.27 | 1.62 | 1.43 | 1.43 | 1.43 |
| 3 | 0.23 | 1.21 | 1.49 | 1.42 | 1.43 | 1.43 |
| 4 | 0.22 | 1.21 | 1.28 | 1.41 | 1.42 | 1.43 |
| 5 | 0.23 | 1.26 | 1.19 | 1.43 | 1.43 | 1.43 |
| Mean | 0.24 | 1.24 | 1.42 | 1.43 | 1.43 | 1.43 |
| Standard Deviation | 0.02 | 0.03 | 0.18 | 0.01 | 0.00 | 0.00 |

**Table A-10 Tensile strength (MPa) of recycled LDPE at different temperatures ($^{o}$C)**

| Temperature($^{o}$C) | -20 | 0 | 20 | 40 | 60 | 80 |
|---|---|---|---|---|---|---|
| 1 | 18.73 | 16.24 | 14.53 | 10.21 | 7.69 | 5.49 |
| 2 | 18.95 | 16.78 | 13.79 | 10.83 | 7.64 | 5.33 |
| 3 | 19.45 | 16.24 | 12.88 | 10.07 | 7.54 | 4.99 |
| 4 | 19.06 | 16.01 | 13.54 | 10.67 | 7.78 | 5.85 |
| 5 | 19.00 | 16.34 | 11.66 | 10.34 | 7.72 | 5.66 |
| Mean | 19.04 | 16.32 | 13.28 | 10.42 | 7.67 | 5.47 |
| Standard Deviation | 0.26 | 0.28 | 1.08 | 0.32 | 0.09 | 0.33 |

**Table A-11 Tensile strain (mm/mm) of recycled LDPE with 40 wt% talc at different temperatures ($^{o}$C)**

| Temperature($^{o}$C) | -20 | 0 | 20 | 40 | 60 | 80 |
|---|---|---|---|---|---|---|
| 1 | 0.13 | 0.14 | 0.30 | 0.20 | 0.36 | 0.74 |
| 2 | 0.13 | 0.13 | 0.19 | 0.21 | 0.42 | 0.66 |
| 3 | 0.13 | 0.13 | 0.19 | 0.23 | 0.57 | 0.69 |
| 4 | 0.15 | 0.15 | 0.26 | 0.25 | 0.31 | 0.68 |
| 5 | 0.11 | 0.15 | 0.18 | 0.24 | 0.54 | 0.48 |
| Mean | 0.13 | 0.14 | 0.22 | 0.23 | 0.44 | 0.65 |
| Standard Deviation | 0.01 | 0.01 | 0.05 | 0.02 | 0.11 | 0.10 |

**Table A-12 Tensile strength (MPa) of recycled LDPE with 40 wt% talc at different temperatures ($^{o}$C)**

| Temperature($^{o}$C) | -20 | 0 | 20 | 40 | 60 | 80 |
|---|---|---|---|---|---|---|
| 1 | 21.81 | 19.87 | 14.83 | 13.09 | 10.65 | 7.30 |
| 2 | 23.52 | 19.53 | 14.16 | 13.53 | 10.27 | 7.75 |
| 3 | 22.03 | 19.80 | 14.01 | 12.83 | 10.16 | 7.56 |
| 4 | 23.66 | 18.69 | 14.81 | 12.59 | 9.65 | 7.82 |
| 5 | 21.19 | 19.13 | 14.46 | 12.98 | 9.57 | 8.06 |
| Mean | 22.40 | 19.40 | 14.45 | 13.00 | 10.06 | 7.70 |
| Standard Deviation | 1.09 | 0.49 | 0.37 | 0.35 | 0.45 | 0.29 |

**Table A-13 Tensile strain (mm/mm) of recycled LDPE with 45 wt% talc at different temperatures ($^{o}$C)**

| Temperature($^{o}$C) | -20 | 0 | 20 | 40 | 60 | 80 |
|---|---|---|---|---|---|---|
| 1 | 0.11 | 0.11 | 0.15 | 0.15 | 0.27 | 0.39 |
| 2 | 0.11 | 0.10 | 0.14 | 0.14 | 0.21 | 0.37 |
| 3 | 0.12 | 0.12 | 0.15 | 0.16 | 0.24 | 0.22 |
| 4 | 0.11 | 0.11 | 0.15 | 0.15 | 0.25 | 0.48 |
| 5 | 0.11 | 0.11 | 0.15 | 0.15 | 0.23 | 0.44 |
| Mean | 0.11 | 0.11 | 0.15 | 0.15 | 0.24 | 0.38 |
| Standard Deviation | 0.00 | 0.01 | 0.00 | 0.01 | 0.02 | 0.10 |

**Table A-14 Tensile strength (MPa) of recycled LDPE with 45 wt% talc at different temperatures ($^{o}$C)**

| Temperature($^{o}$C) | -20 | 0 | 20 | 40 | 60 | 80 |
|---|---|---|---|---|---|---|
| 1 | 23.83 | 19.52 | 15.45 | 13.94 | 11.05 | 8.62 |
| 2 | 24.33 | 20.97 | 14.9 | 14.22 | 11.05 | 7.87 |
| 3 | 25.14 | 21.04 | 15.2 | 15.43 | 11.04 | 9.29 |
| 4 | 23.79 | 20.11 | 15.17 | 14.61 | 11 | 8.98 |
| 5 | 23.31 | 19.56 | 15.16 | 14.45 | 11.1 | 8.19 |
| Mean | 24.08 | 20.24 | 15.18 | 14.53 | 11.05 | 8.59 |
| Standard Deviation | 1.09 | 0.49 | 0.37 | 0.35 | 0.45 | 0.29 |

**Table A-15 Tensile strain (mm/mm) of recycled LDPE with 50 wt% talc at different temperatures ($^{o}$C)**

| Temperature($^{o}$C) | -20 | 0 | 20 | 40 | 60 | 80 |
|---|---|---|---|---|---|---|
| 1 | 0.06 | 0.11 | 0.13 | 0.14 | 0.24 | 0.26 |
| 2 | 0.05 | 0.10 | 0.13 | 0.13 | 0.22 | 0.27 |
| 3 | 0.03 | 0.10 | 0.12 | 0.14 | 0.23 | 0.27 |
| 4 | 0.04 | 0.10 | 0.13 | 0.16 | 0.22 | 0.32 |
| 5 | 0.05 | 0.11 | 0.13 | 0.16 | 0.26 | 0.26 |
| Mean | 0.05 | 0.10 | 0.13 | 0.15 | 0.23 | 0.27 |
| Standard Deviation | 0.01 | 0.01 | 0.00 | 0.01 | 0.02 | 0.03 |

**Table A-16 Tensile strength (MPa) of recycled LDPE with 50 wt% talc at different temperatures ($^{o}$C)**

| Temperature($^{o}$C) | -20.00 | 0.00 | 20.00 | 40.00 | 60.00 | 80.00 |
|---|---|---|---|---|---|---|
| 1 | 25.12 | 22.50 | 16.28 | 16.33 | 11.63 | 9.69 |
| 2 | 24.99 | 22.49 | 16.01 | 14.44 | 11.27 | 8.92 |
| 3 | 25.21 | 23.11 | 15.80 | 15.31 | 11.37 | 9.37 |
| 4 | 23.98 | 22.23 | 17.58 | 15.45 | 10.77 | 9.44 |
| 5 | 21.10 | 21.32 | 17.43 | 14.83 | 10.89 | 9.01 |
| Mean | 24.08 | 22.33 | 16.62 | 15.27 | 11.19 | 9.29 |
| Standard Deviation | 1.74 | 0.65 | 0.83 | 0.71 | 0.35 | 0.32 |

**Table A-17 Tensile strain (mm/mm) of recycled LDPE with 40 wt% glass fibre at different temperatures ($^{o}$C)**

| Temperature($^{o}$C) | -20 | 0 | 20 | 40 | 60 | 80 |
|---|---|---|---|---|---|---|
| 1 | 0.03 | 0.05 | 0.13 | 0.9 | 1.49 | 1.55 |
| 2 | 0.03 | 0.07 | 0.14 | 0.84 | 0.92 | 1.64 |
| 3 | 0.03 | 0.07 | 0.12 | 0.81 | 1.44 | 1.18 |
| 4 | 0.03 | 0.04 | 0.13 | 1.21 | 0.9 | 1.2 |
| 5 | 0.03 | 0.05 | 0.13 | 1.19 | 1.15 | 1.58 |
| Mean | 0.03 | 0.06 | 0.13 | 0.99 | 1.18 | 1.43 |
| Standard Deviation | 0.00 | 0.01 | 0.01 | 0.19 | 0.27 | 0.22 |

**Table A-18 Tensile strength (MPa) of recycled LDPE with 40 wt% glass fibre at different temperatures ($^{o}$C)**

| Temperature($^{o}$C) | -20 | 0 | 20 | 40 | 60 | 80 |
|---|---|---|---|---|---|---|
| 1 | 24.39 | 22.30 | 14.03 | 9.28 | 7.77 | 6.56 |
| 2 | 24.39 | 22.42 | 15.44 | 10.17 | 7.51 | 6.66 |
| 3 | 24.39 | 22.23 | 16.77 | 9.61 | 7.90 | 5.94 |
| 4 | 24.39 | 21.92 | 14.68 | 10.43 | 8.10 | 6.75 |
| 5 | 24.39 | 20.08 | 16.78 | 9.51 | 7.58 | 7.19 |
| Mean | 24.39 | 21.79 | 15.54 | 9.80 | 7.77 | 6.62 |
| Standard Deviation | 0.00 | 0.01 | 1.23 | 0.48 | 0.24 | 0.45 |

**Table A-19 Tensile strain (mm/mm) of recycled LDPE with 45 wt% glass fibre at different temperatures ($^{o}$C)**

| Temperature($^{o}$C) | -20 | 0 | 20 | 40 | 60 | 80 |
|---|---|---|---|---|---|---|
| 1 | 0.03 | 0.06 | 0.09 | 0.25 | 0.82 | 1.63 |
| 2 | 0.03 | 0.03 | 0.16 | 0.24 | 0.76 | 0.84 |
| 3 | 0.03 | 0.04 | 0.09 | 0.67 | 1.25 | 1.05 |
| 4 | 0.03 | 0.05 | 0.10 | 0.21 | 0.91 | 1.54 |
| 5 | 0.03 | 0.04 | 0.16 | 0.48 | 1.57 | 0.92 |
| Mean | 0.03 | 0.04 | 0.12 | 0.37 | 1.06 | 1.20 |
| Standard Deviation | 0.00 | 0.01 | 0.04 | 0.20 | 0.34 | 0.36 |

**Table A-20 Tensile strength (MPa) of recycled LDPE with 45 wt% glass fibre at different temperatures ($^{o}$C)**

| Temperature($^{o}$C) | -20 | 0 | 20 | 40 | 60 | 80 |
|---|---|---|---|---|---|---|
| 1 | 24.39 | 21.45 | 16.91 | 10.41 | 7.85 | 6.78 |
| 2 | 24.39 | 22.27 | 15.99 | 11.67 | 8.09 | 5.51 |
| 3 | 24.39 | 22.60 | 16.08 | 13.11 | 7.89 | 5.97 |
| 4 | 24.39 | 22.29 | 16.74 | 9.20 | 7.85 | 6.26 |
| 5 | 24.39 | 21.49 | 16.02 | 10.36 | 8.01 | 5.46 |
| Mean | 24.39 | 22.02 | 16.34 | 10.95 | 7.94 | 5.99 |
| Standard Deviation | 0.00 | 0.01 | 0.44 | 1.49 | 0.11 | 0.55 |

**Table A-21 Tensile strain (mm/mm) of recycled LDPE with 50 wt% glass fibre at different temperatures ($^{o}$C)**

| Temperature($^{o}$C) | -20 | 0 | 20 | 40 | 60 | 80 |
|---|---|---|---|---|---|---|
| 1 | 0.03 | 0.03 | 0.05 | 0.14 | 1.24 | 1.22 |
| 2 | 0.03 | 0.03 | 0.04 | 0.15 | 0.94 | 1.20 |
| 3 | 0.03 | 0.04 | 0.07 | 0.12 | 0.19 | 1.24 |
| 4 | 0.03 | 0.04 | 0.04 | 0.14 | 0.73 | 1.21 |
| 5 | 0.03 | 0.03 | 0.04 | 0.10 | 0.56 | 1.23 |
| Mean | 0.03 | 0.04 | 0.05 | 0.13 | 0.70 | 1.22 |
| Standard Deviation | 0.00 | 0.01 | 0.01 | 0.02 | 0.40 | 0.02 |

**Table A-22 Tensile strength (MPa) of recycled LDPE with 50 wt% glass fibre at different temperatures ($^{o}$C)**

| Temperature($^{o}$C) | -20 | 0 | 20 | 40 | 60 | 80 |
|---|---|---|---|---|---|---|
| 1 | 24.39 | 23.58 | 15.22 | 10.57 | 7.78 | 6.64 |
| 2 | 24.39 | 23.81 | 14.55 | 10.76 | 7.42 | 5.54 |
| 3 | 24.39 | 23.35 | 13.85 | 10.45 | 8.53 | 5.28 |
| 4 | 24.39 | 23.08 | 15.05 | 10.27 | 7.08 | 5.26 |
| 5 | 24.39 | 24.08 | 13.23 | 9.95 | 7.14 | 4.76 |
| Mean | 24.39 | 23.58 | 14.38 | 10.40 | 7.59 | 5.50 |
| Standard Deviation | 0.00 | 0.39 | 0.83 | 0.31 | 0.59 | 0.70 |

# APPENDIX B: ANALYSIS OF FTIR SPECTRA

Carbonyl Index is defined as:

$$\text{Carbonyl Index} = \frac{\text{Absorbance for carbonyl group (at } 1714\text{cm}^{-1}\text{)}}{\text{Absorbance for PE band (at } 1470\text{ cm}^{-1}\text{)}} = \frac{A}{B}$$

A, B can be obtained for FTIR spectra.

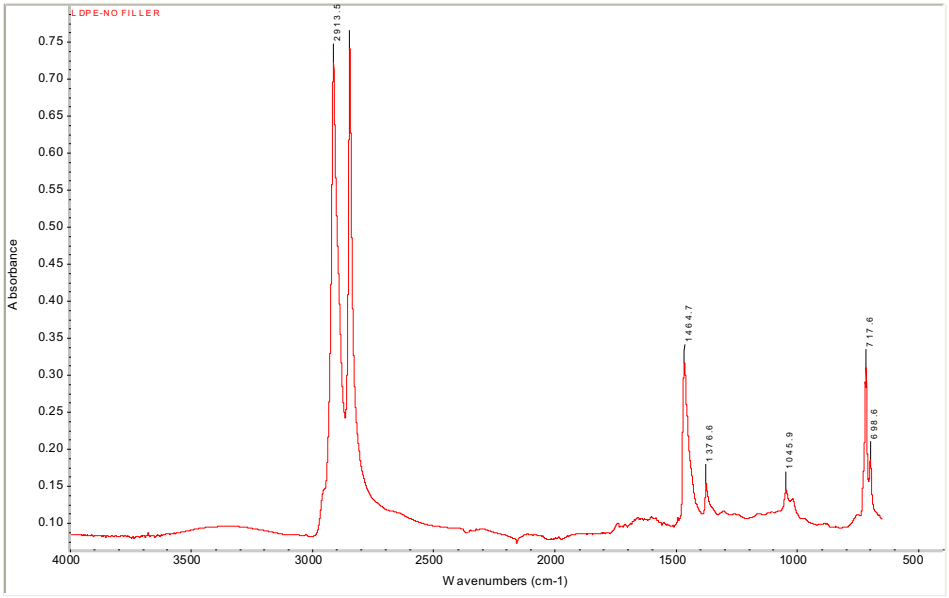


**Figure B-1. FTIR Spectra of recycled LDPE without UV exposing**

Calculation for Carbonyl Index: A= 0.097

B= 0.282

Carbonyl index of recycled LDPE without UV exposing: A/B= 0.344

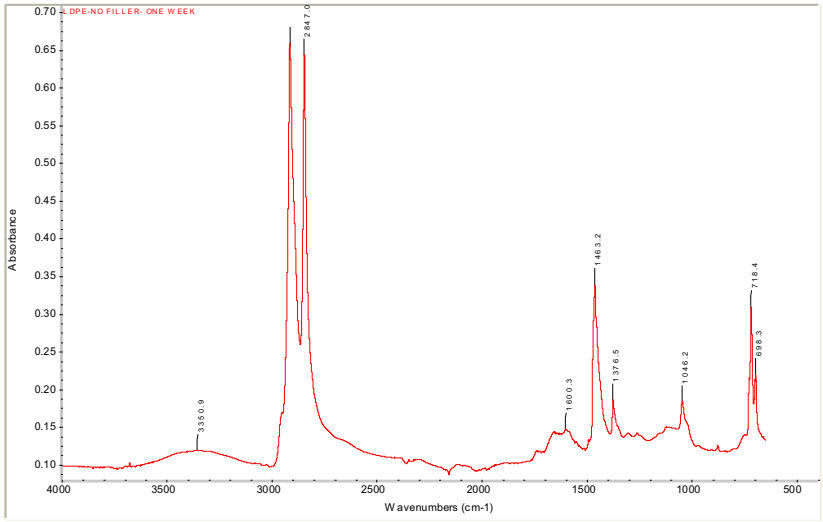


**Figure B-2. FTIR Spectra of recycled LDPE exposed under UV for one week**

Calculation for Carbonyl Index: A= 0.117

B= 0.283

Carbonyl Index of recycled LDPE without filled exposed under UV for one week: A/B= 0.414

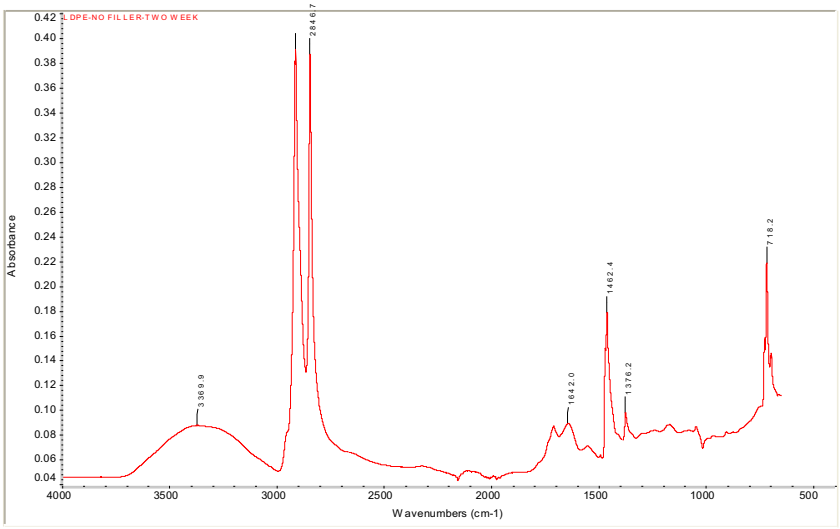


**Figure B-3. FTIR Spectra of recycled LDPE exposed under UV for two weeks**

Calculation for Carbonyl Index: A= 0.087

B= 0.149

Carbonyl Index for recycled LDPE exposed under UV for two weeks: A/B= 0.584

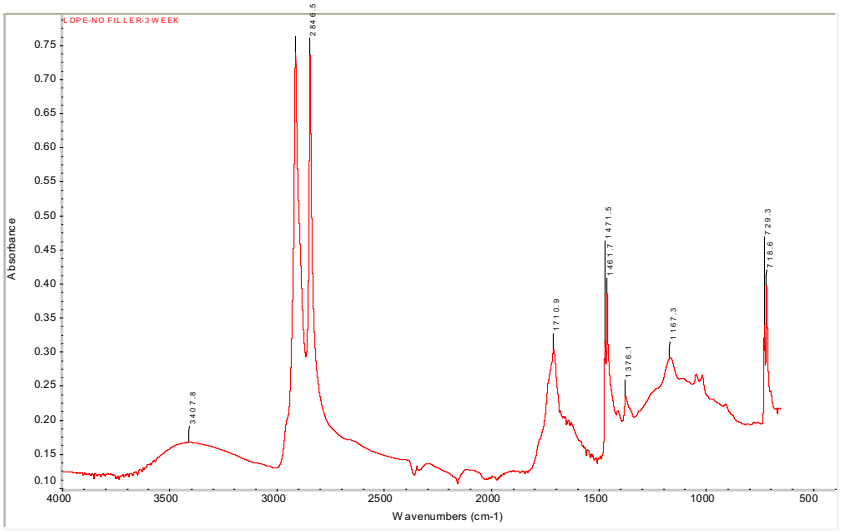


**Figure B-4. FTIR Spectra of recycled LDPE exposed under UV for three weeks**

Calculation for Carbonyl Index: A= 0.302

B= 0.309

Carbonyl Index for recycled LDPE exposed under UV for three weeks: A/B= 0.977

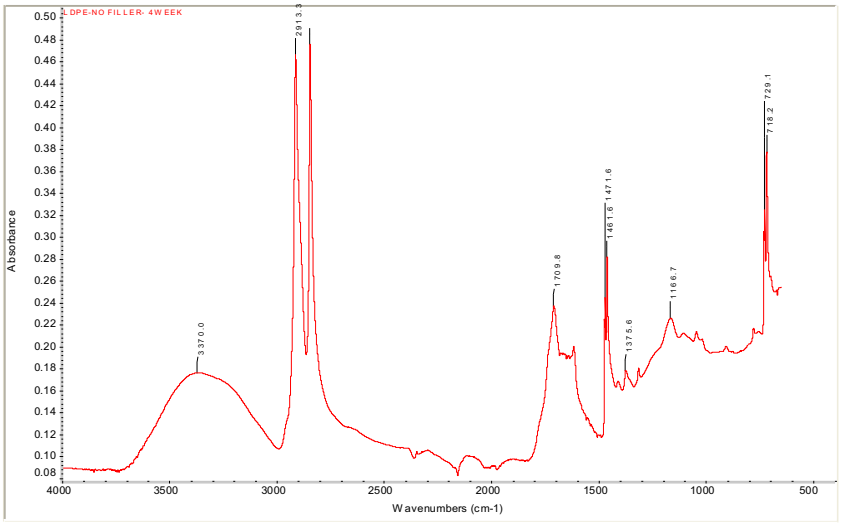


**Figure B-5. FTIR Spectra of recycled LDPE exposed under UV for four weeks**

Calculation for Carbonyl Index: A= 0.230

B= 0.237

Carbonyl Index for recycled LDPE exposed under UV for four weeks: A/B= 1.030

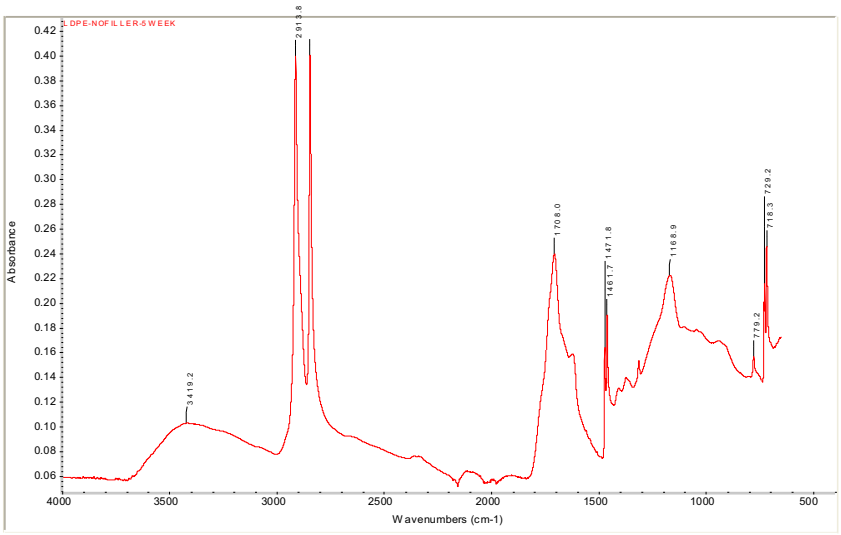


**Figure B-6. FTIR Spectra of recycled LDPE exposed under UV for five weeks**

Calculation for Carbonyl Index: A= 0.239

B= 0.161

Carbonyl Index for recycled LDPE exposed under UV for five weeks: A/B= 1.484

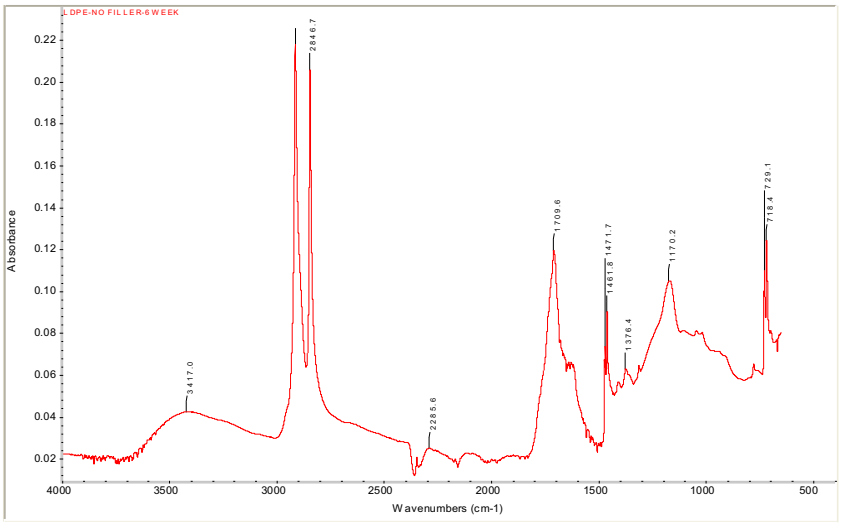


**Figure B-7. FTIR Spectra of recycled LDPE exposed under UV for six weeks**

Calculation for Carbonyl Index: A= 0.12

B= 0.073

Carbonyl Index for recycled LDPE exposed under UV for six weeks: A/B= 1.643

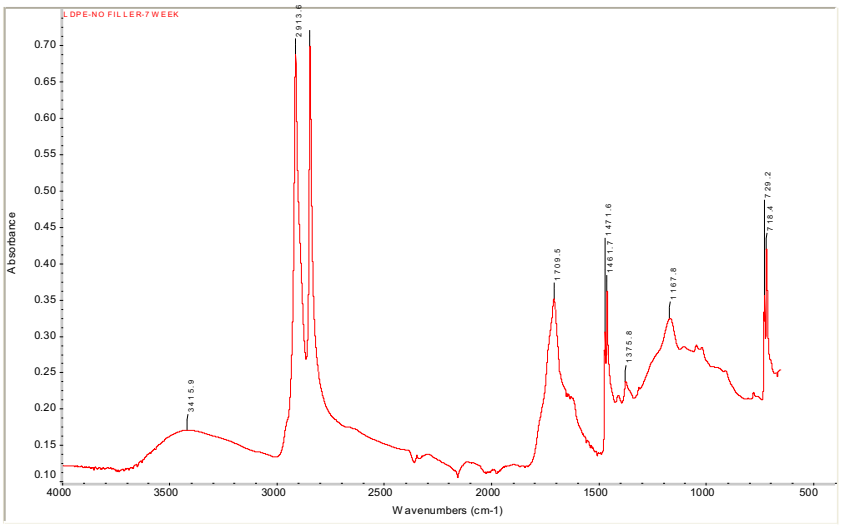


**Figure B-8. FTIR Spectra of recycled LDPE exposed under UV for seven weeks**

Calculation for Carbonyl Index: A= 0.198

B= 0.351

Carbonyl Index for recycled LDPE exposed under UV for six weeks: A/B= 1.766

**Table B-1. Carbonyl Index of recycled LDPE exposed under UV for different time (week)**

| | 0 | 1 | 2 | 3 | 4 | 5 | 6 | 7 |
|---|---|---|---|---|---|---|---|---|
| Carbonyl Index | 0.344 | 0.414 | 0.584 | 0.977 | 1.030 | 1.484 | 1.643 | 1.766 |

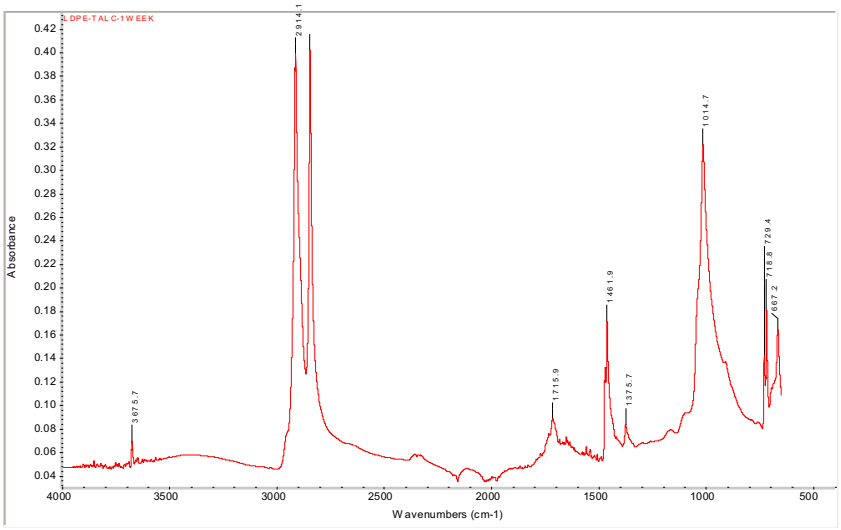


**Figure B-9. FTIR Spectra of recycled LDPE filled with 30wt% fine talc exposed under UV for one week**

Calculation for Carbonyl Index: A= 0.086

B= 0.130

Carbonyl Index of recycled LDPE with 30 wt% talc exposed under UV for one week:

A/B= 0.661

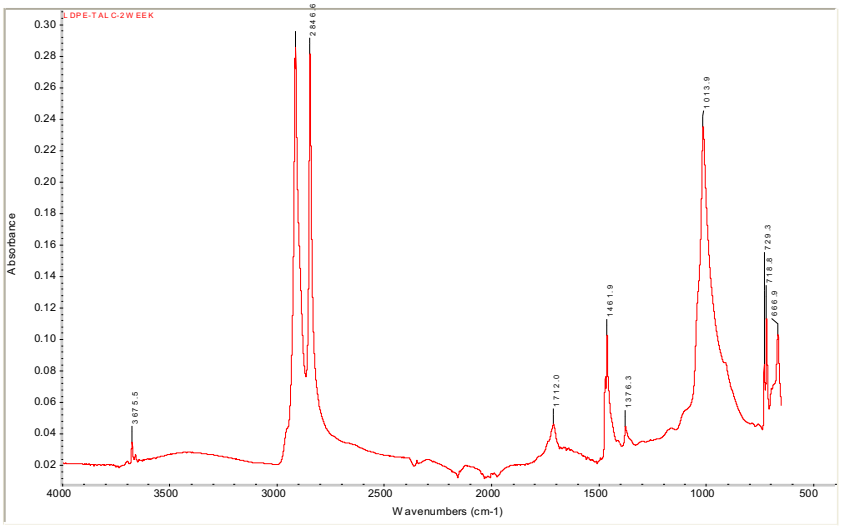


**Figure B-10. FTIR Spectra of recycled LDPE filled with 30wt% fine talc exposed under UV for two weeks**

Calculation for Carbonyl Index: A= 0.045

B= 0.074

Carbonyl Index of recycled LDPE with 30wt% talc exposed under UV for two weeks:

A/B= 0.608

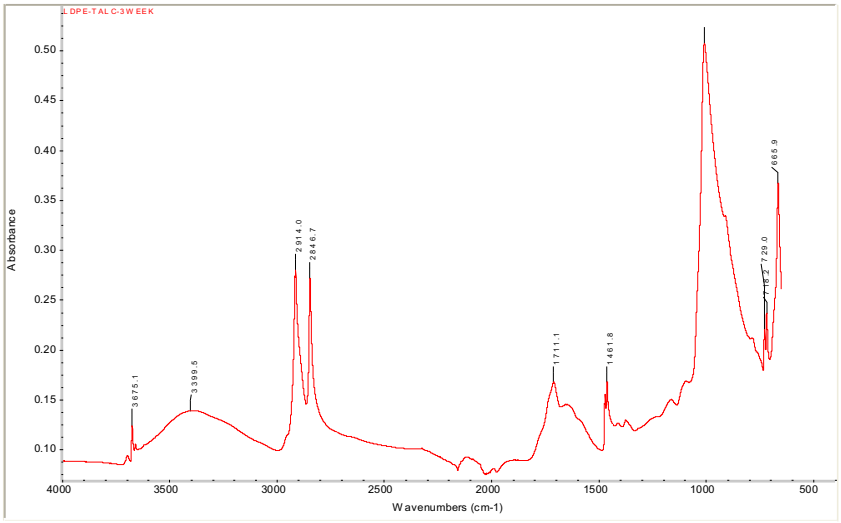


**Figure B-11. FTIR Spectra of recycled LDPE filled with 30wt% fine talc exposed under UV for three weeks**

Calculation for Carbonyl Index: A= 0.166

B= 0.270

Carbonyl Index of recycled LDPE with 30wt% talc exposed under UV for three weeks:

A/B= 0.614

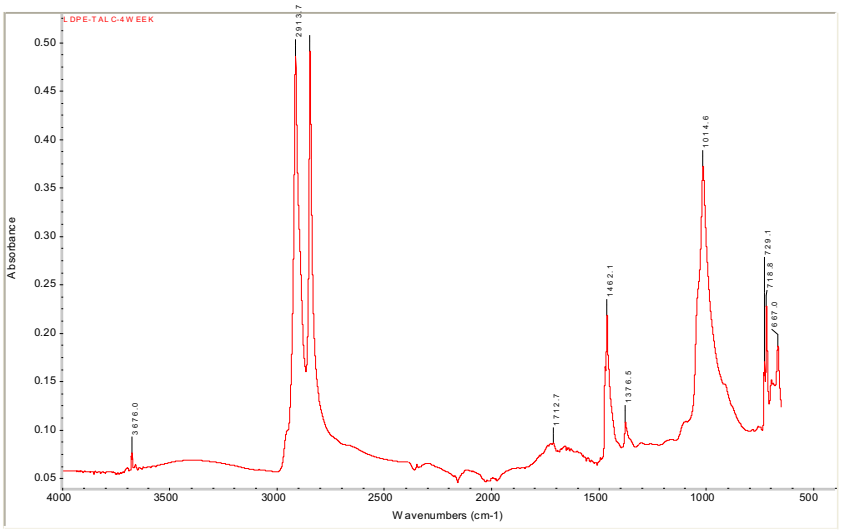


**Figure B-12. FTIR Spectra of recycled LDPE filled with 30wt% fine talc exposed under UV for four weeks**

Calculation for Carbonyl Index: A= 0.088

B= 0.087

Carbonyl Index of recycled LDPE with 30wt% talc exposed under UV for four weeks:

A/B= 0.982

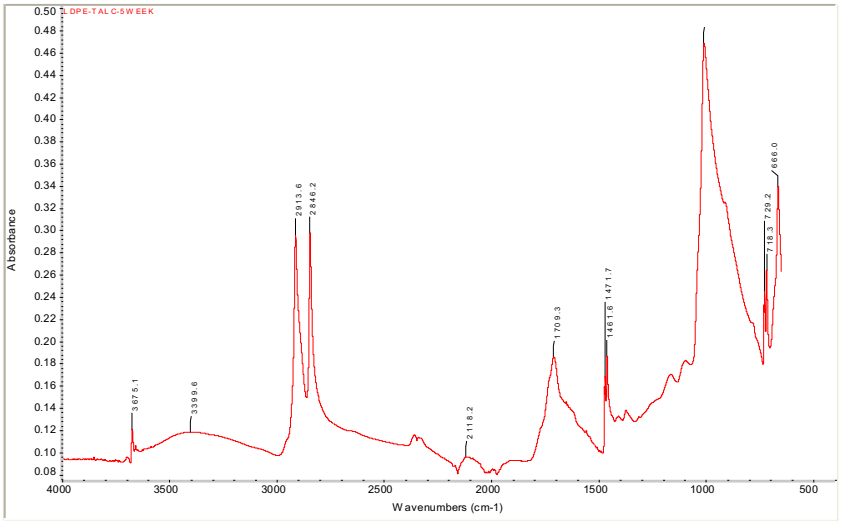


**Figure B-13. FTIR Spectra of recycled LDPE filled with 30wt% fine talc exposed under UV for five weeks**

Calculation for Carbonyl Index: A= 0.186

B= 0.168

Carbonyl Index of recycled LDPE with 30wt% talc exposed under UV for five weeks:

A/B= 1.107

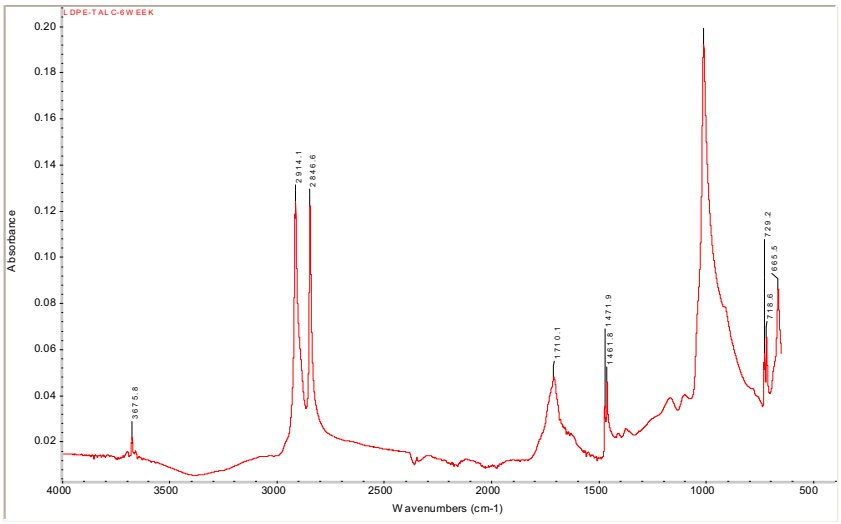


**Figure B-14. FTIR Spectra of recycled LDPE filled with 30wt% fine talc exposed under UV for six weeks**

Calculation for Carbonyl Index: A= 0.048

B= 0.036

Carbonyl Index of recycled LDPE with 30wt% talc exposed under UV for six weeks:

A/B= 1.333

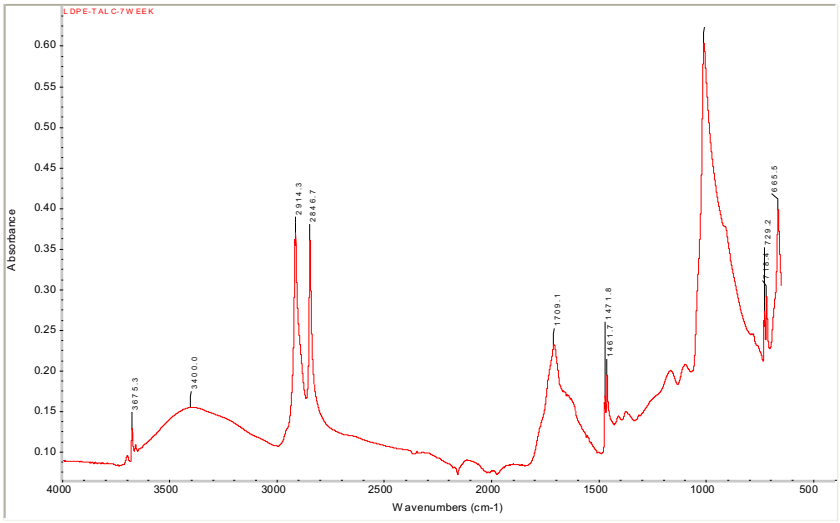


**Figure B-15. FTIR Spectra of recycled LDPE filled with 30wt% fine talc exposed under UV for seven weeks**

Calculation for Carbonyl Index: A= 0.232

B= 0.167

Carbonyl Index of recycled LDPE with 30wt% talc exposed under UV for seven weeks:

A/B= 1.389

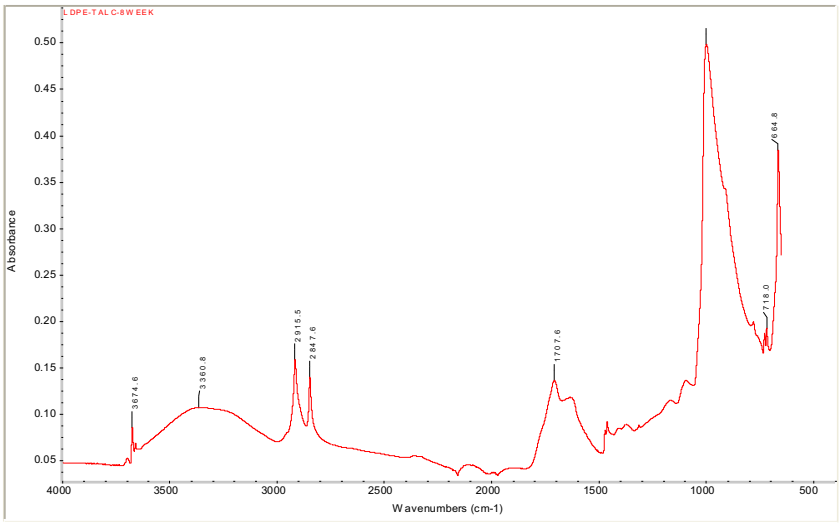


**Figure B-16. FTIR Spectra of recycled LDPE filled with 30wt% fine talc exposed under UV for eight weeks**

Calculation for Carbonyl Index: A= 0.135

B= 0.081

Carbonyl Index of recycled LDPE with 30wt% talc exposed under UV for seven weeks:

A/B= 1.667

**Table B-2. Carbonyl Index of recycled LDPE with 30 wt% fine talc exposed under UV for different time (week)**

| | 0 | 1 | 2 | 3 | 4 | 5 | 6 | 7 | 8 |
|---|---|---|---|---|---|---|---|---|---|
| Carbonyl Index | 0.454 | 0.661 | 0.608 | 0.614 | 0.982 | 1.107 | 1.333 | 1.389 | 1.667 |

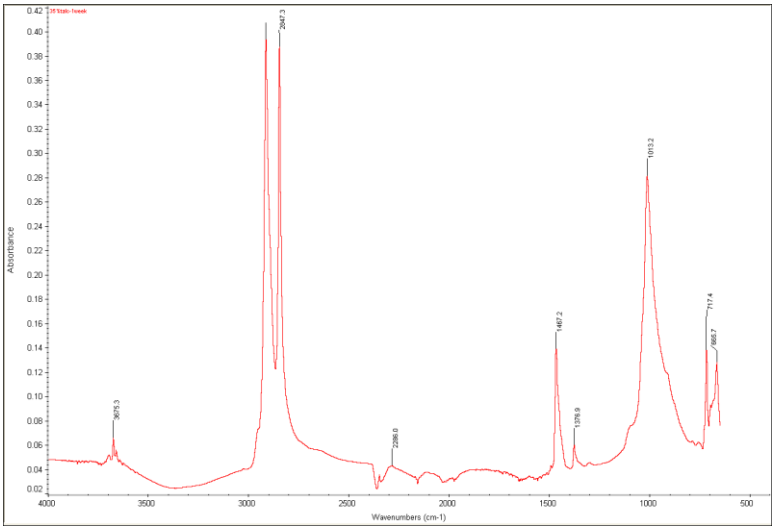


**Figure B-17. FTIR Spectra of recycled LDPE filled with 35wt% fine talc exposed under UV for one week**

Calculation for Carbonyl Index: A= 0.041

B= 0.129

Carbonyl Index of recycled LDPE with 35wt% talc exposed under UV for one week:

A/B= 0.3178

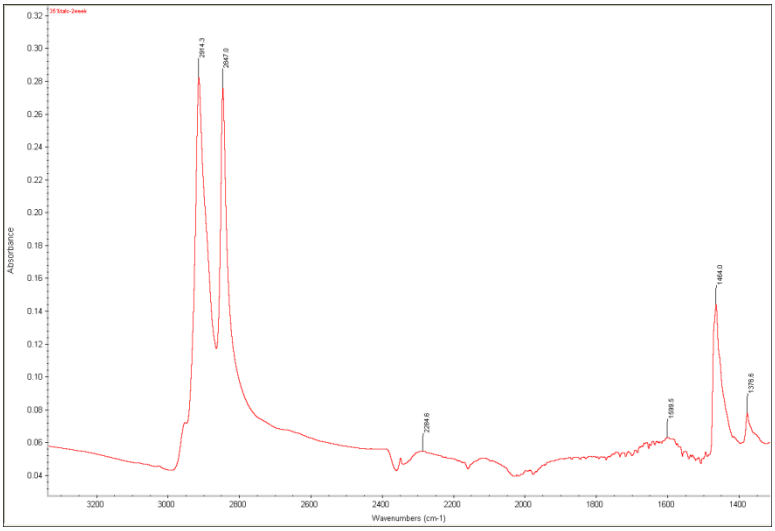


**Figure B-18. FTIR Spectra of recycled LDPE filled with 35wt% fine talc exposed under UV for two weeks**

Calculation for Carbonyl Index: A= 0.056

B= 0.131

Carbonyl Index of recycled LDPE with 35wt% talc exposed under UV for two weeks:

A/B= 0.4274

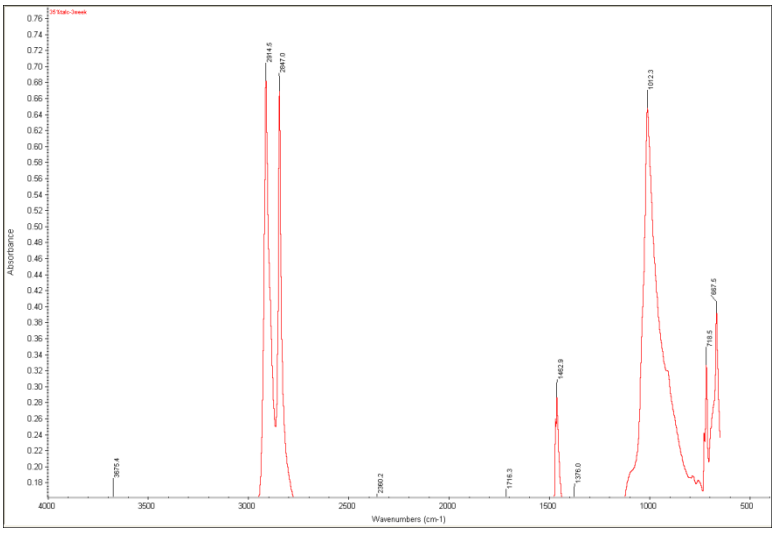


**Figure B-19. FTIR Spectra of recycled LDPE filled with 35wt% fine talc exposed under UV for three weeks**

Calculation for Carbonyl Index: A= 0.173

B= 0.396

Carbonyl Index of recycled LDPE with 35wt% talc exposed under UV for three weeks:

A/B= 0.4368

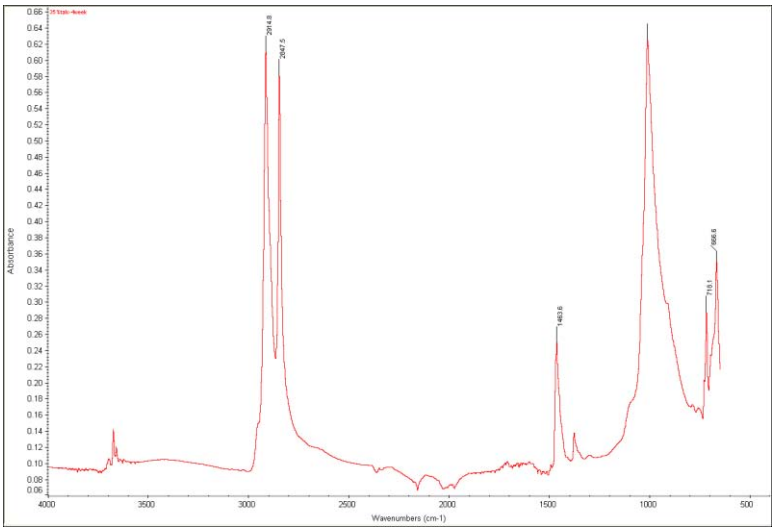


**Figure B-20. FTIR Spectra of recycled LDPE filled with 35wt% fine talc exposed under UV for four weeks**

Calculation for Carbonyl Index: A= 0.102

B= 0.228

Carbonyl Index of recycled LDPE with 35wt% talc exposed under UV for four weeks:

A/B= 0.4473

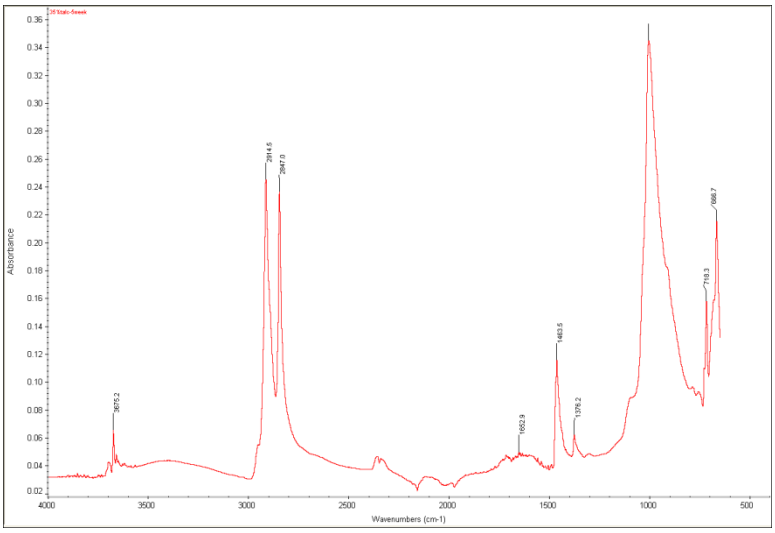


**Figure B-21. FTIR Spectra of recycled LDPE filled with 35wt% fine talc exposed under UV for five weeks**

Calculation for Carbonyl Index: A= 0.103

B= 0.243

Carbonyl Index of recycled LDPE with 35wt% talc exposed under UV for five weeks:

A/B= 0.4238

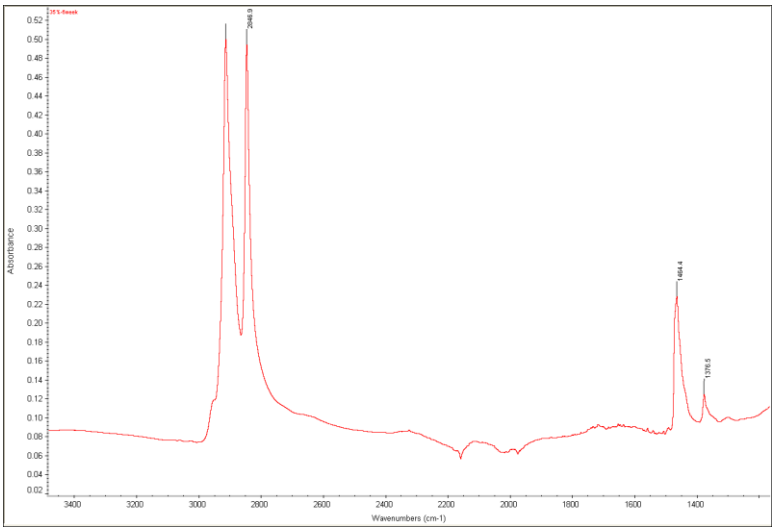


**Figure B-22. FTIR Spectra of recycled LDPE filled with 35wt% fine talc exposed under UV for six weeks**

Calculation for Carbonyl Index: A= 0.094

B= 0.212

Carbonyl Index of recycled LDPE with 35wt% talc exposed under UV for six weeks:

A/B= 0.4433

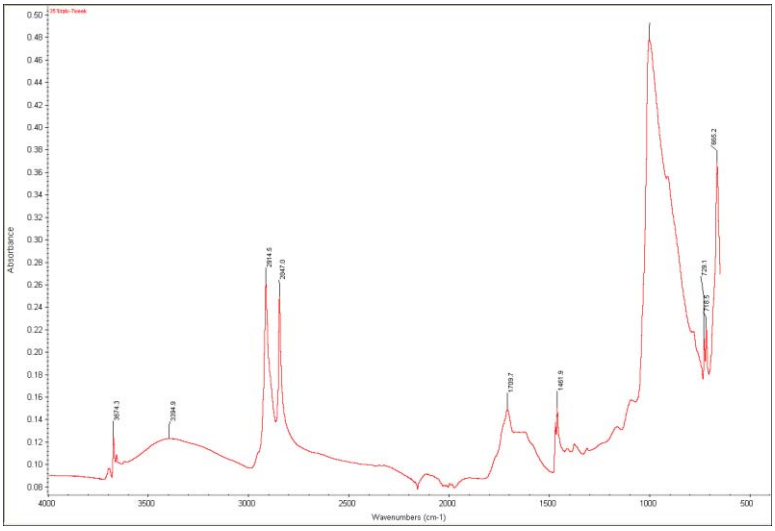


**Figure B-23. FTIR Spectra of recycled LDPE filled with 35wt% fine talc exposed under UV for seven weeks**

Calculation for Carbonyl Index: A= 0.150

B= 0.145

Carbonyl Index of recycled LDPE with 35wt% talc exposed under UV for seven weeks:

A/B= 1.0344

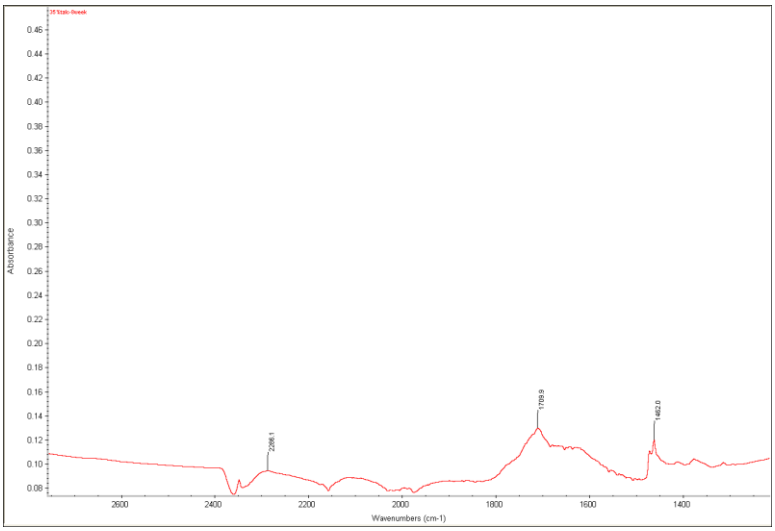


**Figure B-24. FTIR Spectra of recycled LDPE filled with 35wt% fine talc exposed under UV for eight weeks**

Calculation for Carbonyl Index: A= 0.148

B= 0.129

Carbonyl Index of recycled LDPE with 35wt% talc exposed under UV for eight weeks:

A/B= 1.147

**Table B-3. Carbonyl Index of recycled LDPE with 35 wt% fine talc exposed under UV for different time (week)**

| | 0 | 1 | 2 | 3 | 4 | 5 | 6 | 7 | 8 |
|---|---|---|---|---|---|---|---|---|---|
| Carbonyl Index | 0.461 | 0.381 | 0.427 | 0.436 | 0.447 | 0.423 | 0.443 | 1.034 | 1.147 |

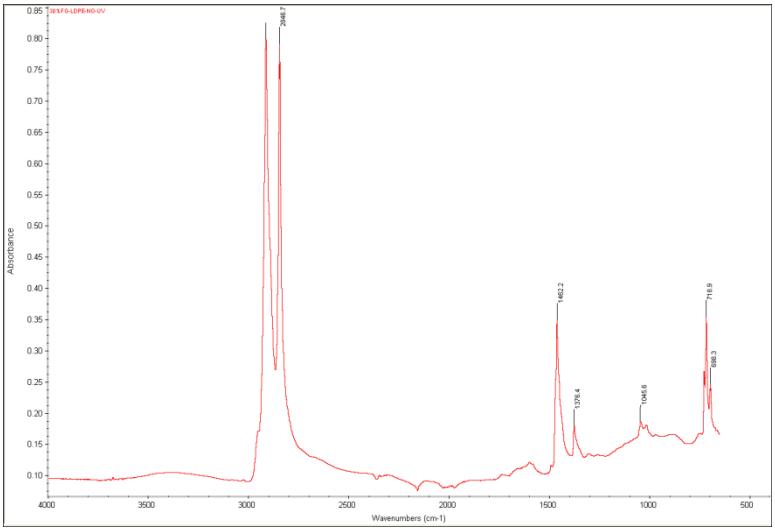


**Figure B-25. FTIR Spectra of recycled LDPE filled with 30wt% glass fibre exposed without UV exposing**

Calculation for Carbonyl Index: A= 0.088

B= 0.231

Carbonyl Index of recycled LDPE with 30wt% glass fibre without UV exposing:

A/B= 0.381

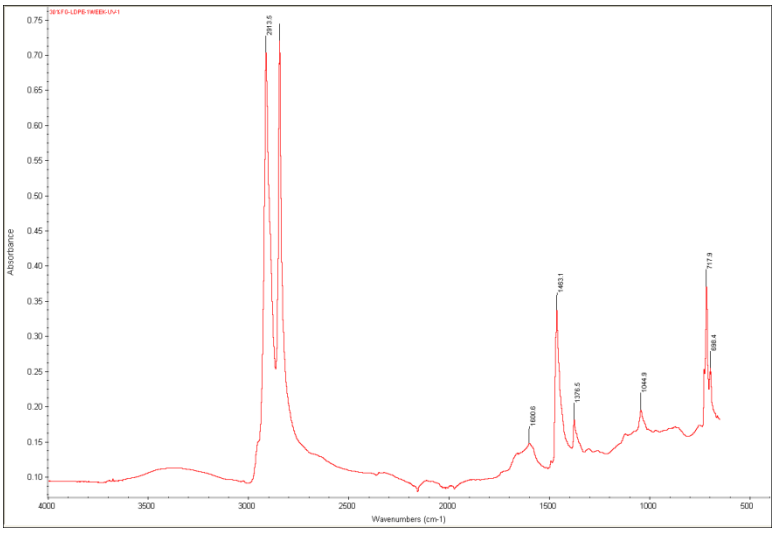


**Figure B-26. FTIR Spectra of recycled LDPE filled with 30wt% glass fibre exposed under UV for one week**

Calculation for Carbonyl Index: A= 0.104

B= 0.242

Carbonyl Index of recycled LDPE with 30wt% glass fibre exposed under UV for one week:

A/B= 0.429

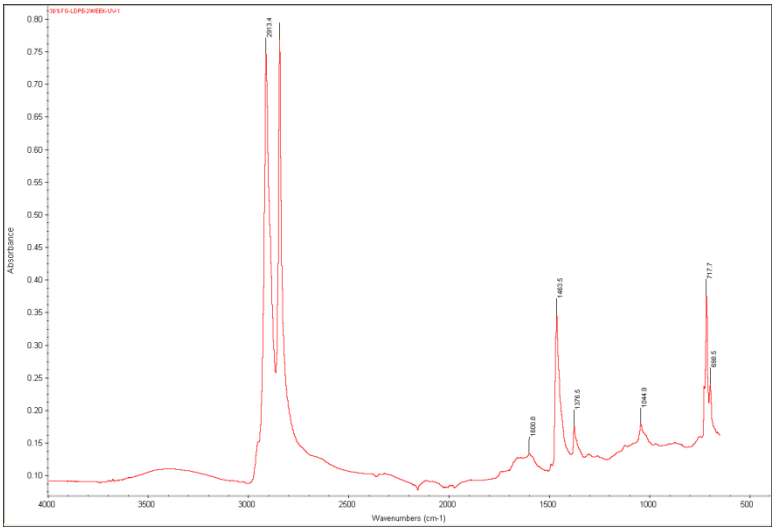


**Figure B-27. FTIR Spectra of recycled LDPE filled with 30wt% glass fibre exposed under UV for two weeks**

Calculation for Carbonyl Index: A= 0.105

B= 0.252

Carbonyl Index of recycled LDPE with 30wt% glass fibre exposed under UV for two weeks:

A/B= 0.3968

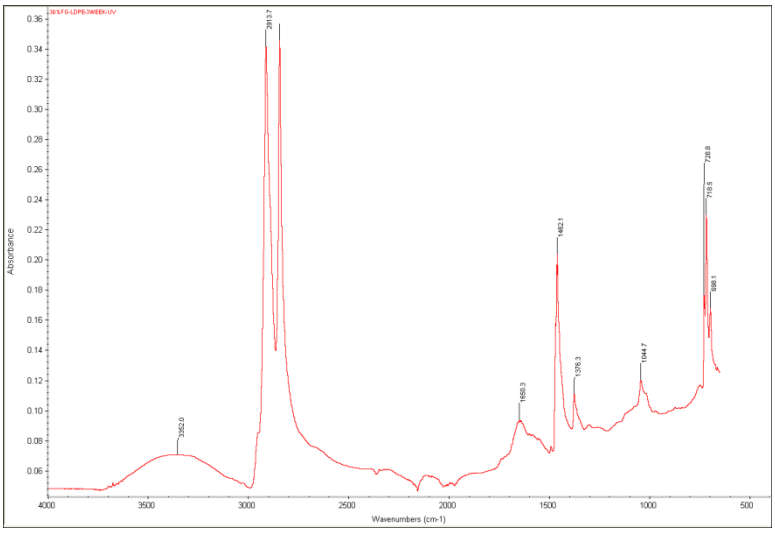


**Figure B-28. FTIR Spectra of recycled LDPE filled with 30wt% glass fibre exposed under UV for three weeks**

Calculation for Carbonyl Index: A= 0.111

B= 0.243

Carbonyl Index of recycled LDPE with 30wt% glass fibre exposed under UV for three weeks:

A/B= 0.456

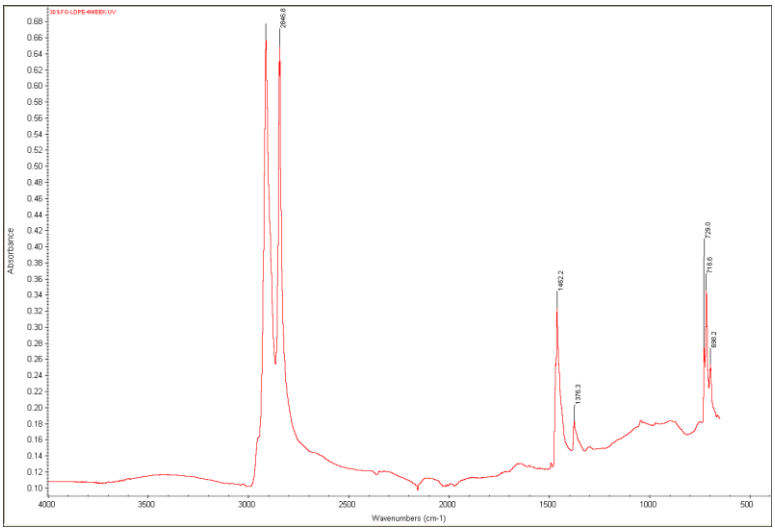


**Figure B-29. FTIR Spectra of recycled LDPE filled with 30wt% glass fibre exposed under UV for four weeks**

Calculation for Carbonyl Index: A= 0.110

B= 0.237

Carbonyl Index of recycled LDPE with 30wt% glass fibre exposed under UV for four weeks:

A/B= 0.464

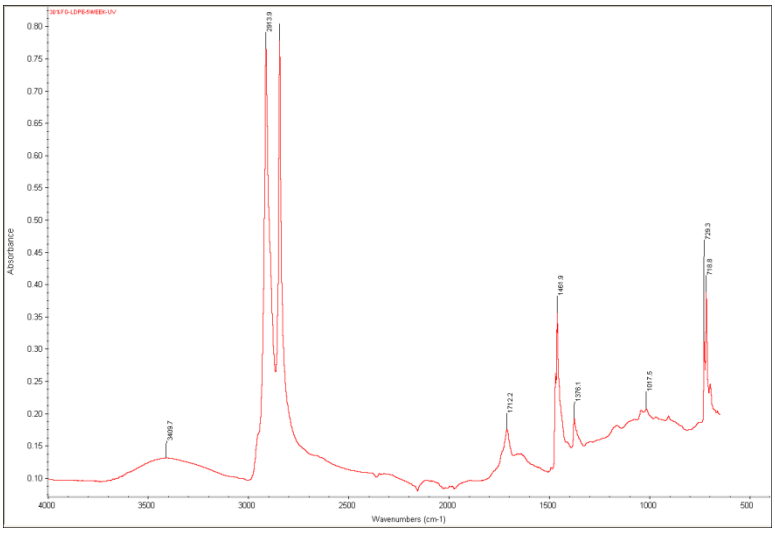


**Figure B-30. FTIR Spectra of recycled LDPE filled with 30wt% glass fibre exposed under UV for five weeks**

Calculation for Carbonyl Index: A= 0.105

B= 0.238

Carbonyl Index of recycled LDPE with 30wt% glass fibre exposed under UV for five weeks:

A/B= 0.441

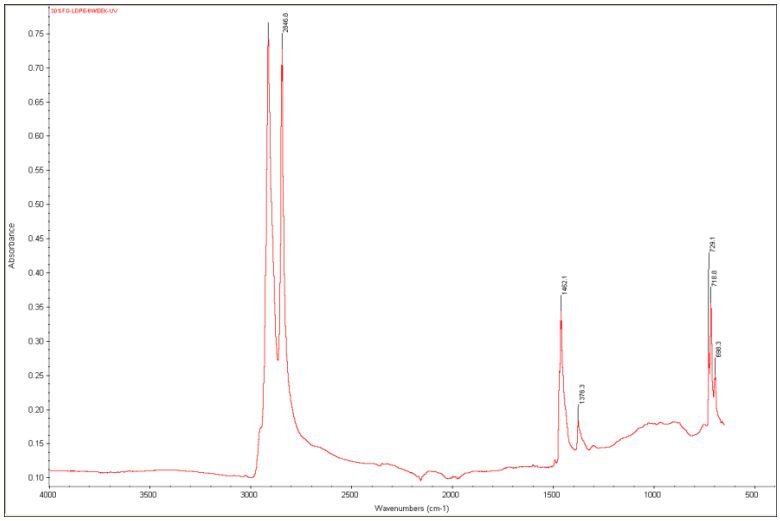


**Figure B-31. FTIR Spectra of recycled LDPE filled with 30wt% glass fibre exposed under UV for six weeks**

Calculation for Carbonyl Index: A= 0.114

B= 0.224

Carbonyl Index of recycled LDPE with 30wt% glass fibre exposed under UV for six weeks:

A/B= 0.508

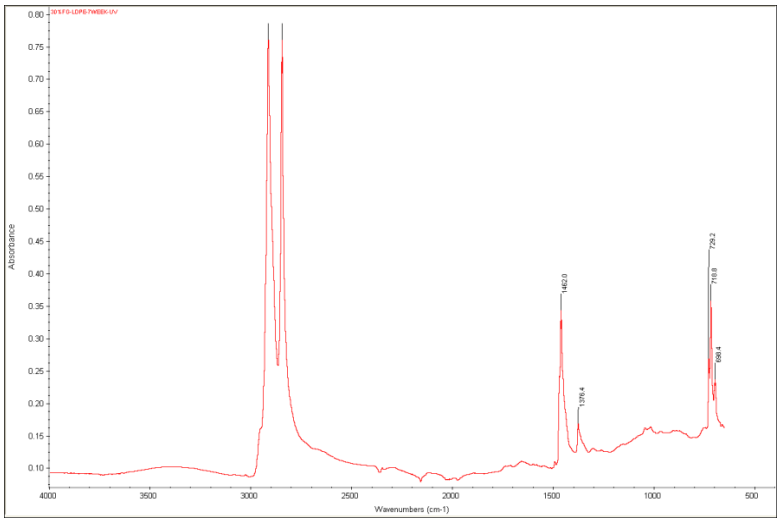


**Figure B-32. FTIR Spectra of recycled LDPE filled with 30wt% glass fibre exposed under UV for seven weeks**

Calculation for Carbonyl Index: A= 0.118

B= 0.238

Carbonyl Index of recycled LDPE with 30wt% glass fibre exposed under UV for seven weeks:

A/B= 0.495

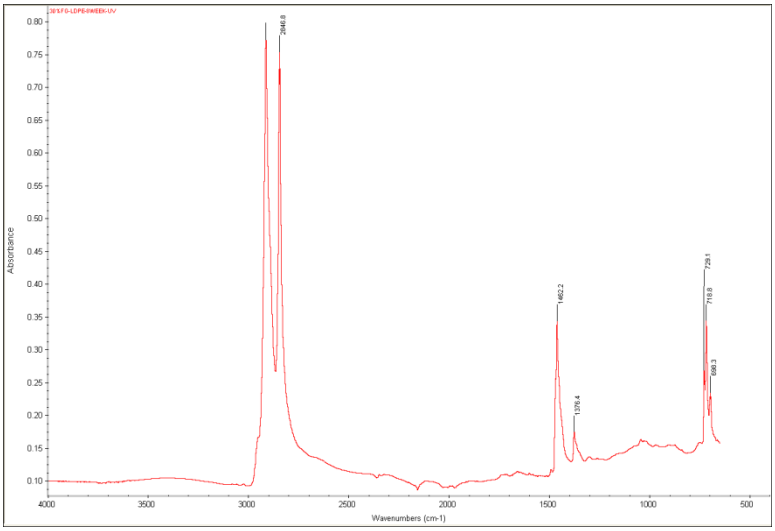


**Figure B-33. FTIR Spectra of recycled LDPE filled with 30wt% glass fibre exposed under UV for eight weeks**

Calculation for Carbonyl Index: A= 0.097

B= 0.181

Carbonyl Index of recycled LDPE with 30wt% glass fibre exposed under UV for eight weeks:

A/B= 0.535

**Table B-4. Carbonyl Index of recycled LDPE with 30 wt% glass fibre exposed under UV for different time (week)**

| | 0 | 1 | 2 | 3 | 4 | 5 | 6 | 7 | 8 |
|---|---|---|---|---|---|---|---|---|---|
| Carbonyl Index | 0.381 | 0.429 | 0.397 | 0.456 | 0.464 | 0.441 | 0.508 | 0.495 | 0.535 |

**Table B-5 Characteristic IR Absorption Frequencies of Organic Functional Groups (UPS n.d)**

NOTE:
This table is included on pages 98-99 of the print copy of the thesis held in the University of Adelaide Library.

# APPENDIX C: DSC TEST RESULTS

**Table C-1 Crystallization properties of recycled LDPE sample one**

| | Crystallization temperature peak ($^{o}$C) | Heat of crystallization (J/g of composites) | Heat of crystallization (J/g of LDPE) |
|---|---|---|---|
| 1 | 127.95 | 25.82 | 25.82 |
| 2 | 128.04 | 23.32 | 23.32 |
| 3 | 128.01 | 25.74 | 25.74 |
| Mean | 128.00 | 24.96 | 24.96 |
| Standard Deviation | 0.04 | 1.42 | 1.42 |

**Table C-2 Crystallization properties of recycled LDPE sample one filled with 30 wt% talc**

| | Crystallization temperature peak ($^{o}$C) | Heat of crystallization (J/g of composites) | Heat of crystallization (J/g of LDPE) |
|---|---|---|---|
| 1 | 128.67 | 24.90 | 35.57 |
| 2 | 128.14 | 26.34 | 37.63 |
| 3 | 129.9 | 24.98 | 35.68 |
| Mean | 128.9 | 25.40 | 36.29 |
| Standard Deviation | 0.90 | 0.80 | 1.16 |

**Table C-3 Crystallization properties of recycled LDPE sample one filled with 35 wt% talc**

| | Crystallization temperature peak ($^{o}$C) | Heat of crystallization (J/g of composites) | Heat of crystallization (J/g of LDPE) |
|---|---|---|---|
| 1 | 128.50 | 24.52 | 37.72 |
| 2 | 128.76 | 25.41 | 39.09 |
| 3 | 129.73 | 26.68 | 41.04 |
| Mean | 128.99 | 25.53 | 39.28 |
| Standard Deviation | 0.64 | 1.08 | 1.67 |

**Table C-4 Crystallization properties of recycled LDPE sample two**

| | Crystallization temperature peak ($^{o}$C) | Heat of crystallization (J/g of composites) | Heat of crystallization (J/g of LDPE) |
|---|---|---|---|
| 1 | 133.91 | 68.50 | 68.50 |
| 2 | 135.07 | 67.55 | 67.55 |
| 3 | 132.86 | 70.98 | 70.98 |
| Mean | 133.94 | 69.01 | 69.01 |
| Standard Deviation | 1.10 | 1.77 | 1.77 |

**Table C-5 Crystallization properties of recycled LDPE sample one filled with 40 wt% talc**

| | Crystallization temperature peak ($^{o}$C) | Heat of crystallization (J/g of composites) | Heat of crystallization (J/g of LDPE) |
|---|---|---|---|
| 1 | 134.70 | 46.99 | 78.32 |
| 2 | 134.68 | 46.79 | 77.98 |
| 3 | 133.04 | 47.13 | 78.55 |
| Mean | 134.14 | 46.97 | 78.28 |
| Standard Deviation | 0.95 | 0.17 | 0.29 |

**Table C-6 Crystallization properties of recycled LDPE sample one filled with 45 wt% talc**

| | Crystallization temperature peak ($^{o}$C) | Heat of crystallization (J/g of composites) | Heat of crystallization (J/g of LDPE) |
|---|---|---|---|
| 1 | 134.59 | 45.41 | 82.56 |
| 2 | 135.37 | 43.76 | 79.56 |
| 3 | 136.22 | 45.09 | 81.98 |
| Mean | 135.39 | 44.75 | 81.36 |
| Standard Deviation | 0.82 | 0.88 | 1.59 |

**Table C-7 Crystallization properties of recycled LDPE sample one filled with 50 wt% talc**

| | Crystallization temperature peak ($^{o}$C) | Heat of crystallization (J/g of composites) | Heat of crystallization (J/g of LDPE) |
|---|---|---|---|
| 1 | 136.94 | 45.05 | 90.01 |
| 2 | 135.93 | 49.91 | 99.82 |
| 3 | 135.45 | 48.00 | 96.00 |
| Mean | 136.11 | 47.65 | 95.27 |
| Standard Deviation | 0.76 | 2.44 | 4.94 |

**Table C-8 Crystallization properties of recycle LDPE filled by talc (wt%)**

| | Recycle LDPE 1 | 30 | 35 | Recycled LDPE 2 | 40 | 45 | 50 |
|---|---|---|---|---|---|---|---|
| Crystallization Temperature ($^{o}$C) | 128.00 | 128.90 | 128.99 | 133.94 | 134.14 | 135.39 | 136.11 |
| Heat of Crystallization (J/g of composites) | 24.96 | 25.40 | 25.53 | 69.01 | 46.97 | 44.75 | 47.65 |
| Heat of crystallization (J/g of LDPE) | 24.96 | 36.29 | 39.28 | 69.01 | 78.28 | 81.36 | 95.27 |
| Degree of crystallinity | 9% | 12% | 14% | 24% | 27% | 28% | 33% |